University of
Stavanger

Faculty of Science and Technology

MASTER'S THESIS

Study program/ Specialization: Offshore Technology/ Marine and Subsea Technology	Spring semester, 2013. Open / ~~Restricted access~~
Writer: Clement Adewale **Obadina**	…………………………………………. (Writer's signature)

Faculty supervisor: Prof. Arnfinn Nergaard, Ph.D.
University of Stavanger, Norway.

External Supervisor: Harald Syse
Reelwell AS, Norway.

Title of thesis: Hydrodynamic Analysis of Drill String in Open Water

Credits (ECTS): 30

Key words: Analysis, Hydrodynamics, Drill String, Open Water, Riserless Drilling.	Pages: 91 + enclosure: 32 + 1 CD Stavanger, June 14, 2013. Date/year

ABSTRACT

Due to a decline in proven petroleum reserves through continued production, exploration of oil and gas has moved into more challenging environment and into deep and ultra-deep water. Over the years, the equipment and facilities needed for exploration in such environments have become more sophisticated, expensive and the technology has become more challenging. This is as a result of the need to accommodate the much heavier weight of the marine riser and its suspension/tensioning systems, the space needed for handling more and advanced equipment, the space required for the mud facilities especially when high density drilling fluid is required and finally, to meet standards set by regulating organization.

One of the challenges of deep water operation is therefore the marine riser. A marine riser connects the drilling rig to the mudline and helps for material circulation between the well and the topside. In some past years when exploration was done in relatively shallow waters it was easy to move into a deeper waters by only increasing the size of the drill rig. As we move into deeper water, the marine riser and its content get bigger and heavier. Because of the heavier weight larger vessels which are very scares and expensive are required. Therefore, a method that can eliminate the marine riser would be one of attractive alternatives to explore oil fields in deep and ultra-deep water economically. This drilling method without the marine riser is known as Riserless drilling.

Riserless drilling is an unconventional drilling technique where the marine riser is eliminated and replaced with a different method to take the return and a control bundle. The control bundle serves as a means of communication between the well and the rig. Reelwell Drilling Method – Riserless (RDM-R) is one of such riserless drilling methods. The RDM-R method utilizes a dual pipe where the return of the circulation fluid is the inner pipe. The company that offers the RDM-R method claims that the benefits of the method includes: reduction in the numbers of casing points - Longer sections, less space requirement, dual gradient drilling, easier station keeping, less weight capacity requirement, less fluid volume and pumping capacity, etc.

This report will focus on the effects of hydrodynamic forces and vessel movements on the RDM-R drill string without the marine riser. Emphasis will be made upon the forces and stresses developed during the static and the dynamic phases of the simulation. This report will discuss oscillating loading and the Magnus Effect on the drill string. It will also define for the audience fatigue damage analysis. The RDM-R pipe will be checked for burst and collapse failure with reference to DNV-OS-F201. In this report we will also make comparison of the axial load requirements for a RDM-R method and the CRD method which will be an input for the drill vessel requirements.

The input data are referenced from a project undertaken by the Reelwell AS Company in Santos Basin, Brazil. Orcaflex Software will be used for the design of the mechanical model and for the simulation.

Acknowledgement

I would like to dedicate this report to the glory of the Almighty GOD, thank you Lord.

I am exceedingly grateful to my supervisor and lecturer, Professor Arnfinn Nergaard, whose fatherly care and guidance made this report a success.

My gratitude also goes to Reelwell AS, Stavanger, Norway for granting me the opportunity to undertake this task and providing me with an enabling office space for the successful completion of this project. My profound gratitude goes to all staffs and management of Reelwell AS for being there to answer my questions and making me feel welcomed during the course of this work.

Finally, I express my endless thanks to my gift from GOD - my parents and my siblings especially Rev. Fr. A.O. Obadina (CMF), for always being there.

Clement Adewale Obadina

Stavanger, June, 2013.

Table of Contents

List of Figures

List of Tables

Abbreviations

ALS	Accidental Limit State
API	American Petroleum Institute
BHP	Bottom Hole Pressure
BOP	Blowout Preventer
CBHP	Constant Bottom Hole Pressure
CCS	Continuous Circulation System
CMC	Controlled Mud Cap
CRD	Conventional Riser Drilling
DDP	Dual Drill Pipe
DNV	Det Norske Veritas
DP	Dynamic Positioning
ECD	Equivalent Circulating Density
FLS	Fatigue Limit State
FPSO	Floating Production Storage and Offloading
HSE	Health Safety and Environment
IADC	International Association of Drilling Contractors
JOHNSWAP	Joint North Sea Wave Project
LRFD	Load and Resistance Factor Design
MODU	Mobile Offshore Drilling Units
MPD	Managed Pressure Drilling
NPT	Non Production Time
PMCD	Pressurized Mud Cap Drilling
RAO	Response Amplitude Operator
RCD	Rotating Control Device
RD	Riserless Drilling
RDM-R	Reelwell Drilling Method – Riserless
RP	Recommended Practice
SCF	Stress Concentration Factor

SLS	Serviceability Limit State
SPE	Society of Petroleum Engineers
SWL	Safe Working Load
TVD	Total Vertical Depth
TLP	Tension Leg Platform
UBD	Underbalanced Drilling Operation
ULS	Ultimate Limit State
VIV	Vortex Induced Vibration
WSD	Working Stress Design

Chapter 1: Introduction

1.1 Background

As the industry moves into deep and ultra-deep waters in harsh environments that present high technical and economic risks, the drill rig size has tripled in the past 50 years with corresponding increase in cost. The oil and gas industry requires attractive and cost effective alternatives for exploration without undermining the environment. One of such alternatives is the Reelwell Drilling Method (RDM) which eliminates the use of marine riser and substitutes it with a small internal pipe to take return of the circulating fluid. The present development in the ultra-deep waters has stalled at 10000 ft., RDM is one avenue to reach 13000 ft. (Reelwell, 2013) and with the marine riser eliminated older generations of drilling rigs, say 3rd and 4th could be used in ultra-deep well operations to save cost. Using 3rd and 4th generation rigs for deep water wells at a 25 - 35 % lower day rates may results to cost savings in excess of 45% (Reelwell, 2013).

1.2 Objectives

The objective of this report is to investigate the effects of hydrodynamic forces on the drill string in open water. The following are what we will carry out in the course of this report:

- **Establish a design basis**: Using DNV-OS-F201, DNV-OS-F101 and API RP 2RD we will establish the relevant design criteria that the RDM-R drill pipe must meet and identify its limit states. We will also set up the characteristics of the proposed RDM-R drill pipes and establish a model for the RDM-R dual drill pipes in OrcaFlex 9.5.
- **Establish a mechanical model**: Using OrcaFlex 9.5, we will establish a model of the dual concentric pipe, the environment and the conditions in the well from our base case. Our base case would be the BG presalt wells in Santos basin in Brazil. As such, all data relating to this report will be taken from this deep water development in Brazil.
- **Perform analysis of the model**: We will run both static and dynamic analysis of the established model.
- **Present the results and discuss the result**.
- **Make recommendation for further studies**.

Chapter 2: State of the Art in Drilling Technology

2.1 Introduction

Well drilling is the process of drilling a hole through the earth to access its resources. Over the years, well drilling has become very advanced, challenging and its engineering has become even more sophisticated as exploration of gas and oil moves into more hostile environments. These advancements and high-tech engineering are results of the limitations in applications of the marine riser, the narrow operating window between formation pore pressure and fracture pressure, to mention a few. These features are even more challenging in the deep and ultra-deep water environments.

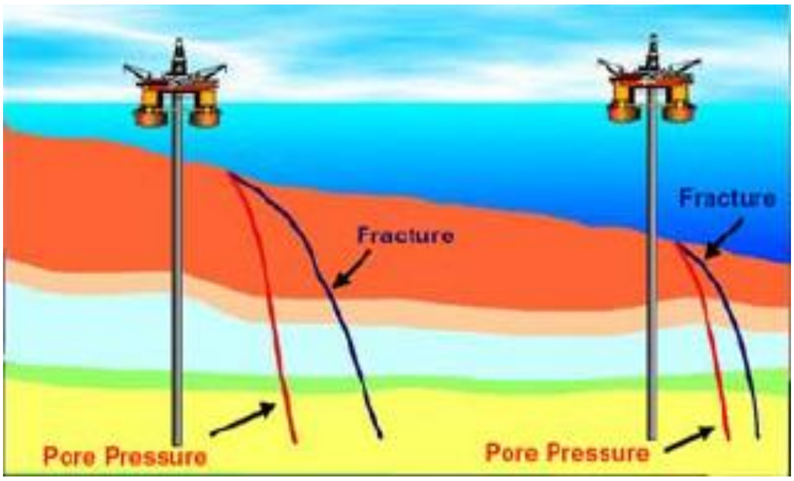

Figure 1: Pressure profiles (Fjelde k., 2011)

Since it is impossible to manipulate the nature of the environment in terms of the water depth and the pressure profile of a well, we need to improve our present technology to accommodate and adapt to this new environment. In the words of Royal Dutch Shell's boss, Peter Voser, "Given the rise in the population and the rise in the developing world of energy needs, we will have to develop those resources in deep waters, so my expectation is that we will go forward with it, but it will need some changes" (Energy Bulletin, 2013). Figure 2 below shows deep water discoveries made in the industry since 1982 till date.

The deep water environment is very promising as new discoveries are made regularly. However, to make these vast resources available for exploration in an economic and safe manner it will push the existing technology to its limits. These are due to reasons like the marine riser and the pressure profiles in the deep and ultra-deep environments area as highlighted above but the more challenging is the use of marine riser.

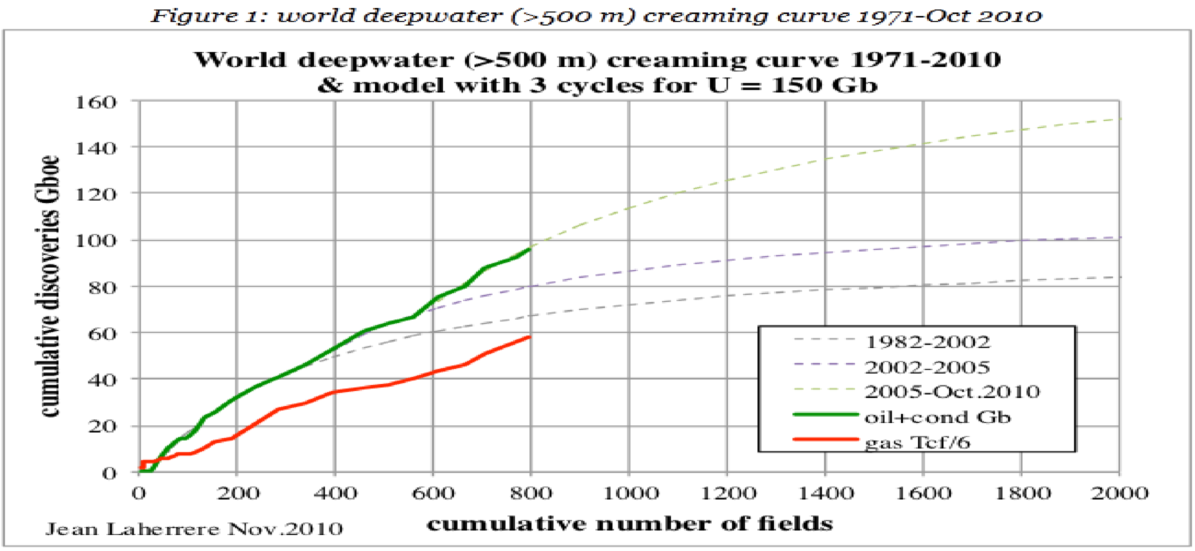

Figure 2: Increasing Discoveries in the Ultra-Deep Waters in Recent Years from 2005-2010 (The oildrum, 2013)

As operation moves into the deep and ultra-deep waters the size of the applicable marine riser gets bigger. In some cases a typical 21" marine riser can increase up to 50" when kill line, choke line, control line and booster line are attached (Leach. C. et al, 2002). An increment in the length and diameter of the riser implies that the mud needed to fill it becomes much and quite heavy. To accommodate for the resulting increase in pressure and stresses the thickness of the marine riser has to increase. The thickness and size of the marine riser determines the unit's cost in price of the riser. This is why it becomes very expensive and very difficult to use a large diameter marine riser drill a well beyond 6,000 ft. The marine riser has although been used successfully for water depth more than 7,000 ft. but it is impractical to extrapolate current technologies to 10,000 ft. water depth (Jonggeun C, 1998). Apart from this, the required tools and installation time add a huge expense to deep water operations. Furthermore, high weighted mud column in the riser if not properly managed can result into fracture of the well.

2.2 Oil Well Drilling

An oil well drilling is basically making a hole through the surface of the earth to access oil and often times, natural gas is produced along with the oil. The process of making the hole is made possible by a drilling rig. A typical oil rig is as shown in figure 3 below.

Offshore drilling rigs are massive structures that houses equipment that are used to carry out operations on site. Such operations may include drilling oil wells, drilling natural gas extraction wells, sub-surface physical properties sampling, mineral deposits investigation, rock sampling, and sub-surface fabrications. They are capable of drilling hundreds of meters through the earth which is, amongst other factors, affected by how well cooling the drill bit and removing the cuttings or cleaning the hole are administered. Simultaneous cooling and cleaning is achieved by circulating drilling mud or slurry. The circulation is done through the drill bit and up the annulus while drilling. After boring a hole, pipe sections or casings are installed in the hole which may be cemented in place.

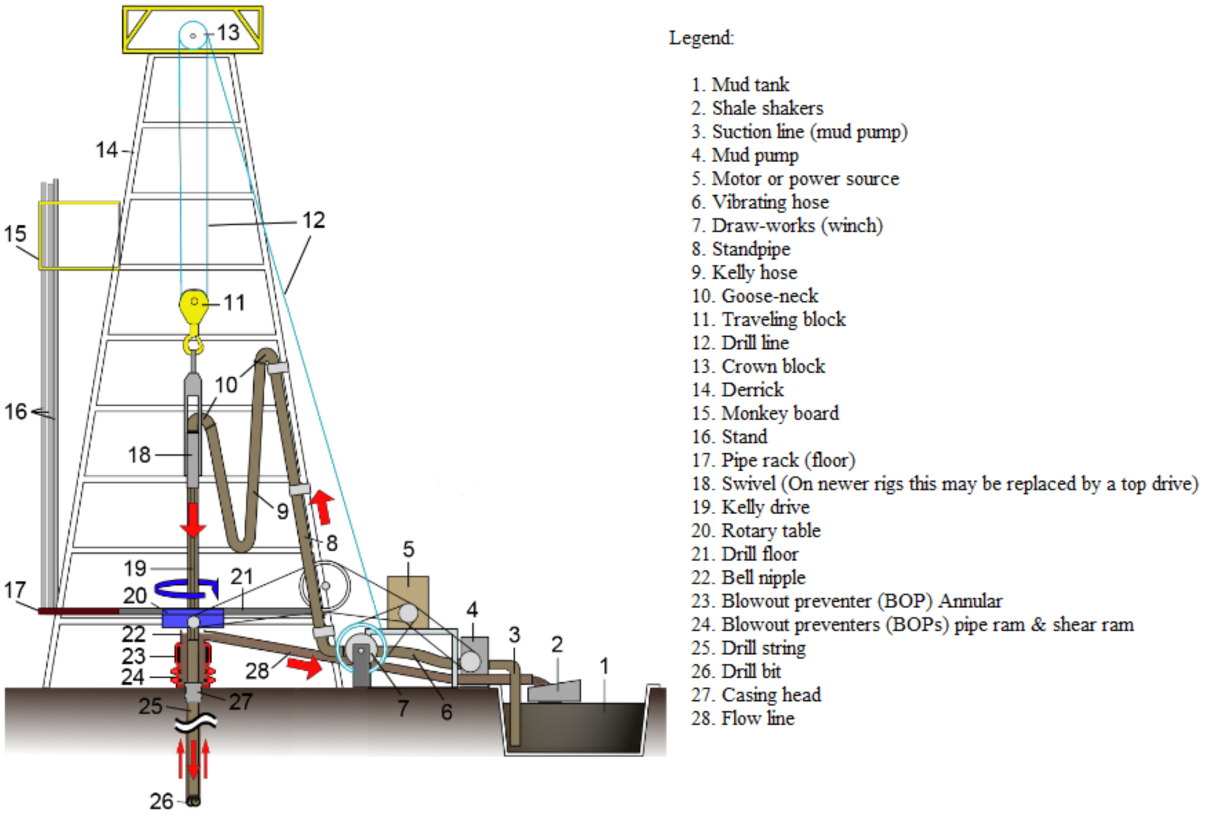

Figure 3: Oil Rig (Wikipedia, 2008)

These casings serve the purpose of providing structural integrity to subsequent drilled holes and isolates dangerous high pressure zones from the surface.

2.3 Offshore Drilling Units.

Offshore drilling in deep and ultra-deep water depth greater than 500 meters may require that operations be carried out from a floating vessel, as fixed structures are not practical. These floating vessels are referred to as mobile offshore drilling units (MODU). The selection of a MODU for a particular operation depends on several factors, among which are its limitation, capacity and cost.

2.3.1 Jackup Rigs: The main components of a Jackup unit are the hull, the legs/footings, and the equipment. It is designed in such a way that allows for it to be towed to a site and installed by simply lowering its legs into the seabed and elevating or jack-up its hull. A typical modern drilling Jackup is capable of working in harsh environment like wave heights up to 25m and in wind speeds up of 100 knots (Marine Wiki, 2010), in water depth from 20 feet to 550 feet maximum depth. In some textbooks 350 feet has been cited as the maximum depth a jackup can operate, however Petroleum Engineering Handbook has cited a water depth of 550 feet in the Gulf of Mexico (Petrocenter, 2008).

Figure 4: Jackup Drilling Rig (Bennett Offshore, 2012)

The advantages of the jackup rig include work platform stability, low mobilization cost, readily available, competitive day rate, and unlike other MODU, it can be enhanced or updated easily.

The limitations include relatively lesser load carrying capabilities, environmental limits, drilling limits, and soil (foundation) limits.

2.3.2 Drill ships: The Drill ships are vessels that have features like derrick and moon pool for drilling. It is a typical deep and ultra-deep water drilling rig and can be used in water depths from 2,000 to about 10,000 feet (Rigzone, 2013). Its long hull results into its characteristics high motion in six degrees of freedom. Advancements in dynamic positioning and mooring systems of the drillship have led to a phenomenon improvement in the capability of drilling in harsh environments.

Figure 5: Drillship (gCaptain, 2013)

The advantages of modern drill ships is in their ability to operate in waters more than 2500 m. Ease and quick mobilization, time saving in moving between fields and they are independent, that is, unlike semi-submersible, a drillship can move by itself from one place to the other especially during emergency disconnect.

The limitation of a drillship is in its susceptibility to wind, current and waves especially during drilling.

2.3.3 Semisubmersible Rigs: It is the most stable of all the floating rigs with the ability to stand rough waters and as such chosen mostly for most operations in the harsh environments. Semisubmersible rigs have pontoons and columns that allow the operator controls the draft of the unit by managing the level of flooded water in the columns. The draft of the column allows for better stability against wave energy and minimizing surge, sway, heave, roll, pitch, and yaw motions.

The combined actions of wind and waves on the semisubmersible make it difficult for position-keeping in the ocean and due to the preciseness of the wellbore, it is very necessary to keep position. Mooring lines are used for proper position-keeping. There a several patterns of mooring that can be used to keep the rig in position; examples are 45i-90i nine-line, symmetric twelve-line, six-line, and eight-line, etc.

The disadvantage of a semisubmersible is that it relies on a transport vessel for movements and has a lesser equipment holding capacity in comparison with the drillship.

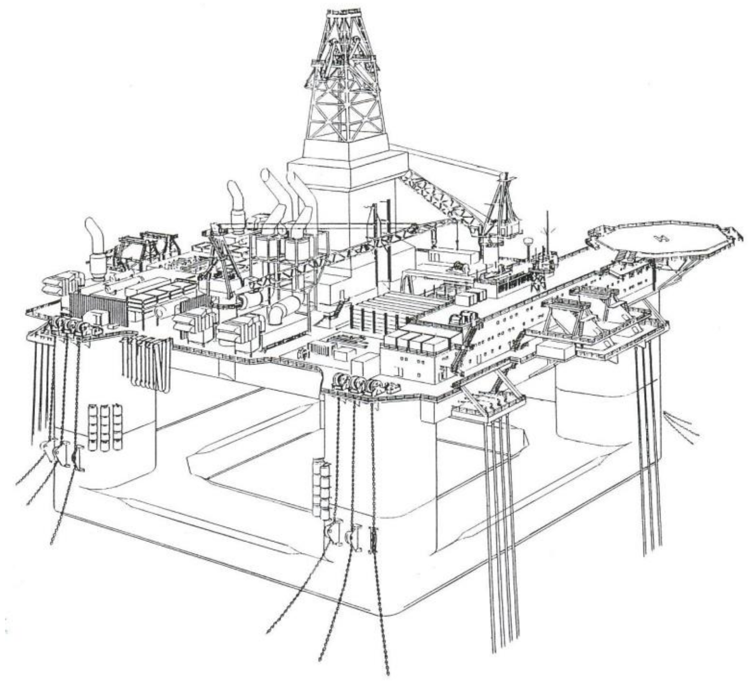

Figure 6: Semi-submersible Drilling Rig (Lim E.F.H. et al, 2012)

Semisubmersible drilling rigs are commonly subdivided into generations. Appendix A shows some notable semisubmersible designs and their general characteristics. The table below shows the different generations of the semisubmersible and their features.

Generation	Example	Year	Water Depth (Ft)
1	• Ocean Explore • Bluewater One	Mid 1960 – Late 1960	300 – 600
2	• Pentagone • Ocean Traveller	Mid 1970 – Late 1970	600 – 2000
3	• Odyssey • Aker H3 • Byford Dolphin	Early 1970 – 1985	1500 - 5000
4	• West Alpha • Ocean Victory	Late 1980 – Early 2000	3500 – 5000
5	• Leiv Eriksson • R & B Falcon • Blackford Dolphin	Late 1990 – 2005	5000^{+}
6	• Deepsea Atlantic • Atwood Osprey	2005 - Date	About 10000

Table 1: Generation of Semisubmersibles

2.4: Conventional Riser Drilling (CRD)

Conventional drilling had its beginning at Beaumont, Texas in 1900 (Kenneth P. Malloy et al, 2009). There have been some improvements since then, for example, the movement of the BOP to the seafloor as water depth increased, increment in rig size for more tool handling and work space, increment in the sizes of equipment and development of more sophisticated tools. Also, the former $13\,{}^{5}/_{8}{}''$ wellheads were substituted with the $18\,{}^{3}/_{4}{}''$ wellheads, and the present 21’’ risers were initially $18\,{}^{5}/_{8}{}''$.

Conventional drilling circulation flow path starts from the mud pit; the mud moves down through the drill string, out through the drill bit and up the annulus, the wellbore to the atmosphere. Then to solids control equipment and mud-gas separator then back to the pit for another cycle. The annulus is created by the marine riser which also protects the drill strings. Other function of the riser is that it provides supports for umbilical and other gadgets from the topside to the well.

Figure 7: 50 Years of Semisubmersibles (Reelwell, 2012)

Presently, conventional riser drilling is the most trusted single drilling concept employed in deep-water drilling. But, as water depth increases even further and operations goes into the deep and ultra-deep waters it became glaring that it would be technically impossible and uneconomically viable to continue with the present trend of operation. The size of the marine riser, the rig and equipment has reached their economic and technical limits. Even if we justify that all the problems in connection to the rig and marine riser are solved at a reasonable cost, the problems of drilling operations in the deep and ultra-deep waters are not all about the size and cost of marine drilling risers, dealing with narrow window between the pore pressure and the fracture pressure in deep water environments is also a big challenge that needs to be addressed properly.

2.4.1 Limitations of Conventional Riser Drilling in Deep-water

- Massive space and weight handling requirements
- Heavy mud weight in the marine riser especially as water deepens
- Possible severe stress development in the marine riser as a result of size.
- Severe stresses combined with other hydrodynamic forces may make it difficult for proper station keeping
- Longer non-productive time.
- Numerous casing joints because of narrow pressure window in the deep water.
- Limited fleets of capable drilling rigs able to carry out operations in deep-water environments.

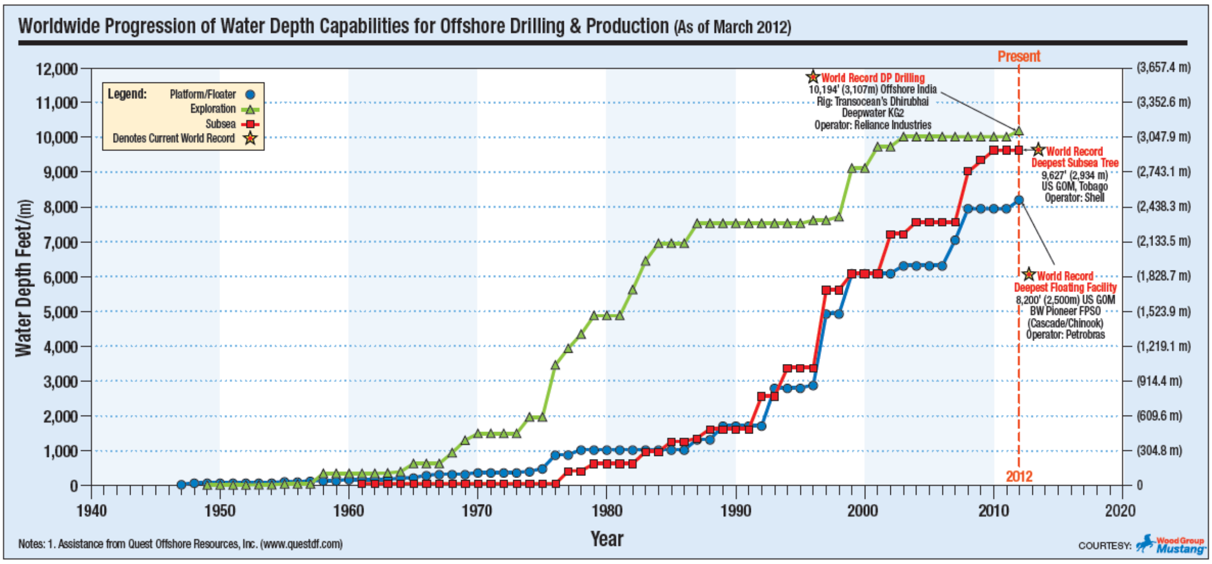

Figure 8: (Mustang, 2012)

Majority of the aforementioned limitations of conventional drilling can be traced to the use of the marine riser. It is the single most challenging problems of conventional drilling for deep-water operations. A marine riser serves as a return path for the mud to the vessel and a guide for the drill pipe into the hole. Presently in deep-water drilling operations a 21 inches outside diameter with 19.5 inches internal diameter marine riser is utilized.

$$Volume\ Capacity\ per\ unit\ Lenght = \frac{\pi d^2}{4}$$

$$= \frac{\pi * 19.5^2}{4} = 298.65\ sqaure\ inches$$

It means that the internal volume capacity is around 1.21bbl. for every unit length in meter. For a steel material, a net weight of 48.77klb for every unit meter length. If we assume a mud with density 14.5ppg inside the riser, it weighs about 70klb per unit meter of length without the weights of additional buoyancy units. In addition, the weights of the couplings, for example, choke line; kill lines will further increase the weight of the riser. Therefore, huge buoyancy units may be required which further increases the outer diameter of the riser and invariably causes other problems like riser handling, VIV, etc.

2.3.2 Other Issues Associated with the Applications of the Marine Riser in Deep-Water.

1. **It may take hydrocarbon to places that it is unwanted**: Example is in the Deepwater Horizon incident in the Gulf of Mexico. In cases where it became difficult to disconnect the rig from the well, the marine riser is a direct passage to the rig.
2. **Exposure to severe stresses**: In order to accommodate burst pressure resulting from huge mud weight the thickness of the riser may need to be further increased. This means that as water depth increases the resulting weight of the riser increases leading to more stresses at the

hook position. Furthermore, the vessel movements, and hydrodynamic effects such as currents, wave and wind also contribute to the measured stress.

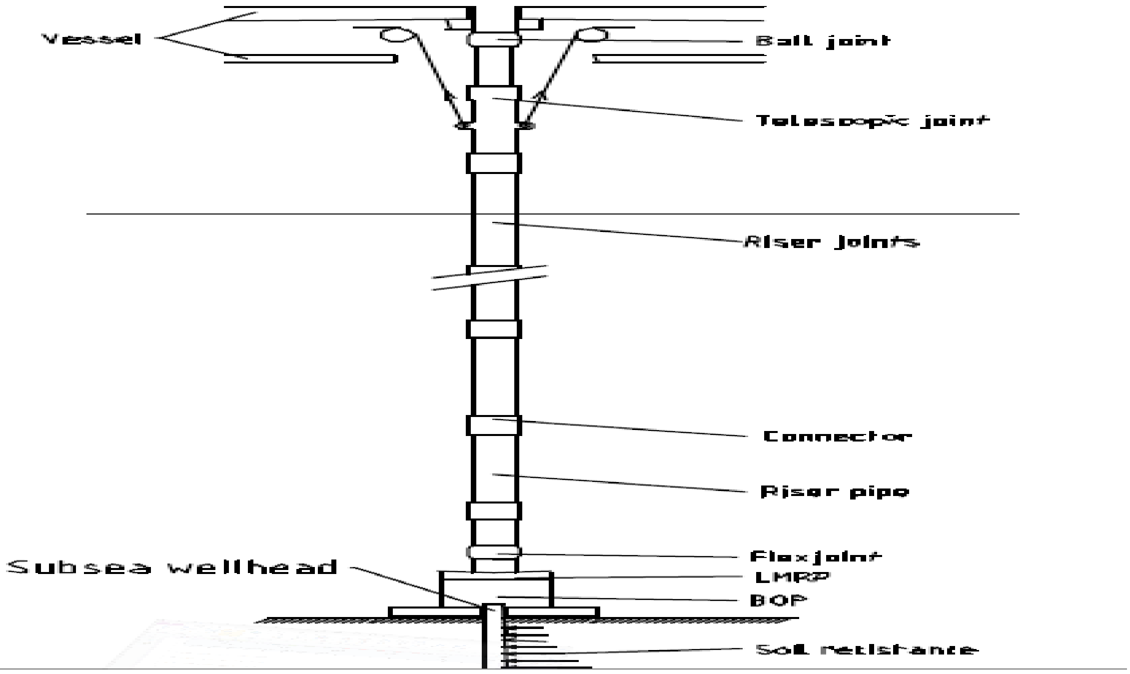

Figure 9: Components of a Marine Riser (DNV, 2010)

3. **Severe current effects**: In harsh environment where current may be high, it will become very difficult to run a long and large diameter riser. Secondly, the effects of VIV are more imminent.
4. **High cost of drilling vessel**: For station keeping, it will require a larger and as such more expensive drilling vessel.
5. **Increases waiting-on-weather time and non-productive time**: As the operation becomes more sophisticated a good weather window will be required for the operation.
6. **Increase numbers of casing**: Deep-water area is characterized with a narrow gap between pore and fracture pressures, therefore, it may require numerous casing points.

In the quest to reduce the size and weight of the marine riser the industry has in recent times developed some methods applicable for deep water exploration. Some of these methods include:

- Reducing the effective density of mud in the marine riser by injecting gas at the BOP level: Gases can be injected to reduce mud hydrostatic pressure in the marine riser. Just like gas lifting, nitrogen gas is used to maintain the hydrostatic pressure in the subsea wellhead equal to the hydrostatic pressure of the seawater at the mudline (Jonggeun C, 1998).
  However, an automatic controller for the gas injection rate is essential for actual application of this system which is not easy because of slow reaction from transient to steady state conditions and gas migration for static and circulating conditions. (Lopes, C.A. et al, 1997)

- Reducing the effective density of mud in the marine riser by using hollow glass: Hollow glass spheres of specific gravity 0.35 – 0.4 can be used to reduce mud density. This will provide better choke pressure control and easy calculation of system pressures because hollow glass spheres are essentially incompressible. (Medley, G.H. Jr. et al, 1995).
  However, cost for the use of hollow glass spheres is highly dependent on the recovery efficiency of the hollow glass spheres from the return mud.
- Reducing the pressure in the annulus beneath the wellhead by installing a subsea pump.

None of these techniques has resulted into the needed improvement in the industry. Even if the huge discoveries in the deep and ultra-deep water environments justifies the huge investments necessary for exploration in the area we still cannot push the application of the marine riser further than its present use.

Chapter 3 Emerging Drilling Operations

3.1 Introduction

Drilling operation in the deep water environment can be very intimidating due to the colossal floating package used and the downhole drilling hazards. As stated in chapter 2 of this report, many of these operations are carried out with a 21” marine riser that connects the mudline to the surface. To handle the huge mud column, an enormous rig with large space and good tensioning capabilities is vital. Various drilling operations have been developed over the past decade, amongst which is managed pressure drilling operation (MPD) and underbalanced drilling operation (UBD). The common denominator is to remove the hydrostatic head associated with the weight of the mud in the marine riser. Figure 10 below shows the illustration of the domain of managed pressure drilling operation, Underbalanced drilling operation, and conventional riser drilling operation.

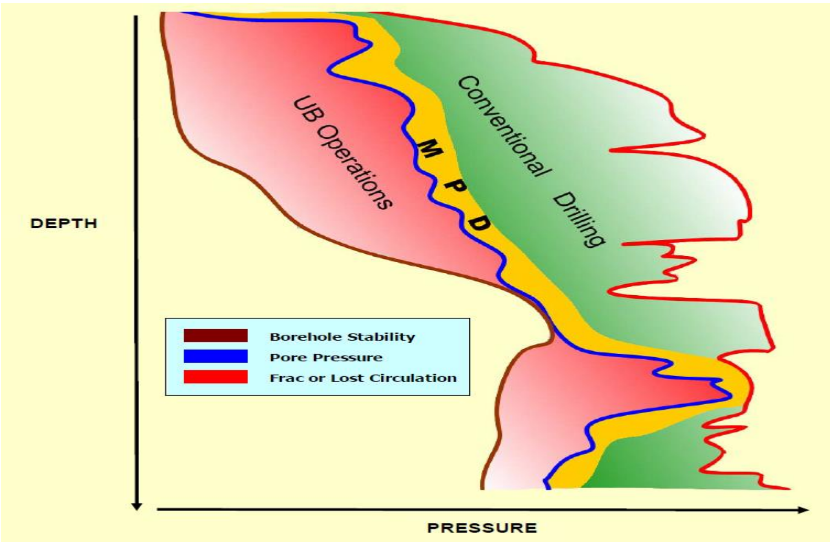

Figure 10: Drilling Windows for Drilling Operations (Kenneth P. Malloy et al, 2009).

3.2 Underbalanced Drilling Operation (UBD)

Underbalanced drilling operation enhances the productivity of a reservoir and it is achieved when the pressure exerted in the wellbore is intentionally kept equal or less than the pore pressure in any part of the bore. The intent is to bring formation fluids to the surface. The major objective of this drilling operation is to protect the reservoir during drilling operation in order not to compromise well potentials or to prevent formation damage that normally occurs during conventional drilling. This therefore maximizes recovery and at the same time minimizes drilling problems. In order for this to be obtained, hydrocarbon is encouraged to flow. The flow is allowed to travel up the borehole and controlled at the surface. The three major surface control devices are (Kenneth P. Malloy et al, 2009):

- Rotating Control Device (RCD)
- Multiple Phase Separator

- Drilling Choke Manifold

3.2.1 Objectives of UBD

- Early production: Production may start as soon as drilling begins.
- Reduced stimulation: Hydraulic fracture stimulation is eliminated since there is no solids invasion in the reservoir.
- Enhanced recovery: It makes the recovery of bypassed hydrocarbons possible. The improved productivity of an underbalanced well also results into a lower drawdown which can reduce water coning.
- Increased reservoir knowledge: During an underbalanced drilling operation, the produced fluids can be analyzed.
- No losses: Since there is a reduction in the hydrostatic pressure in the annulus fluid losses into a reservoir formation is reduced.

3.2.2 Advantages and Disadvantages of UBD

Advantages	Disadvantages
Increases rate of penetration	Possible wellbore stability problems
Decreases formation damage	Increases drilling costs (Based on system used)
Eliminates risk of differential sticking	Higher risk with more inherent problems
Reduces risk of lost circulation and Increases reservoir knowledge	Possible excessive borehole erosion
Improves bit life	Possible increased torque and drag

Table 2: Advantages and Disadvantages of UBD

3.3 Managed Pressure Drilling (MPD)

The Underbalanced operation and managed pressure drilling committee of the International Association of Drilling Contractors (IADC) as defined MPD as

"*An adaptive drilling process used to more precisely control the annular pressure profile throughout the well bore. The objectives are to ascertain the downhole pressure environment limits and to manage the annular hydraulics pressure profile accordingly. This may include the control of back pressure by using a closed and pressurized mud return system, downhole annular pump or other such mechanical devices. Managed pressure drilling generally will avoid flow into the well bore*"

In conventional drilling, mud returns to an open environment and as such makes it very difficult to monitor the annular pressure which presents great problems to drilling personnel. In static condition, the annular pressure is the weight of the mud or the hydrostatic head in the column while in dynamic condition annular pressure is the combination of the mud weight and annular frictional pressure as shown in the figure 11 below. Managed Pressure drilling has peculiar features to counter the limitations of having a narrow pressure window and in turn reduces the cost on non-production time (NPT).

MPD is a modified and more improved method of underbalanced drilling. According to Steve Nas (2011), as the pressure of the well is precisely controlled to prevent any formation influx into the well bore, managed pressure drilling is a primary well control. Being as it were, it is important that during drilling all the secondary well control equipment like the blow out preventer, rig choke manifolds, must be ready for operations at all times and not used for routine drilling operations. The system is a completely closed pressurized loop. A typical flow diagram for a MPD system is as shown in figure 12

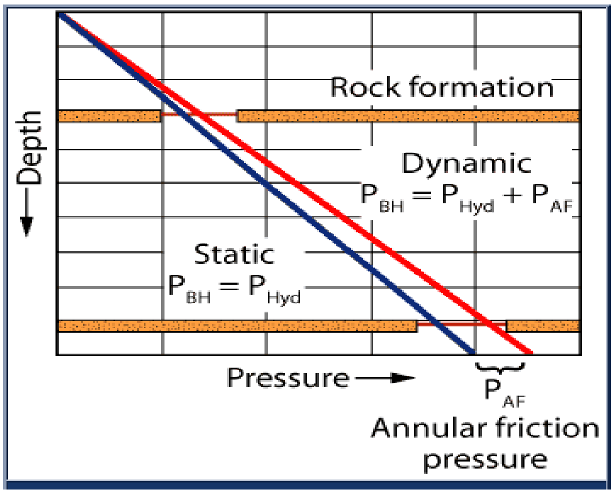

Figure 11: Static and Dynamic Pressure (World Oil, 2007)

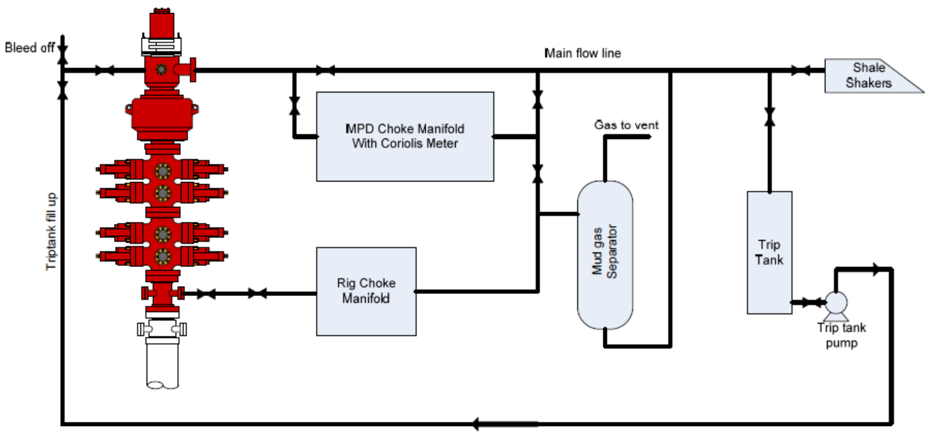

Figure 12: MPD Process Flow Diagram in a Closed Wellbore (Steve Nas, 2011)

The Underbalanced operation and managed pressure drilling committee also presented the following summarized technical paper (D. Hannegan, 2006):

"MPD processes employ a collection of tools and techniques which may mitigate the risks and costs associated with drilling wells that have narrow downhole environmental limits, by proactively managing the annular hydraulic pressure profile".

"MPD may include control of back pressure, fluid density, fluid rheology, annular fluid level, circulating friction, and the hole geometry, or combinations thereof"

"MPD may allow faster corrective action to deal with observed pressure variations. The ability to dynamically control annular pressures facilitates drilling of what might otherwise be economically unattainable prospects".

"MPD techniques may be used to avoid formation influx. Any flow incidental to the operations will be safely contained using an appropriate process".

3.3.1 Categories of MPD

The Underbalanced operation and managed pressure drilling committee of the IADC identifies that MPD can be categorized into reactive and proactive MPDs.

- **Reactive**: In the reactive MPD the well is drilled conventionally but with extra tools like the RCD, chokes or drill string float. The tools are added in case of any emergency or as a contingency plan. For example, say the mud system in the hole becomes less suitable to handle the current situation and there is a need to replace the mud system which will require so much precious time, a safer and more rapid mode of arresting the situation is possible MPD in place. The goal of installing the tools is to be able to safely and efficiently control any abnormal and unexpected downhole pressure environment that may be higher or lower than the expected fracture pressure or pore pressure respectively.
- **Proactive**: It is also known as "walk the line category" and it presents far greater benefits to drilling operations. The fluids programs, wells casing and operations are designed from the outset with a fluid systems, casing and open hole program that will take the advantage of the ability to more accurately manage the downhole pressure environment. It reduces the non-productive time and can be used in areas that were thought to be operationally and economically challenging.

3.3.2 Variations of MPD

3.3.2.1 Return Flow Control (HSE)

This is simplest in all the variations of MPD. It ensures that annular fluid returns are more safely contained than in the case of conventional drilling where the mud returns is open to the atmosphere. A closed drilling fluid return system is employed with the addition of a rotating control device (RCD) above the blowout preventer. This system totally diverts annulus flow away from rig. This variation does not however control any annular pressure and it differs from the conventional method only by the presence of the RCD.

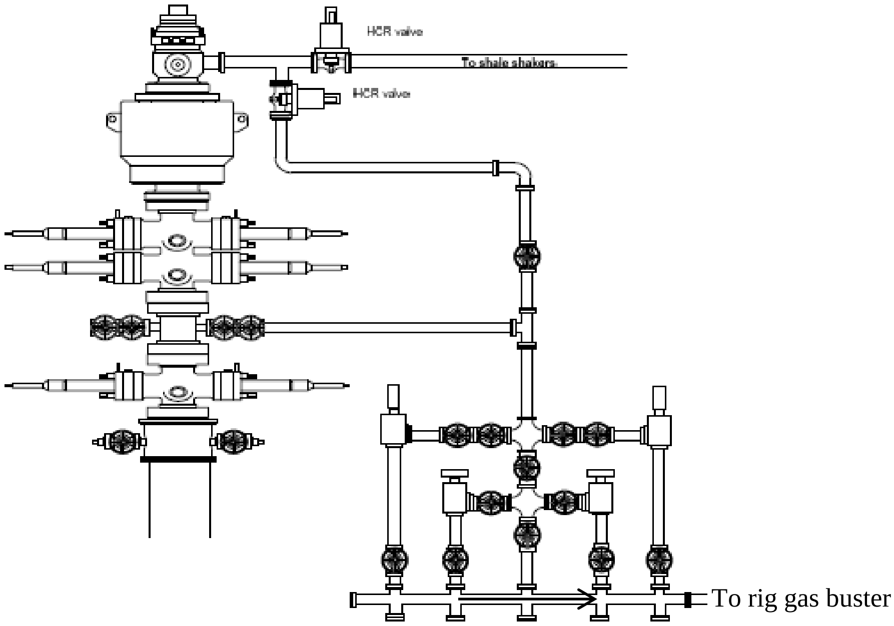

Figure 13: Return Flow Control (Steve Nas, 2009)

3.3.2.1.1 Features and Benefits of Return Flow Control

- It eliminates the risk of releasing hazardous gases to the environment by total containment of all annular returns.
- The risk of people exposure to hazardous gases is reduced and pump and dump eliminated.
- The risk of triggering facility gas alarms and associated automated shutdown systems is removed, and related production loss is avoided. (Weatherford International LTD, 2006)

3.3.2.2 Constant Bottom Hole Pressure (CBHP)

Constant bottom hole pressure is a category of MPD that allows "walking the line" between fracture pressure and pore pressure gradient. The objective is to drill in a way that the bottom hole pressure (BHP) is constant, whether during circulation of the fluid column or in static condition. During static condition, the loss of annulus flowing pressure is balanced by applied surface backpressure. A combination of an additional choke and a rotating control device (RCD) installed up above the blowout preventer facilitates this control. In effect, as shown in figure 14, the change in bottom hole pressure which is case in conventional drilling caused as a result of equivalent circulating density (ECD) is moved to surface. In short words, the drop in pressure is made up with surface annulus pressure. During drilling when the mud pumps are stopped the choke is activated and a surface back pressure is applied to maintain a constant BHP.

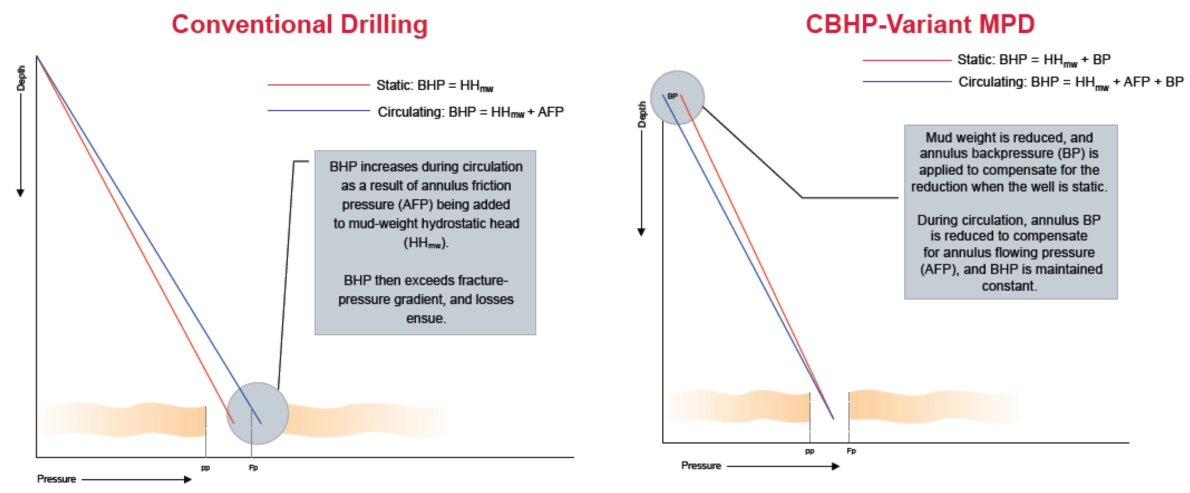

Figure 14: Comparison of CBHP MPD and Conventional drilling (Weatherford, 2010)

CBHP drilled wells, as compared to the conventionally drilled wells can be carried out with less ECD, it is less likely to exceed the formation fracture-pressure of the well and because fluid losses are not incurred the deeper hole sections can be drilled.

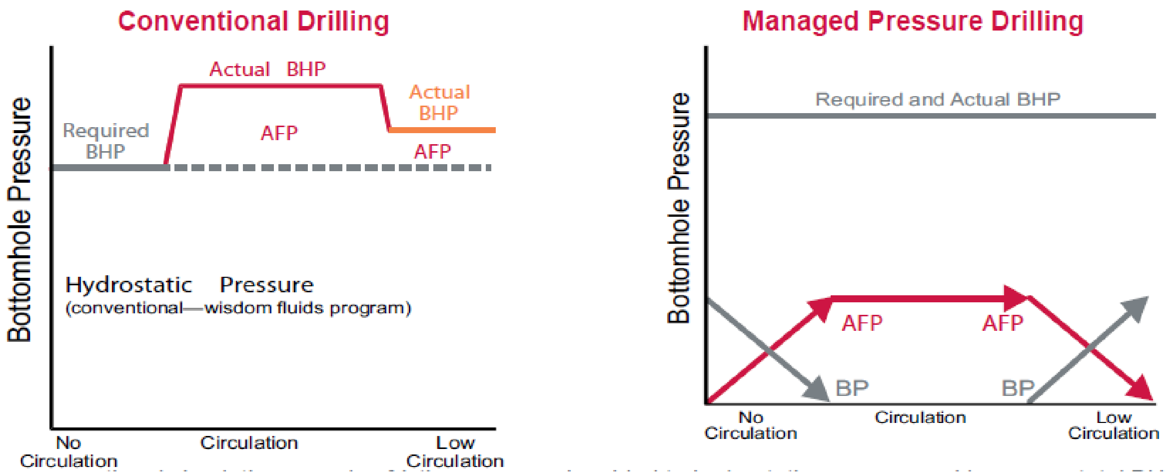

Figure 15: Constant Bottomhole Pressure (Weatherford, 2010)

Another variation to the constant bottom hole pressure is the Continuous circulation system (CCS). In this variation of CBHP the equivalent circulation density is kept by maintaining a constant interrupting circulation throughout the operation even during pipe connections and other the non-drilling operations. It is mostly used during extended reach operations where it is necessary to keep the annular frictional pressure constant so as to properly clean the well and prevent cutting from settling. Figure 16 shows the main element of a CCS. Closing the RCD seals the annulus to form a closed loop and leads the flow through the choke system. The flow is pressured by back pressure pump and by regulating the opening of the choke a required back pressure can be maintained.

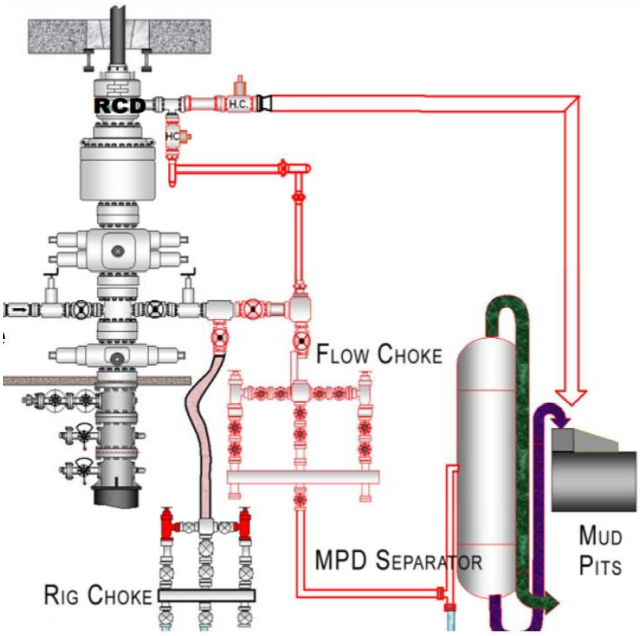

Figure 16: Main Elements of the CCS System (Hannegan, D.M., 2007)

3.3.2.2.1 Features and Benefits of CBHP

- Using a dedicated choke, changes in bottom hole pressure which normally occurs when operating the mud pumps do not occur. The annulus backpressure is controlled at surface.
- It makes it easy to maintain the BHP within a narrow pressure window since the BHP is constant whether the mud column is static or dynamic.
- Hole section can be drilled deeper because CBHP has the attributes to accurately "walk the line" between the pressure gradients.
- With the RCD controlling the applied backpressure, it allows for a proper control of the BHP keeping it constant and below the formation fracture gradient.
- By just adjusting the applied annulus backpressure the uncertainties in the estimates of pore pressure which is often the situation with high temperature/high-pressure (HTHP) well drilling and complex environments like the pre-salt can be easily accommodated.

3.3.2.3 Dual Gradient Drilling

International Association of Drilling Contractors (IADC) defines dual gradient drilling as

"*a variation of managed pressure drilling that uses two or more pressure gradients within selected sections to manage the well pressure profile*."

This variation of MPD is best suited for deep water drilling where large marine riser results in large mud weight. In a conventional drilling operation, the entire volume of the marine riser is filled with the drilling fluid that exerts pressure on the well. This method inadvertently affects the design of the casings and creates many downhole problems. In dual-gradient drilling however, the marine riser is filled with a lighter fluid say sea water. In simple word, drilling of the wellbore is carried out with two or more different annulus fluid gradients. The operating window and environment determines how this is accomplished. Dual gradient MPD results in lesser downhole pressure upon the well and improves safety.

Some of the techniques use to achieve a dual gradient MPD include continuous pumping of fluid returns through another duct external to the seawater-filled riser from the seafloor. Another one is injecting through the marine riser a lower-density fluid, say water or air/gas. The objective in all these cases is to be able to adjust the bottomhole pressure (BHP) within the predetermined window without changing the weight of the base drilling mud. For example, the pumps for an artificial mud lift system are installed on the seabed. The mud return is directed to these pumps which pumps it through a separate line to the rig. Therefore, two fluid systems are used: the sea-water fluid system in the marine riser and the base drilling fluid in the well. Figure 18 below shows the component of a detachable artificial mud lift system, another duct is used for mud return.

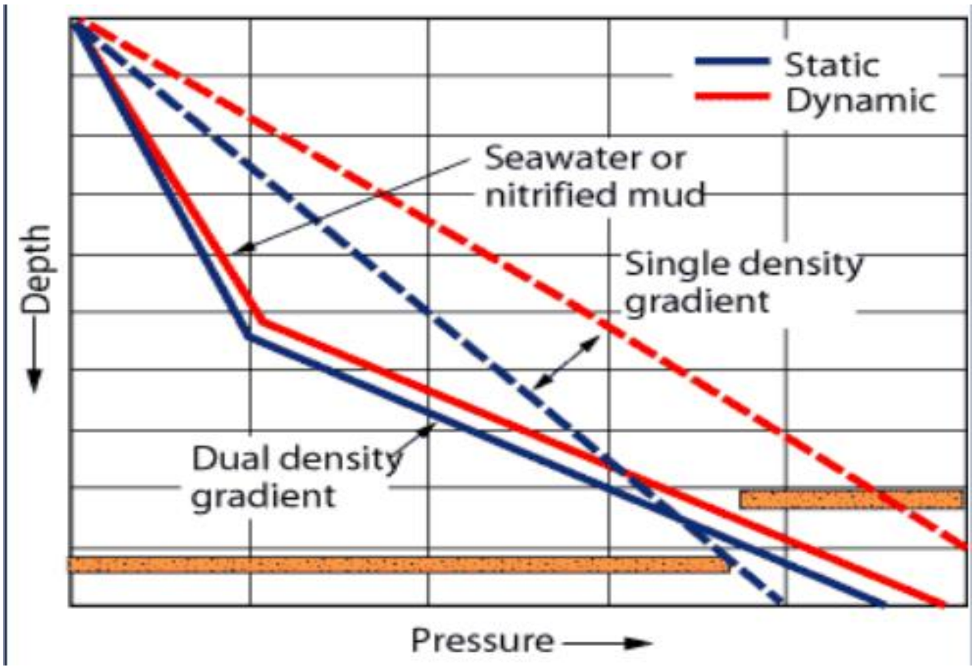

Figure 17: Dual Gradient MPD with Two Density Gradients (World Oil, 2007)

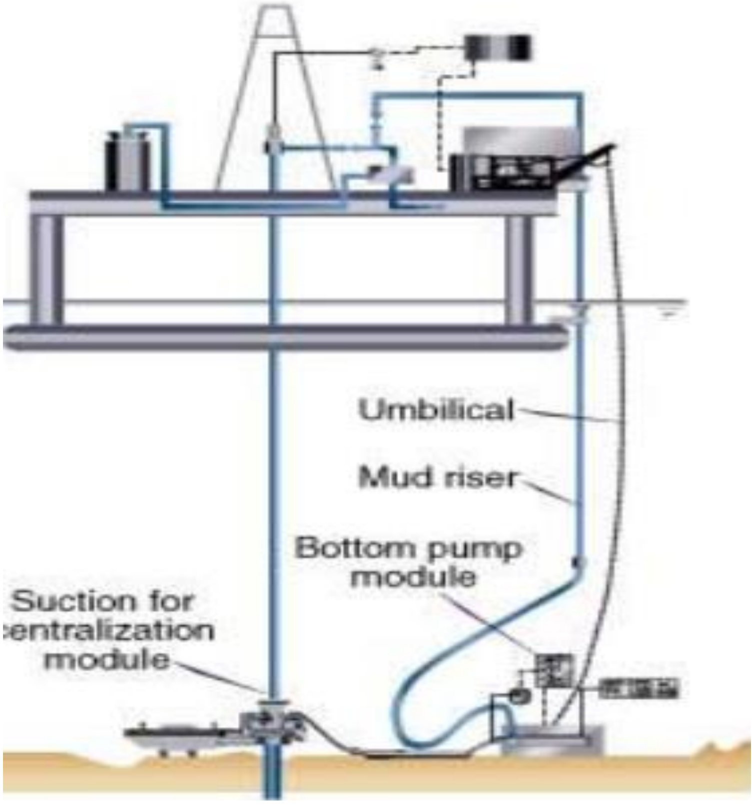

Figure 18: Detachable Artificial Mud Lift System (Offshore, 2012)

3.3.2.3.1 Features and Benefits of Dual Gradient MPD

- Dual gradient drilling eliminates non-productive time that is otherwise used to perform a mud-density change. It makes it possible to be able to adjust the effective bottom hole pressure or the equivalent mud weight.
- From a hydraulic point of view, drilling in deep water using dual gradient effectively moves the rig nearer to the mud line.
- The dual gradient variation is most often known to have some challenges in deep water drilling from floating vessel; however, it is more applicable in drilling on land or deep wells in shallow water.
- Dual gradient MPD can be easily integrated with other MPD techniques, for example, constant bottomhole pressure (CBHP), Pressurized mud cap drilling (PMCD), etc.

3.3.2.4 Pressurized Mud Cap Drilling (PMCD)

Whenever a reservoir could result in a severe circulation loss, for instance, depleted reservoirs with lower reservoir pressures as a result of production from neighboring wells or when wellbore pressure is significantly higher than the reservoir pressure, pressurized mud cap drilling technique (PMCD) is used. When circulation is lost, there would be a decrease in the hydrostatic pressure of the wellbore which takes the wellbore pressure way below the reservoir pressure. At this point, gas begins to flow into the wellbore. To keep the gas influx from reaching the rig floor a heavier mud is pumped in the annulus. This is what PMCD is.

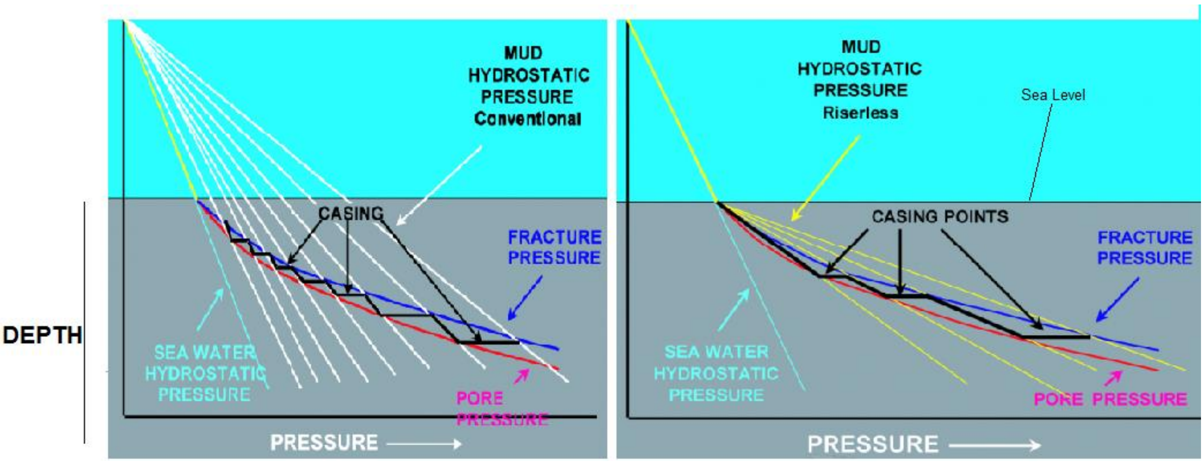

Figure 19: Borehole Gradient in Dual Gradient MPD allows Significantly Longer Open Hole (SPE International)

Figure 19 shows the pressure profile of PMCD. A lighter fluid is used to drill section while the heavier fluid at the top forces all returns into the depleted zone to keep the well under control at all times. The advantage of the PMCD method ranges from increased the rate of penetration (ROP), rig protection but at a severe loss of the formation and less cost of lighter drilling fluid. Another additional advantage with the use of lighter fluid is underbalanced drilling which results in less damage to the reservoir.

Another concept to the mud cap family similar to PMCD is the controlled mud cap system (CMC). In this variation the mud cap level is adjusted by a mud pump in the quest to better manage the bottom hole pressure.

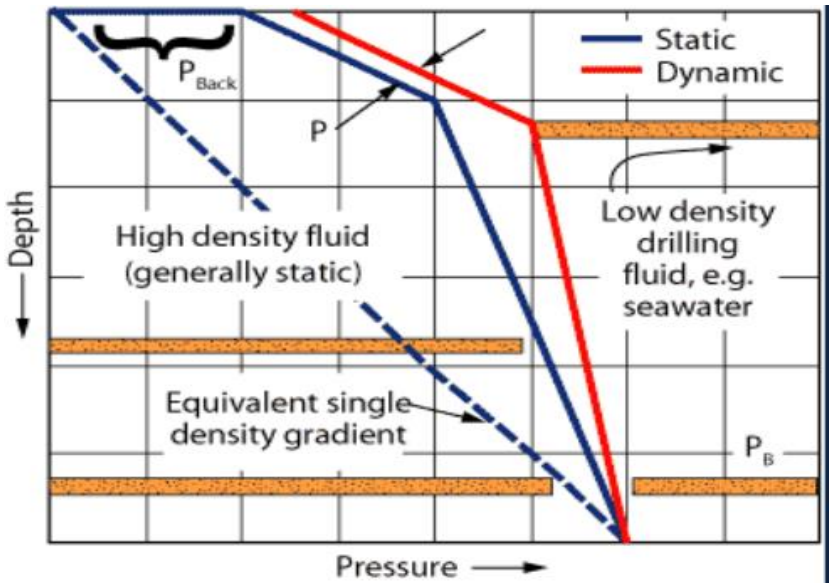

Figure 20: Mud Cap MPD (Kenneth P.M., 2007)

Figure 21 below shows the setup of a CMC system for deep water well. A subsea mud-lift-pump is connected to the mud pits by a return line and to the riser. All through the marine riser, pressure sensors are located so that the level of the mud in the riser can be determined. To manage the BHP and compensate for ECD the marine riser from the mud cap is filled with air.

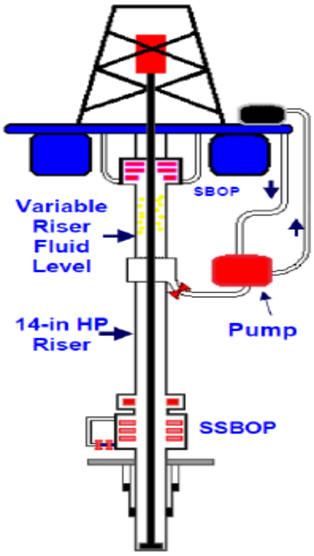

Figure 21: Controlled Mud Cap System Set-up (Rohani M. R., 2011)

3.3.3 Issues with MPD Methods

A paper Presented in 2010 at SPE/IADC Drilling Conference and Exhibition held in Amsterdam, Netherlands by Steve Nas et al on Offshore Managed Pressure Drilling Experiences in Asian Pacific says that rig modification requirements for MPD operations is minimal and the operation have been done with minimal down time. Other advantages of MPD includes good hole cleaning, limiting circulation loss, general reduction in NPT and well bore instability, increased penetration rate, and other numerous merits.

Having mentioned this, the following are the issues concerning the application of MPD:

- High initial cost of project.
- Needs for personnel training
- MPD operation is a complex operation. (Philip Frink, 2006).
- Unavailability of a suitable reference documents (Ian C. Coker, 2004).

Figure 22: Merits of MPD (Hannegan, D.M. 2007)

3.3.4 MPD Tools

Hannegan, D.M. in his SPE distinguished lecturer series on “Managed Pressure Drilling: A new way of looking at drilling hydraulics… Overcoming conventional drilling challenges”, identified some essential MPD tools, they are:

- Floating rigs Rotating Control Device (RCD)
  - External Riser RCD
  - Subsea RCD
  - Internal Riser RCD (IRRCH)
- Fixed rigs RCD (no wave heave)
  - Passive & Active annular seal design “land” models
  - Marine Diverter Converter RCD
  - Bell Nipple Insert RCD
  - Internal Riser Rotating Control Head (IRRCH)
- Non Return Valves
- MPD Choke
  - Manual
  - Semi-automatic
  - PC Controlled Automatic

Other tools include:

- Downhole Casing Isolation Valve (Downhole Deployment Valve)
- Nitrogen Production Unit
- ECD Reduction Tool
- Real time Pressure & Flow Rate Monitoring
- Continuous “Valve” or “System”

3.3.4.1 Rotating Control Device (RCD)

The rotating control device (RCD) is first barrier against the flow of well fluids during drilling operations into areas they are unwanted and as such, it is a key well control tool. By far, it is the most important and most common of all the tools of MPD. RCD has many important functions, amongst which are maintaining tight pressure barrier in the annulus section, allowing diversion of flow through choke to surface handling equipment and lastly and most importantly, allowing drill pipe to be rotated when performing other operation. Figure 23 shows the position of a RCD in a subsea stack assembly.

RCD usage started 1930’s where it was used to divert flow of air (Bill Rehm et al). Modern technology of the device consists of an advance sealing element that seals around drill string and provides additional vertical movement allowance for the pipe. The secondary housing houses the sealing sleeve that permits unrestricted movements of pipe and at the same time maintains seals (Paco Vieira et al, 2009). The RCD system can be divided into the passive system and active system.

The passive system makes use of the prevailing well pressure for actuating the sealing elements. It comprises of rotating packer which has an under size annular seal to drill pipe it is therefore forced-fitted onto the pipe. As the sealing element is exposed directly to well pressure any increment in the well pressure is exerted on sealing rubbers. On the other hand, the active system has its sealing mechanism actuated by a hydraulic pressure operated from rig floor. This system of RCD utilizes a pressurized diaphragm that works by squeezing a packer element against the pipe.

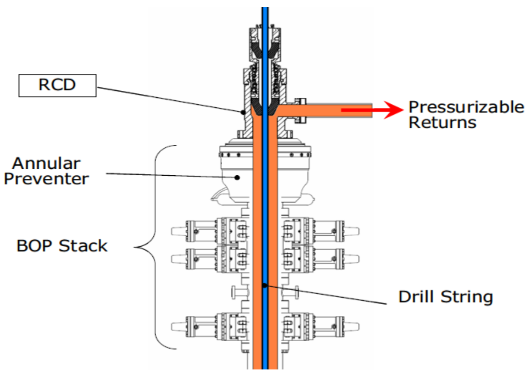

Figure 23: Typical Alignment of RCD (Paco Vieira et al, 2009)

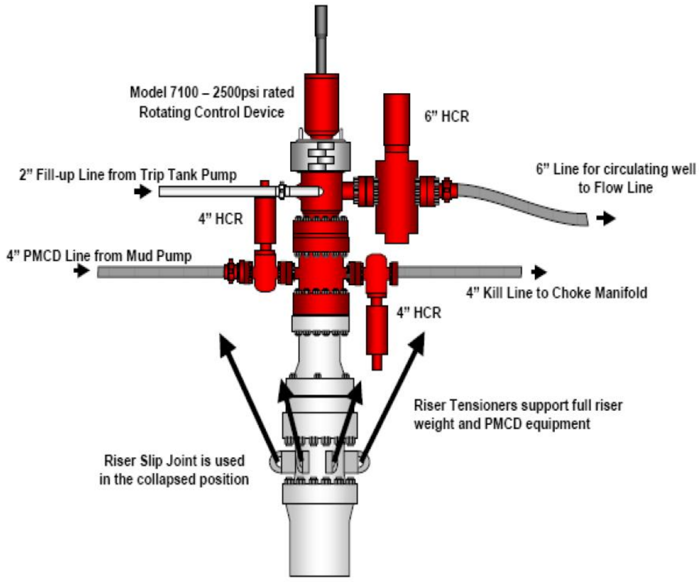

Figure 24: External Riser RCD on a Riser Cap (Chustz M.J. et al, 2008)

3.3.4.2 Non Return Valve (NRV)

Drill-pipe non return valve is essential tool in MPD to control the U-tube effects in drilling operations. The U-tube effect is present whenever a dual gradient MPD is used in drilling operation or the operation is carried out with a low riser return system (LRRS). What initiates the U-tube effect in LRRS is the shutting down of the surface pump and in the case of dual gradient MPD it is as a result of difference in the density of the drilling mud and the pressure at the inlet of the pump at the seafloor which is close to the hydrostatic pressure of seawater. In order to balance the pressure differentials between the annulus and the drill string, there would be a drop in the level of the mud in the string until the pressure in the annulus is equal to the pressure in the drill string.

Figure 25 below shows a pipe non return valves and the section through it. It can also be called a one way valve because it only allows flow in one desired direction. Different types of NRV are currently in the market today, examples are: Hydrostatic Control Valve, Basic Piston-Type Float, Retrievable NRV (Bill Rehm et al).

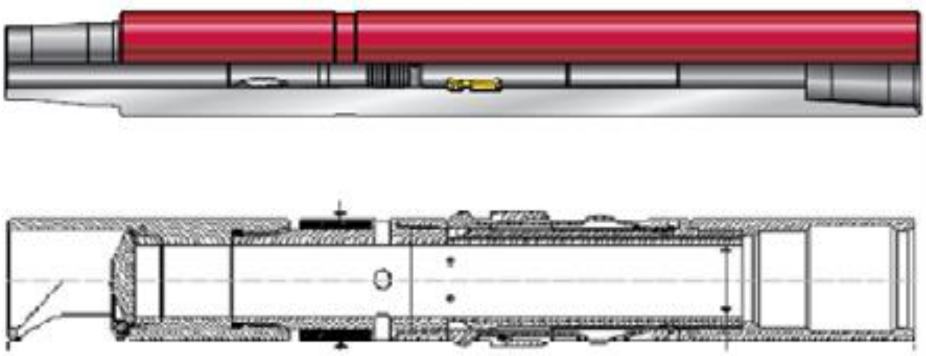

Figure 25: Pipe Non Return Valves (Weatherford, 2010)

3.3.4.3 MPD Choke Manifold

Chokes valves are key tools in MPD application to precisely control the flow. It is extensively used during CBHP operations in the return line so that back pressure can be applied during the drilling. They are classified according to their closure system, namely: choke gates, sliding plates and shuttles. The ability to energize the choke by pumping across the wellhead is incorporated so that surface pressure can be applied to the choke. A separate MPD choke manifold should be installed and used whenever possible so as ensure that secondary barrier equipment is not used for routine drilling (Nas, S., 2009). There are three choke options in the applications of MPD; manual choke, semi-automatic choke and PC controlled automatic choke.

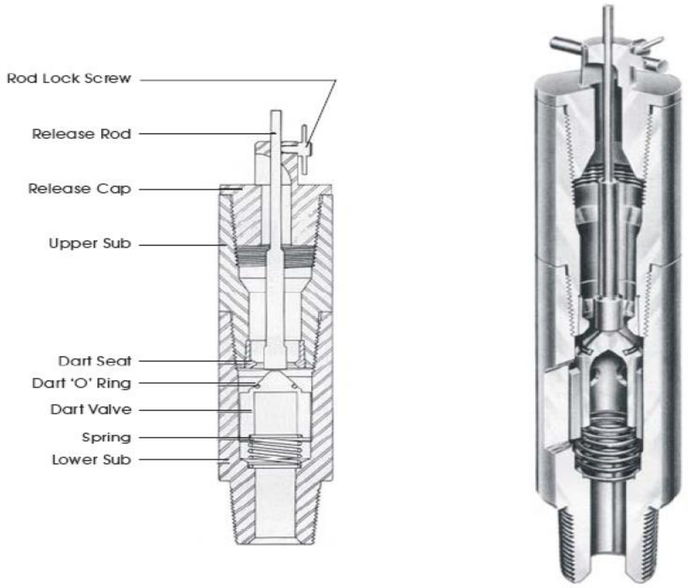

Figure 26: Inside BOP Pump-Down Check Valve (Erdem Tercan, 2010)

In conventional drilling chokes are used as secondary well barrier equipment, this is not the case with MPD operations. Bearing in mind that in MPD operation, flow of fluid is not allowed to the surface, therefore MPD chokes are more employed for pressure control than for flow control. Depending upon its operation it is classified as: manual choke, semi-automatic and automatic. Figure 27 below shows schematics of a semi-automatic when fully open and fully closed.

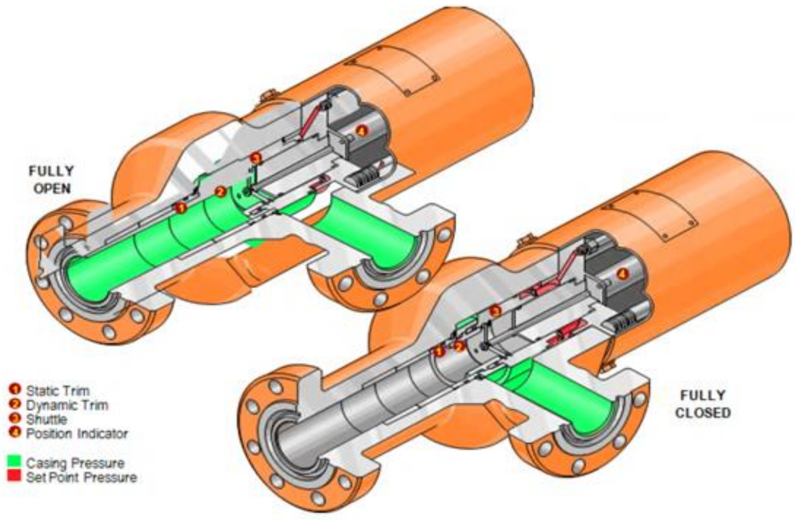

Figure 27: Semi-Automatic Choke (Arnone, M., 2010)

3.3.4.4 Coriolis Flowmeter

In most automated pressure control system there may be need to also take supplementary measurements, the Coriolis Flowmeter is an important tool in MPD operations to measure data even with the automated pressure control systems. The principle measurement is based on the control of Coriolis force generation. The Coriolis force is an apparent force that deflects moving objects to the left in the southern hemisphere and to the right in the northern hemisphere and as a result of the earth's rotation. It is possible to measure the mass flow rate and the density of the fluid. The fluid density can be accurately determined directly with great precision by measuring the time it takes to complete one oscillation in wave period (Malloy, K.P. et al, 2008). The change in fluid density can be sensed in a split second since the oscillation happens in the range of tens of thousands per second.

Figure 28 below shows the working schemes of a Coriolis Flowmeter.

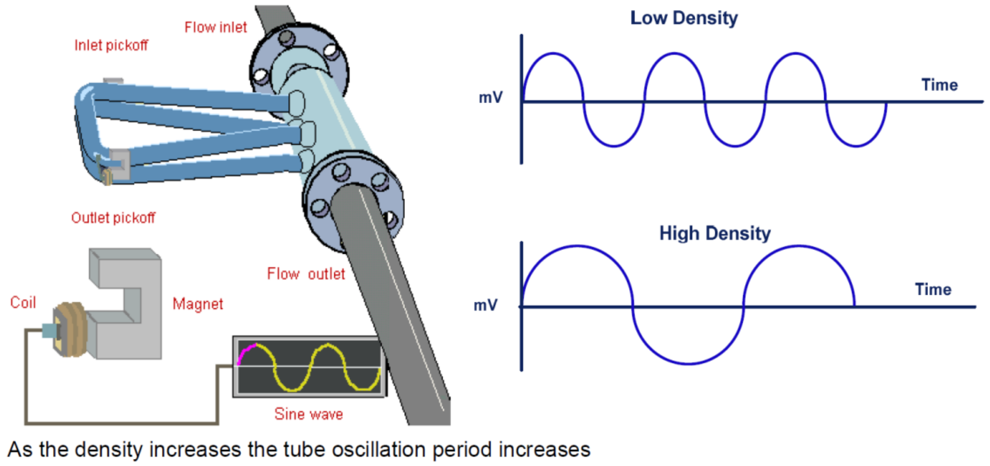

Figure 28: Coriolis Flowmeter Working Schemes (Malloy, K.P., 2008)

3.4 Riserless Drilling

Some years ago when offshore oil development was in its early stage and operations were carried out in shallow waters, the challenges of water depth increase were tackled by simply increasing the size of subsea wellhead and marine riser. However, it is not visible to extend current technologies using the large diameter marine riser to drill beyond 10,000 feet water depth (Reelwell, 2012). As the industry moves into deep and ultra-deep waters in environments that present high technical and economic risks, the drill rig size has tripled in the past 50 years with corresponding increase in cost. The oil and gas industry requires attractive and cost effective alternatives for exploration without undermining the environment. Even if the huge discoveries in the deep and ultra-deep water environments justifies the huge investments necessary for exploration in the area we still cannot push the application of the marine riser further than its present use. Many methods have be developed to reduce the weight from the marine riser amongst which were reducing the effective density of mud in the marine riser by using hollow glass, reducing the effective density of mud in the marine riser by injecting gas at the BOP level and lots more but none of these techniques has resulted into the needed improvement in the industry. Another method that totally eliminates the use of marine riser has been introduced to the industry. This method is called Riserless Drilling (RD).

Riserless drilling concept is a managed pressure drilling (MPD) method without the use of a marine riser. It simultaneously solves the two major challenges in deep and ultra-deep operations:

1. The issues of narrow window between the formation pressure and the pore pressure are taken care of by isolating the system from the environment using the MPD method.
2. The limitation in the use of the marine riser is taken care of by totally eliminating the riser.

The riserless method basically requires a small diameter pipe for mud return instead of the marine riser, a blowout preventer (BOP) for well control, a rotary control device (RCD) - an annular barrier for pressure containment, a umbilical riser to maintain communication with the well, and an option for a pump to enhance flow and reduce pressure head in the well.

There are speculations that riserless drilling method may be the concept that probably eliminates all the issues concerning conventional drilling today but being a new technology, it has not yet been tested for a long period and as such the conventional method is still the most trusted and widely used drilling method.

3.4.1 Advantages of Riserless Drilling

- **Better well control**: Better hazard detection and accurate response results in less risk to well as a whole and also provide low risk of environmental hazards.
- **Fewer Casing strings**: Riserless drilling allows driller to reduce the additional hydrostatic pressure head from the drilling mud in the riser which results in a wider drilling window,

resulting into extending the casing setting depth and invariably fewer strings to complete the well.

- **More Completion Opportunities**: Provides opportunities for better well completion because of its simple well designs.
- **Improve well integrity**: As a result of better completion jobs the overall well integrity will improve.
- **Better Station Keeping**: The hydrodynamic effects on the vessel are exacerbated as a result of the size and weight of the marine riser, because this weight is drastically reduced, station keeping in riserless drilling is easier.
- **Utilization of older generation rigs**: Because the weight and space requirement has been reduced a 3rd or 4th generation rigs can be used for riserless operations.
- **Reduced Drilling Cost**: With the aforementioned points, riserless drilling method is more economical in comparison to the conventional method of drilling

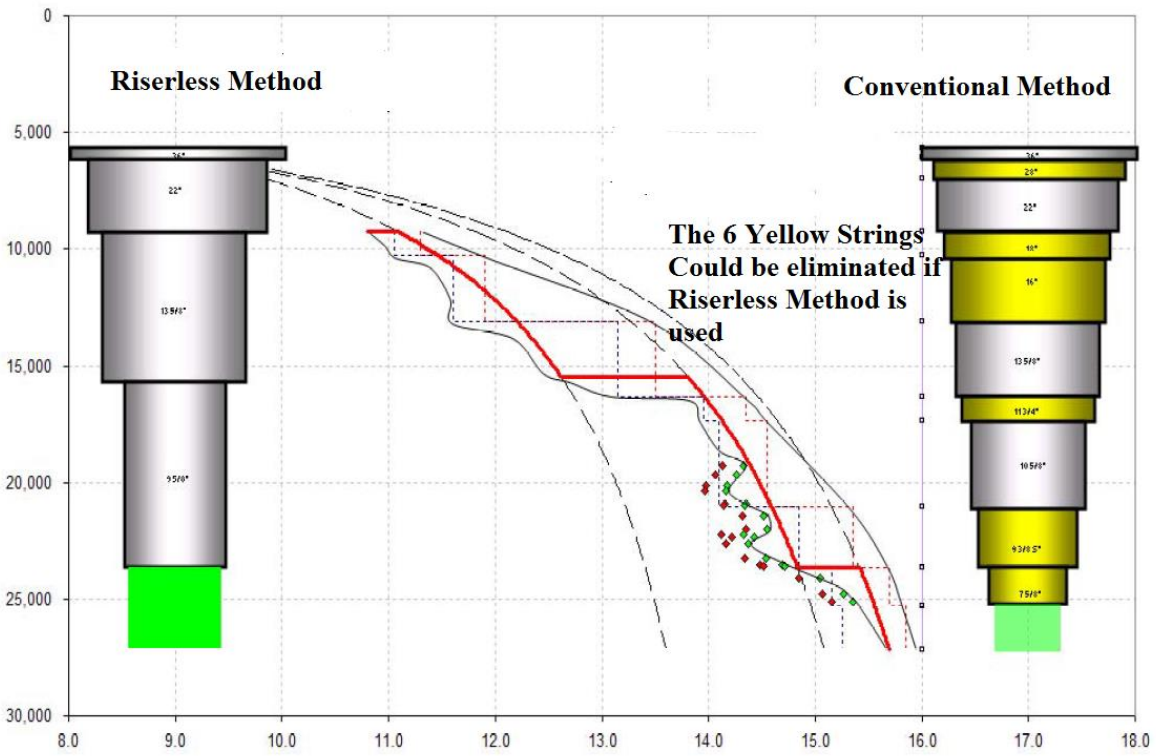

Figure 29: Riserless Method Eliminates Casing Strings (Ken Smith, 2009)

3.4.2 Concepts in Riserless Drilling

3.4.2.1 Riserless Mud Recovery (RMR)

One major problem with deep well drilling in deep and ultra-deep waters is how to manage and control the circulation and recirculation of drilling mud. The drilling mud serves the functions of cooling down the drilling process, serving as a barrier element, flushing rock cuttings out from the well and general cleaning of the hole. Commonly, top-holes in deep-water wells are drilled before the riser is installed (riserless) with the process of pump and dump which disperses the rock cuttings and mud on the seabed. Apart from the economic consequences it is also not environmental friendly.

RMR is a riserless mud recovery system that enables re-use of the drilling mud. Figure 30 shows a RMR system where drilling mud pumped through the drill pipe comes out through the drill bit, returns to the sea surface outside of the drill pipe and is thereafter captured and pumped to the surface. The pumping process is made possible by the installed subsea pump located as shown.

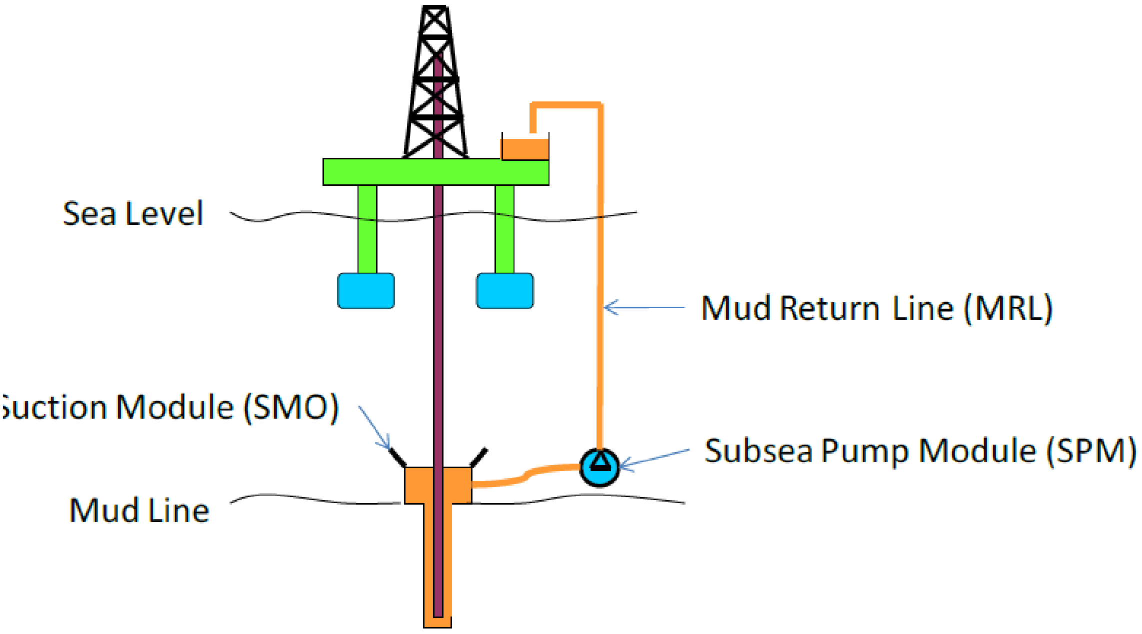

Figure 30: Shallow Water RMR System (Dave Smith et al, 2010)

A joint industry group comprising Norwegian Research Council's DEMO 2000 program, AGR Subsea, Shell, BP America and supported by PETRONAS undertook a work to advance the shallow water RMR technology to function in deep water environment. Figure 31 below shows the configuration of a typical deep water RDM system.

Advantages of RMR (Stave R., et al, 2005)

- *Improved hole stability and reduced washouts due to possibility to use inhibited and weighted mud.*
- *Use of weighted mud improves well control both with regard to shallow gas and shallow water flows vs. using seawater and gel sweeps.*
- *Improved gas detection, accurate flow checks and mud volume control.*
- *Separation of drill cuttings prevents accumulation on subsea templates and prevents dispersion in areas with special environmental restrictions.*

- *Sometimes possible to increase depth of the surface casing. Hence, possibility for reducing hole and casing sizes and number of casings required.*

Disadvantages of RMR (BG Brazil, 2012)

- *It is difficult to scale up subsea pumps.*
- *It requires casing to be suspended to act as return line.*
- *Requires rotating head.*
- *Failure of pump can lead to losses.*
- *Complicated well control procedures.*

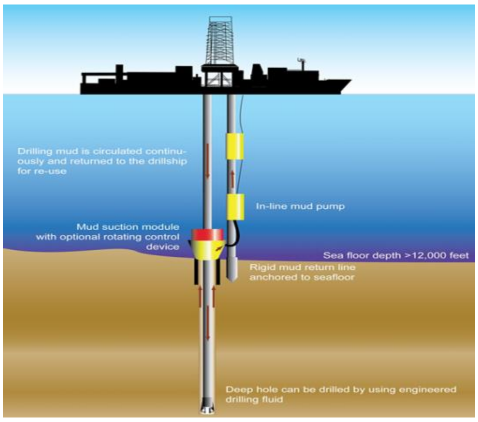

Figure 31: Deep Water RMR (Putra R., 2009)

3.4.2.2 E-Duct Return - Managed Pressure Drilling (EDR-MPD)

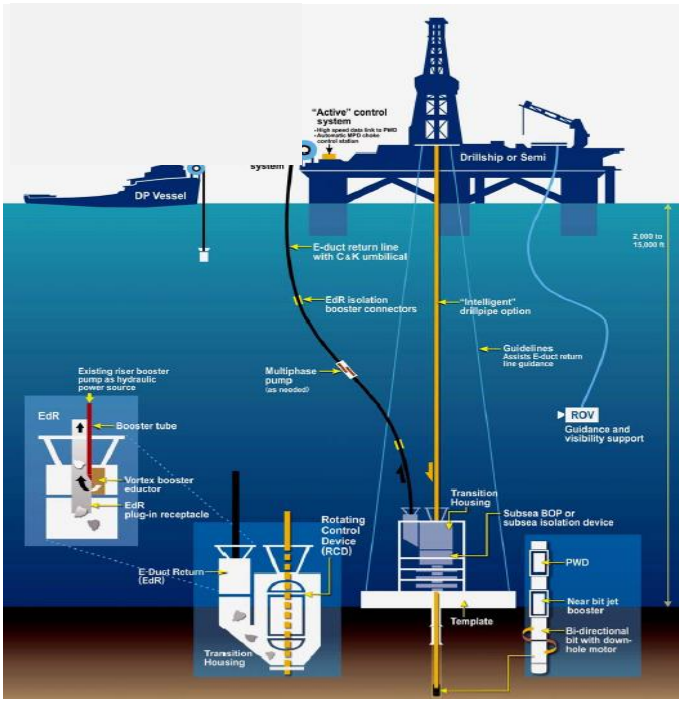

Figure 32: Riserless EDR-MP (Carter G., et al, 2005)

The EDR-MP system consists primarily of an active control station on the MODU, an E-ductor return line, a subsea RCD and an in-line Multi-phase pump. Modifications of the subsea BOP and installation of an additional subsea well control housing unit is necessary to enable the E-duct line function as the return line while operation is carried out without a drilling riser. Also, to pump the return circulating mud with cuttings, an in-line multiphase pump or an existing booster pump on the rig is installed.
The figure 32 is schematic diagram of the entire system. The transition housing houses the rotating control through which the return drilling mud is diverted.

Advantages of EDR-MPD (Carter G., et al, 2005)

- *Mitigates Riser Fatigue and Joint Leaks.*
- *Enables Reverse Circulation.*
- *Increases Riser Angle Limits.*
- *Minimizes VIV Issues*
- *Greater Degree of Vessel Drifting.*
- *Quicker Emergency Break-Away.*
- *Potential Elimination of "Pump and Dump".*
- *Cost Savings: Mitigates Capital Costs of Riser Pipe; Eliminates Riser Tensioning & maintenance; Reduced Installation Time; Less Mud Volumes to Fill Riser; Lower Inspection & Handling Costs; and Selection of Lower Cost Drilling Vessels.*

Disadvantages of EDR-MPD (BG Brazil, 2012)

- *Subsea pumps difficult to scale up.*
- *Requires casing to be suspended / hung-off to act as return line.*
- *Requires rotating head.*
- *Casing running presents complexities: Circulating while running casing. Running & landing hanger.*
- *If dual gradient: Failure of pump can lead to losses: Complicated well control procedures.*

3.4.2.3 Reelwell Drilling Method-Riserless (RDM-R)

Just like other riserless drilling method the RDM transfers the circulation mud and the cuttings to the surface, but in this case, in an unconventional manner. As shown in figure 33 below, a specially designed internal pipe is hanged in the drill pipe leaving the assembly a concentric drill string system.
In this new system, the inner pipe takes the role of the low pressure marine riser. The only difference between them is that the inner pipe is a high pressure pipe and can therefore be used to realize a pressured fluid system for performing a managed or controlled pressure drilling. The circulation returns flow to the surface through the inner pipe eliminating totally the need for any type and size of the marine riser. Eliminating the marine riser means that all riser handling tools, corresponding

accessories and other requirements that are found on the drilling vessel as a result of the use of the riser are uninvolved.

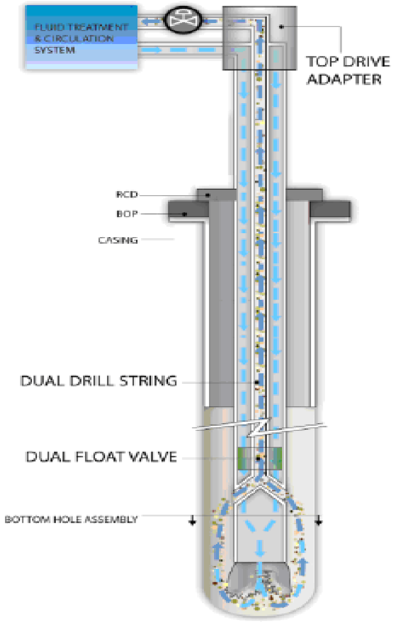

Figure 33: RDM-R Configuration (Rajabi, M.M. et al, 2010)

In deep and ultra-deep water conventional riser drilling, a colossal rig system, say 5th or 6th generations rig is required in order to accommodate the large size and heavy weighted marine riser. In addition, enough tension must be applied on the riser, therefore, need for a good tensioning system is required which may be too expensive or unavailable. The RDM-R could be operated on a 3rd or 4th generation rigs to drill in deep and ultra-deep environments with much less technical limitations and difficulties. Rajabi, M.M. et al says that "*Riserless RDM can be deployed in water depths of 12.000 ft or even deeper by floating drilling vessels that are currently used for conventional riser drilling in water depths shallower than 4.000 ft of water depth. If the rig is to be a conversion, not much modification is required on it. Almost all current floating drilling vessels may be a candidate for conversion in order for riserless Reelwell drilling in deep-water*". The advantage of the RDM-R to be able to drill in deep-water with smaller rigs is very important for the industry as it eliminates one of the present limitations in the use of limited fleets of 5th and 6th generation of drilling vessels whose costs are considerably higher than older fleets of drilling vessels.

Advantages of RDM-R (Rajabi, M.M. et al, 2010)

- *Cost saving: Riserless drilling in ultra-deep water with smaller rigs (lower day rates).*
- *Extension of water depth capability: Riserless RDM enables drilling at any water depth even beyond 12000 ft as the main limiting component (marine drilling riser) is eliminated.*
- *Wait-On-Weather time reduction: Wider operational radius due to relaxed station keeping.*

- *Non-productive time reduction: Many downhole drilling hazards in offshore drilling are addressed by RDM as it proves to be a reliable tool for MPD.*
- *Improved primary well control: Any small amount of kick is immediately detected and controlled by the dynamic return pressure and flow control system on the surface.*

Disadvantages of RDM-R (BG Brazil, 2012)

- *Lots of new components required.*
- *Requires rotating head.*
- *Unconventional Well Control procedures.*
- *Might require Casing isolation valve when pulling BHA.*
- *Casing running presents complexities*

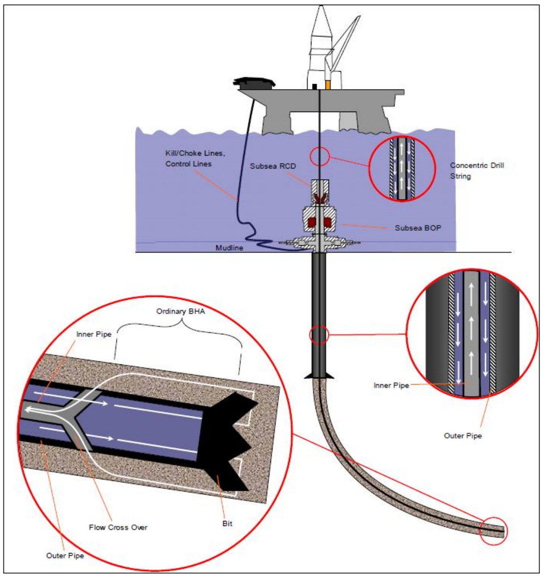

Figure 34: RDM-R from a Drill Vessel (Rajabi, M.M. et al, 2010)

In the present stage of development of the RDM-R method, the following are some of the issues that are been faced:

- System configuration and design:
  - BOP design.
  - Utility riser configuration.
  - Subsurface pump design and configuration.
  - Drill pipe design and configuration.
- Well control
- Hydrodynamics
  - Extreme severe stresses resulting from weight of the pipe and circulating fluid.
  - Effects of surface and sub-surface currents, waves, and winds.
  - Effects of the movements of the vessel.
  - Vortex induced vibration (VIV).

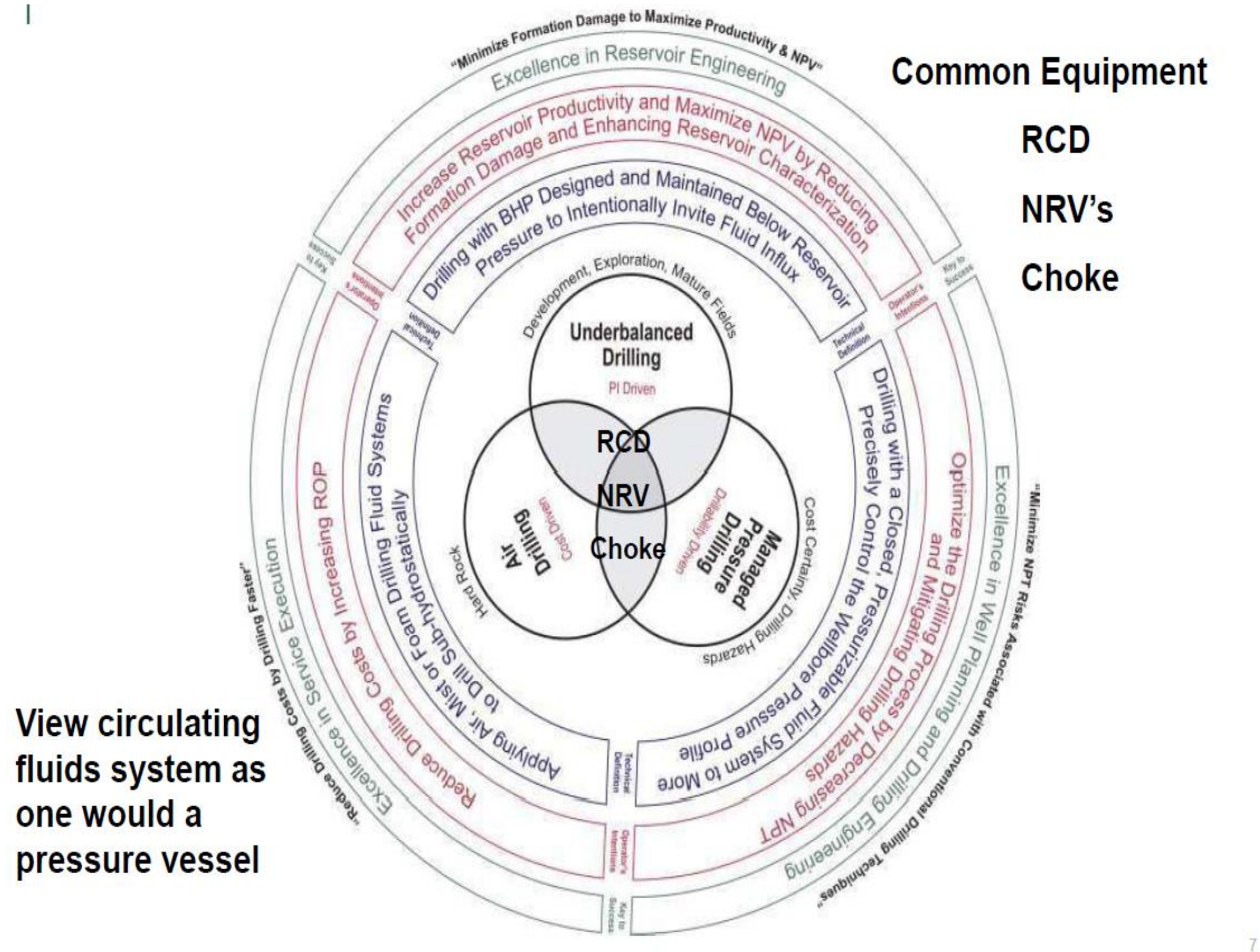

Figure 35: Emerging Drilling Technology (Hannegan, D.M., 2007).

Chapter 4 Hydrodynamics

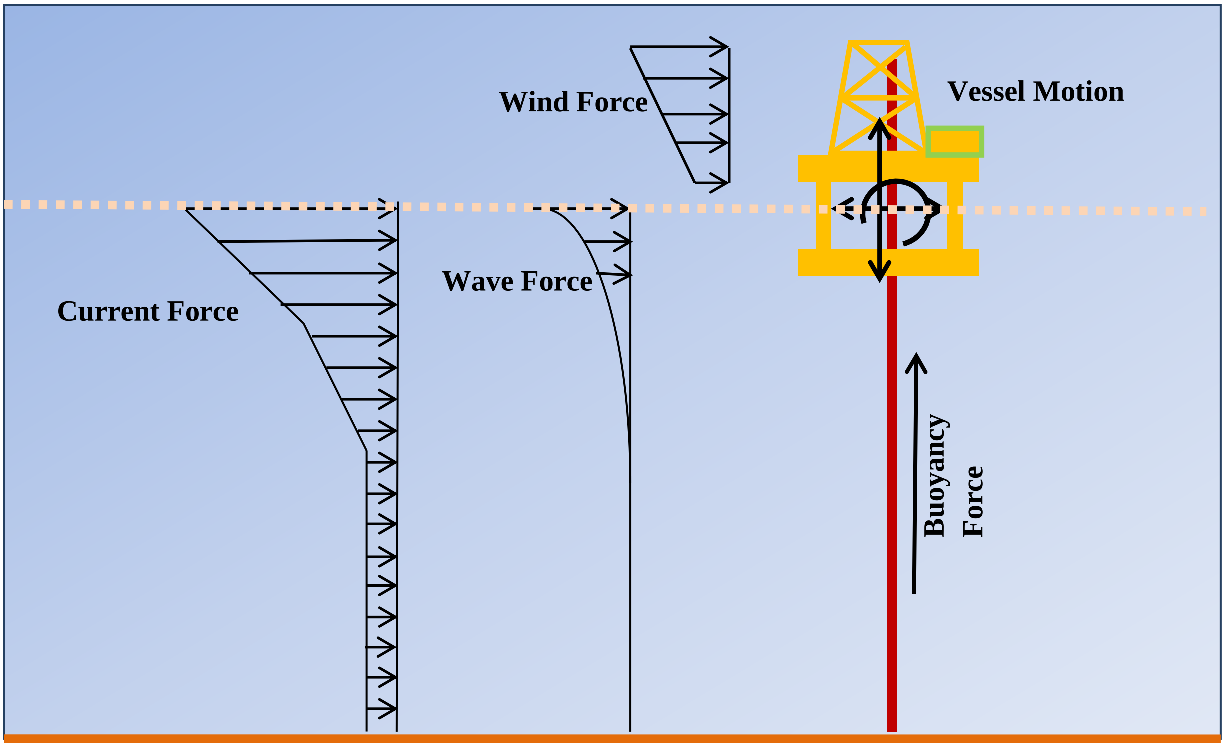

Figure 36: Force on the Drill Pipe

4.1 Vessel Motion

The vessel has 6 degrees of freedom:

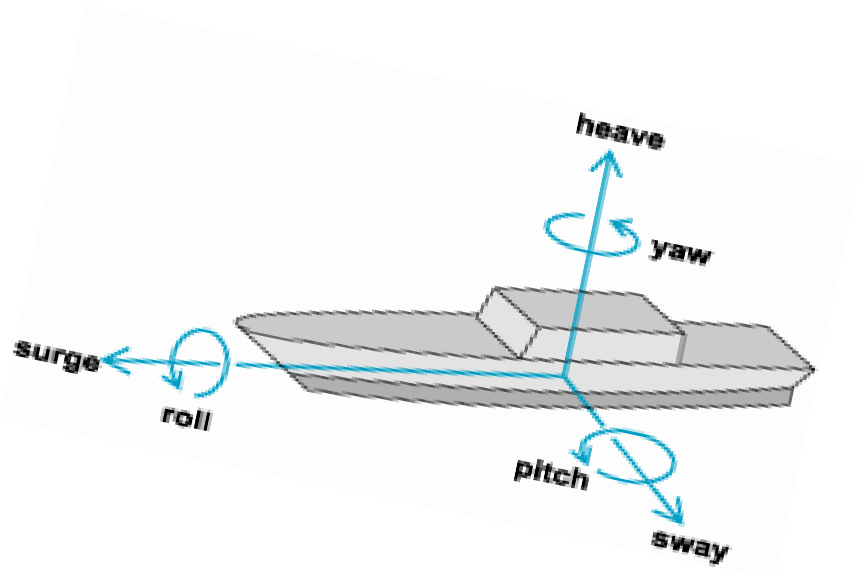

Figure 37: Motions of a FPSO (Gudmestad, O.T, 2012)

- Pitch Motion: Rotation about the transverse axis
- Roll Motion: Combination of translational and rotational motions about a longitudinal axis (an axis that runs from front to back)
- Heave Motion: Vertical translational motion along the spinal axis.
- Yaw Motion: Rotational motion to the left or right of its direction of motion.

- Surge Motion: Horizontal translational motion.
- Sway Motion: sideways motion.

Motion	Translational	Rotational	Simple harmonic
Pitch		√	√
Row		√	√
Heave	√		√
Yaw		√	
Surge	√		
Sway	√		

Table 3: Vessel Motions

4.2 Wave Forces

Wave spectrum gives wave energy as a function of wave frequency in a short term wave condition, typically a three hour storm. This energy may vary with wave direction and can incorporate spreading.

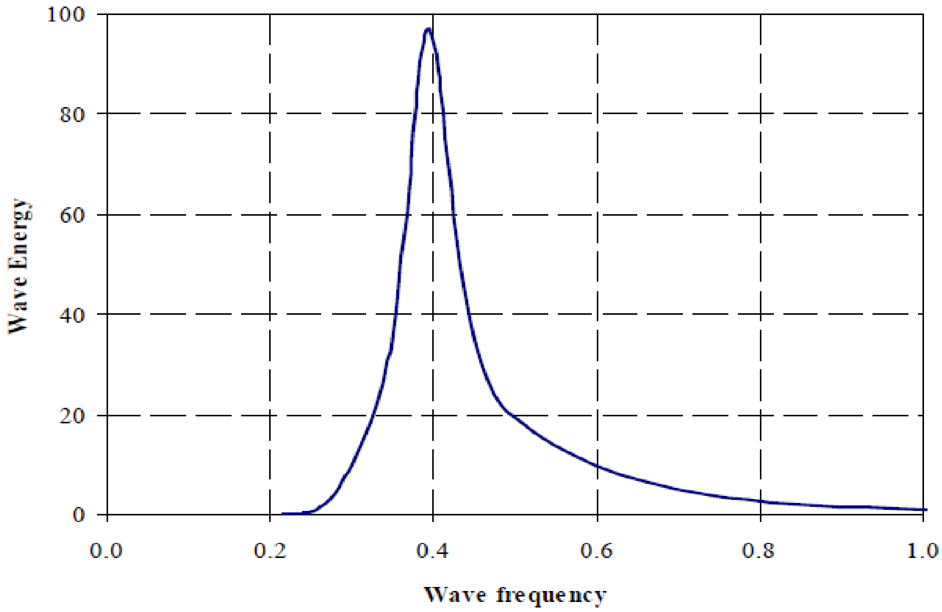

Figure 38: Wave Spectrum (Gudmestad, 2012)

Wave spectra used to represent waves characteristics found in offshore locations include the JONSWAP model, the Bretschneider or ITTC two parameter spectrums, the Ochi-Hubble spectrum model and the Pierson-Moskowitz model. In areas where the fetch length is limited, the JONSWAP (Joint North Sea Wave Project) spectrum is often used to describe the sea state. The equation for the spectrum is given as:

$$S(\omega) = \alpha g^2 \omega^{-5} exp\left(-1.25\left(\frac{\omega}{\omega_p}\right)^{-4}\right).\gamma^{\left(\frac{-(\omega-\omega_p)^2}{2\sigma^2\omega_p^2}\right)}$$

Where:

H_s = Significant Wave Height (It is approximately the average of the 1/3 largest waves).

ω = Angular wave frequency = $\frac{2\pi}{T_\omega}$

ω_p = Angular spectral peak frequency = $\frac{2\pi}{T_p}$

T_ω = Wave period

T_p = Peak wave period (This is the wave period at which the maximum energy density appears)

T_z = Zero up-crossing wave periods → $\frac{T_p}{T_z} = 1.407(1 - 0.287 \ln \gamma)^{1/4}$

G = Acceleration due to gravity

α = $5.058(1 - 0.287 \ln \gamma) \frac{H_s^2}{T_p^4}$

σ = Spectral width parameter = 0.07 for $\omega \leq \omega_p$

= 0.09 for $\omega \geq \omega_p$

γ = Peakedness parameter = 1.0 for $T_p \geq 5\sqrt{H_s}$

= $exp\left(5.75 - 1.15\frac{T_p}{\sqrt{H_s}}\right)$ for $3.6\sqrt{H_s} \leq T_p < 5\sqrt{H_s}$

= 5.0 for $T_p < 3.6\sqrt{H_s}$

The peakedness of the spectrum depends on water depth and peak period

4.2.1 Gaussian Swell

The Gaussian Swell spectrum is used to model long period swells seas. The Gaussian swell spectrum is specified by $H_s, f_m\ and\ \sigma$. The spectrum is based on the normal probability density function defined as:

S (f) = $(\frac{H_s}{4})^2 \sigma^{-1} (2\pi)^{-1/2} \exp\left[\frac{-(f-f_m)^2}{2\sigma^2}\right]$

Where:

$f_m = \frac{1}{T_p}$

σ = Spectral width parameter

H_s = Significant Wave Height.

4.2.2 Dean Stream

Stream function wave theory was developed to examine fully nonlinear water waves numerically. The method used to develop this model involves computing a series solution to the fully nonlinear wave problem, involving the Laplace equation with two boundary conditions - constant pressure and a wave height (Robert A.D, 2012). A vector field φ(x, z) whose partial derivatives are the particle velocities of the fluid. That is

$\frac{\delta\varphi(x,z)}{\delta x} = u$

$\frac{\delta\varphi(x,z)}{\delta z} = v$

The function also satisfies:

- Irrotational Flow: That is $\frac{\delta^2\psi}{\delta x^2} + \frac{\delta^2\psi}{\delta z^2} = 0$ (Laplace's equation)
- Ψ(x, 0) = 0: That is zero at the seabed.
- z = η(x), say ψ(x, η) = -Q: Constant at the free surface.
- Bernoulli's equation; $\frac{1}{2}\left[\left(\frac{\delta\psi}{\delta x}\right)^2 + \left(\frac{\delta\psi}{\delta z}\right)^2\right] + \eta = R$, Where R is a constant.

4.2.1 Velocity, Acceleration and Pressure under a Wave

Wave characteristics found in offshore locations are considered as a superposition of plane waves. Figure 39 shows how approximation of real offshore wave made by combination of several surface waves. A simple surface wave can be represented by a sine or cosine wave.

Sinusoidal wave is represented by the following surface profile:

$\emptyset = \emptyset_0 \sin(\omega t - kx)$

Where:

$\emptyset_0 = Wave\ Amplitude$

t = time

ω = Angular wave frequency

k= wave number

The velocity potential is therefore given as:

$$\emptyset = \frac{\emptyset_0 g}{w} * \frac{\cosh k(z-d)}{\cosh(kd)} * \cos(\omega t - kx)$$

Where:

z = the distance measured from the surface to the seabed.

Therefore, the velocity of the wave in horizontal direction is given by taken the first derivation of the velocity potential.

Horizontal Velocity, $u = {d\emptyset}/{dx} = \frac{\emptyset_0 . g . k}{w} * \frac{\cosh k(z-d)}{\cosh(kd)} * \sin(\omega t - kx)$

Horizontal acceleration, $\dot{u} = \emptyset_0 . g . k * \frac{\cosh k(z-d)}{\cosh(kd)} * \cos(\omega t - kx)$

Vertical Velocity, $w = {}^{d\emptyset}/_{dz} = \frac{\emptyset_0 . g . k}{w} * \frac{\sinh k(z-d)}{\cosh(kd)} * \cos(\omega t - kx)$

Vertical acceleration, $\dot{w} = -\emptyset_0 . g . k * \frac{\sinh k(z-d)}{\cosh(kd)} * \sin(\omega t - kx)$

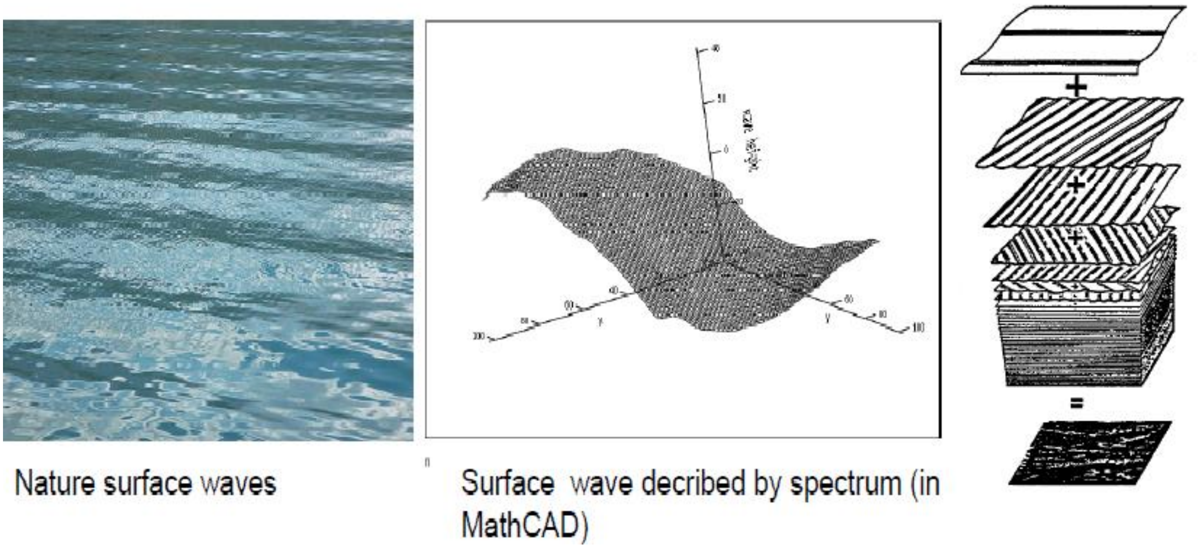

Figure 39: Offshore Wave Approximate (Karunakaran, D., 2012)

To obtain the pressure under the wave we will use Bernoulli equation. Linearizing the equation we obtain:

$P = P_0 - \rho g z - \rho \frac{d\emptyset}{dt}$ (Gudmestad, 2012)

Where:

$P_0 = Atmospheric\ Pressure$

$-\rho g z = Hydrostatic\ Pressure$

$-\rho \frac{d\emptyset}{dt} = Dynamic\ Pressure$ = Pressure under the wave, P_d

$$P_d = -\rho \frac{d\emptyset}{dt} = -\rho \frac{d\left[\frac{\emptyset_0 g}{w} * \frac{\cosh k(z-d)}{\cosh(kd)} * \cos(\omega t - kx)\right]}{dt}$$

$$P_d = \rho * g * \emptyset_0 * \frac{\cosh k(z-d)}{\cosh(kd)} * \sin(\omega t - kx)$$

4.3 Current Forces

Current depends solely on the prevailing local conditions and therefore measured locally. Sometimes during a calm day the effects of waves may be negligible in deeper water but there may be current effects and it is most times neglected. This has caused some avoidable catastrophe in the past. Operations in offshore fields are influenced by current and measurements must be made.

Current is influenced by the following environment factors:

- Currents due to winds
- Tidal effects
- The Gulf Stream
- Temperature differences in the water
- Salinity effects
- Coriolis effects

4.4 Wind Forces

High winds are destructive if not managed properly. The wind speed exerts pressure on structures when it meets it. The intensity of impact of pressure is what we call wind load. New generation drilling vessels are equipped with dynamic positioning (DP) systems to reduce the effects on winds and wave pressure on the vessels.

4.5 Hydrodynamic Loads

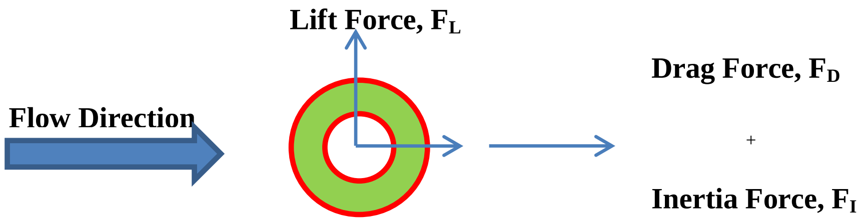

Figure 40: Hydrodynamic Loads

Lift Force: A flowing fluid moving past a body will exert surface force on its surface. The perpendicular component in the oncoming flow direction of this surface force is the lift force. The lift force is proportional to the square of the velocity of flow and it is always upward.

Drag Force: The parallel component in the flow direction of the surface force is called the drag force. The drag force is proportional to the square of flow velocity and changes with flow direction.

Inertia Force: The inertia force is proportional to the acceleration of flow and changes with the change in the direction of acceleration.

4.5.1 Hydrodynamic Load Coefficients

According to DNV-OS-F201 (2010), Morison equation can be used to express the hydrodynamic loading on slender structures (for example, drill pipe) by considering the relative body-fluid velocities and accelerations. The water particle acceleration and velocity vectors are found by using the above equations on wave and current kinematics. A uniform circular cross-section exposed to hydrodynamic loads is represented by the following Morison

$$f_n = \frac{1}{2}\rho C_d D_h |v_n - \dot{r}_n|(v_n - \dot{r}_n) + \rho\frac{\pi D_b^2}{4} C_m \dot{v}_n - \rho\frac{\pi D_b^2}{4}(C_m - 1)\ddot{r}_n$$

Where:

f_n	Force per unit length in normal direction
ρ	Water density
D_h	Hydrodynamic diameter
D_b	Buoyancy diameter (i.e. equivalent diameter for description of resulting buoyancy on a general riser cross section)
$v_n, \dot{v}_n$	Fluid velocity and acceleration in normal direction
$\dot{r}_n, \ddot{r}_n$	Structural velocity and acceleration in normal direction
C_d, C_m	Drag and inertia coefficients in normal direction ($C_m = C_a + 1$)
C_a	Added mass coefficient in the normal direction

Chapter 5: Design Premises

5.1 Limit States Design

The condition of an element above which it no longer satisfies the relevant design criteria is called the limit state design. The idea of any design using limit states is to identify likely failure actions that can occur during the service life of the element and design such structure in a way as to sustain the failure actions and still maintain reliability and fitness for its functions. Hence, it is of utmost importance in any drill pipe design to firstly identify extreme loads that could exceed any of the limit states.

In accordance to DNV-OS-F201 used for dynamic risers, all failure modes expected during the life of the RDM-R drill pipe shall be identified and verifications are to be made to making sure that no corresponding limit states are exceeded. These limit states includes:

- Serviceability Limit State (SLS): Requires that a pipe must remain functional for its intended everyday use. It requires that the drill pipe must be able to remain in service and operate properly. This limit state corresponds to criteria limiting or governing the normal operation (functional use) of the drill pipe.
- Ultimate Limit State (ULS): Requires that the drill pipe must not rapture (burst or collapse) when subjected to the peak design load. That is, it must remain intact, but not necessary be able to operate.
- Accidental Limit State (ALS): Requires that a drill pipe maintains its integrity under infrequent loads. It is a ULS due to accidental loads.
- Fatigue Limit State (FLS): Requires that a drill pipe does not fail under accumulated fatigue, crack growth or cyclic loading (directly or indirectly).

5.2 Failure Modes and Design Requirements

The different types of failure modes that are associated with limit states include bursting, collapse, propagating buckling, fatigue, accidental loads, etc.

The DNV-OS-F201 code identifies the different design approaches used for the above failure modes:

- Design by testing
- Reliability analysis
- Working Stress Design (WSD) method
- Load and Resistance Factor Design (LRFD) method

5.2.1 Working Stress Design (WSD) Method

This method expresses the structural safety margin by a central usage factor or safety factor for each limit state. That is, the uncertainties in the resistance and load effects are accounted for by a one central safety factor. This makes the working stress design method easier to use.

Mathematically, the working stress design method can be expressed as:

$$\sigma_s < C_f\sigma_{a:}\ \text{(API RP 2RD, 2006)}$$

where:

$\sigma_a = C_a\sigma_y$ = Basic allowable resistance

$C_a = {}^2/_3$ = Allowable stress factor

σ_y = Material minimum yield strength

C_f = Design case factor as shown in the table below

σ_s = Load effect

Limit State	C_f	Allowable stress = $C_f\sigma_a$
ULS	1.2	$0.8\sigma_y$
ALS	1.5	$1.0\sigma_y$

Table 4: Design Case Factors and Allowable Stress (API RP 2RD, 2006; DNV-OS-F201, 2010)

5.2.2 Load Resistance Factored Design (LRFD) Method

The WSD differs from the LRFD format in that the uncertainties in the different resistance and load effects in the LRFD approach are represented by different personal safety factors. According to DNV-OS-F201 (2010), the fundamental principle behind this is to make sure that the factorized design load effects is not more than the factored design resistance for all the limit states. Some of the failure modes associated with limit states including bursting, collapse, etc. are discussed in DNV-OS-F201 (2010) code requirements and are explained below.

5.2.2.1 Bursting

It occurs when pipe's membrane open suddenly and/or violently, especially from internal overpressure only. In dynamic riser design, the most critical area for the riser pipe to experience burst is above the seabed where it experiences reduced external pressure at constant internal pressure. In this case, the RDM-R drill pipe is a high pressure dual pipe and should sustain the circulation fluid pressure since it can be used as a pressurized pipe for MPD or CPD.

Pipe members subjected to internal overpressure are required to satisfy the following condition at all cross sections:

$$(P_{li} - P_e) \leq \frac{P_b(t_1)}{\gamma_m\gamma_{sc}}$$

Where:

P_{li} = Local incidental pressure

$P_e = External\ Pressure$

P_b = Burst Resistance = $\frac{2}{\sqrt{3}}\frac{2t}{D-t}\min(f_y{:}\frac{f_u}{1.15})$

t = A "dummy variable" to be substituted by $t_1 or\ t_2$ where relevant

h = height difference between the actual location and the internal pressure reference point

ρi = Density of the internal fluid

γ_m = Material resistance factor (Table 5 below)

γ_{sc} = Safety class resistance factor (Table 5 below)

t_1 = Minimum required wall thickness for a straight pipe without allowances and tolerance

$$t_1 = \frac{D}{\frac{4}{\sqrt{3}} \frac{\min(f_y; \frac{f_u}{1.15})}{\gamma_m \gamma_{sc}(P_{li} - P_e)} + 1}$$

D = Nominal pipe outer diameter

f_y= Yield strength of pipe

f_u = Tensile strength of pipe

Material Resistance Factors γ_m		**Safety Class Resistance Factor γ_{sc}**		
ULS and ALS	SLS and FLS	Low	Normal	High
1.15	1.0	1.04	1.14	1.26

Table 5: Resistance Factors (DNV, 2010)

5.2.2.2 System Hoop Buckling (Collapse)

As we go deeper, the external pressure on the drill pipe increases way more than the internal pressure. This may cause a plastic deformation of the pipe in which the pipe buckles in.

Pipe members subjected to external overpressure are required to satisfy the following condition:

$$(p_e - p_{min}) \leq \frac{p_c(t_1)}{\gamma_m \gamma_{sc}}$$

Where:

p_{min} = Local minimum internal pressure.

$p_c(t)$ = Resistance for external pressure ≫

$$p_c(t) - p_{el}(t) \cdot \left(p_c^2(t) - p_p^2(t)\right) = p_c(t) \cdot p_{el}(t) \cdot p_p(t) \cdot f_0 \cdot \frac{D}{t}$$

DNV-OS-F101 further factored the hoop buckling resistance $p_c(t)$ as follows:

$$p_c(t) = y - \frac{b}{3}$$

$$Where: b = -p_{el}(t)$$

$$c = -\left[p_p(t)^2 + p_{el}(t) \cdot p_p(t) \cdot f_0 \cdot \frac{D}{t}\right]$$

$$d = p_p(t)^2 * p_{el}(t)$$

$$u = \frac{1}{3}\left(-\frac{1}{3}b^2 + c\right)$$

$$v = \frac{1}{2}\left(\frac{2}{27}b^3 - \frac{1}{3}bc + d\right)$$

$$\varphi = \cos^{-1}\left(\frac{-v}{\sqrt{-u^3}}\right)$$

$$y = -2\sqrt{-u}\cos\left(\frac{\varphi}{3} + \frac{60\pi}{180}\right)$$

$p_{el}(t)$ = Elastic collapse pressure = $\frac{2 \cdot E \cdot \left(\frac{t}{D}\right)^3}{1-\vartheta^2}$

$p_p(t)$ = Plastic collapse pressure = $2\frac{t}{D} \cdot f_y \cdot \alpha_{fab}$

E = Young's modulus of pipe material

f_0 = The initial departure from circularity of pipe and pipe ends of pipe (Ovality) = $\frac{D_{max}-D_{min}}{D}$

α_{fab} = Manufacturing process reduction factor

5.2.2.3 Combined Loading

A drill pipe may experience at any time these loads - burst, collapse, moment, tension, and internal overpressure or combination of all of aforementioned loading. DNV-OS-F201 requires that a drill pipe experiencing bending moment, effective tension and net internal overpressure shall be designed to satisfy the following equation:

$$\{\gamma_{sc} \cdot \gamma_m\}\left\{\left(\frac{|M_d|}{M_k} \cdot \sqrt{1 - \left(\frac{p_{ld} - p_e}{p_b(t_2)}\right)^2}\right) + \left(\frac{T_{ed}}{T_k}\right)^2\right\} + \left(\frac{p_{ld} - p_e}{p_b(t_2)}\right)^2 \leq 1$$

And, if in it is experiencing bending moment, effective tension and net external overpressure shall be designed to satisfies the following equation:

$$\{\gamma_{sc} \cdot \gamma_m\}^2\left\{\left(\frac{|M_d|}{M_k}\right) + \left(\frac{T_{ed}}{T_k}\right)^2\right\}^2 + \{\gamma_{sc} \cdot \gamma_m\}^2\left(\frac{p_e - p_{min}}{p_c(t_2)}\right)^2 \leq 1$$

Where:

M_d = Design bending moment = $\gamma_F \cdot M_F + \gamma_E \cdot M_E + \gamma_A \cdot M_A$

M_k = Plastic bending moment resistance

T_{ed}= Design effective tension = $\gamma_F \cdot T_{eF} + \gamma_E \cdot T_{eE} + \gamma_A \cdot T_{eA}$

T_k= Plastic axial force resistance

p_{ld}= Local internal design pressure = $p_d + \rho_i gh$

γ_F= functional load effect factor.

$\gamma_E = $ Environmental load effect factor

$\gamma_A = $ Accidental load effect factor

M_F,= Bending moment for functional loads.

M_E= Bending moment for environmental loads.

M_A= Bending moment for accidental loads.

T_{eF}= Effective tension for functional loads.

T_{eE}= Effective tension for environmental loads

T_{eA}= Effective tension for accidental loads.

p_d = Design pressure.

5.3 Design Acceptance Criteria in Accordance to DNV-OS-F201

The design objective is to attain some level of reliability, below which the drill pipe is said to have failed. All failure modes identified above shall be checked and verified that no limit state is exceeded. The required reliability is based on the consequences of failure of the drill pipe.

$$Risk = \text{Probability of Event} * \text{Consequences}$$

In DNV-OS-F201, the design drill pipes are based on the safety requirement which depends on the safety class that the drill pipe belongs to, namely:

1. Low Safety Class: Low risk of human injury and low environmental consequences.
2. Normal Safety Class: For temporary condition with high risk of human injury and significant environmental consequences.
3. High Safety Class: For operating conditions with high risk of human injury and significant environmental pollution or very high economic or political consequences.

The safety class partial safety factors depend on the fluid category, the location and the operating condition whether permanent condition or temporary condition. These factors are shown in table 5 above.

For the state-of-the-art-design in this report, I will concentrate on the use of load resistance factor design (LRFD) rather than the working stress design (WSD) because it is considered superior to the WSD method (DNV-OS-F201, 2010).

Fundamentally, the applied load (S) must be lesser than the drill pipe resistance (R).

$$S_d\left(S_p; \gamma_F S_f; \gamma_E S_E; \gamma_A S_A; t\right) \leq \frac{R_k}{\gamma_{sc}\gamma_m\gamma_c}$$

Where;

S_p = Pressure loads

S_f = Load effect from functional loads.

S_E = Load effect from environmental load .

S_A = Load effect from accidental loads.

γ_F = Load effect factor for functional loads.

γ_E = Load effect factor for environmental loads.

γ_A = Load effect factor for accidental loads

R_k = Generalised resistance.

γ_{sc} = Resistance factor that takes into account the safety class (i.e. failure consequence).

γ_m = Resistance factor that takes into account the material and resistance uncertainties.

γ_c = Resistance factor that takes into account the special conditions.

t = For systems exposed to time varying excitations.

Chapter 6: Analysis Data and Methodology

This report is written to analyze the hydrodynamic effects on the RDM-R drill pipes in open water. The RDM-R drill pipe is a product of the Reelwell Company and the analysis in this report will be based on the project undertaken by the Reelwell Company for BG Brazil in their presalt well located in Santos basin, Brazil. Santos Basin is one of the largest Brazilian sedimentary basins located 23^0 south and 28^0 south along the Brazilian shelf in the South Atlantic Ocean, about 300 kilometers south east of Sao Paulo. All Metocean data are taken from this environment which is at a water depth in excess of 2000 meters.

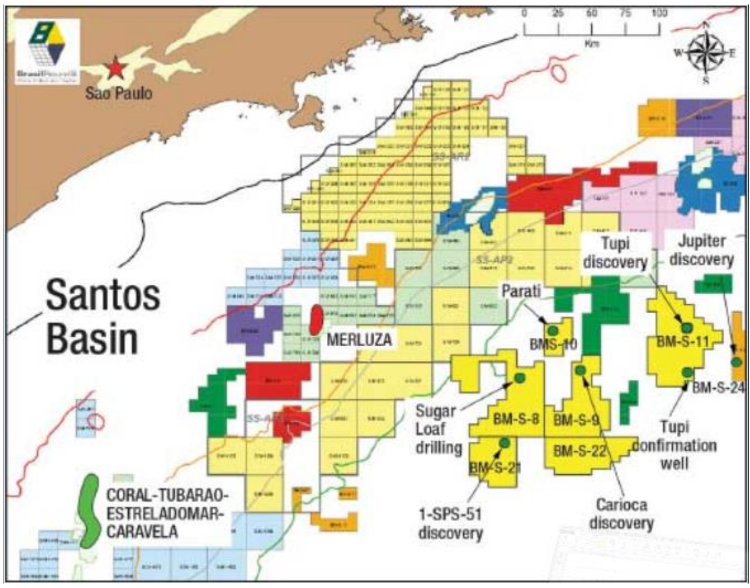

Figure 41: Santos Basin (RMC, 2008)

At the present stage of the project, the top hole has been drilled by another drilling method to a depth of 1000 meters below the mud line. The RDM-R is expected to drill a 2000m subsalt region, that is, in excess of 3000m below the mudline, 5000m below sea level. The purpose of this report is to examine the hydrodynamic forces on the different configurations of the RDM-R drill pipes and evaluate which configuration is best suited for the Santos basin subsalt project with respect to some parameters of interest. The different configurations of RDM-R drill pipes that would be analyzed include the RDM-R steel drill pipe, the RDM-R Aluminum drill pipe and lastly, an assumed steel drill pipe configuration. The different properties of all the aforementioned configurations of drill pipes will be shown in subsequent sub-chapter.

The analysis will be done in two different stages:

1. At 3000m depth from sea level
2. At 5000m depth from sea level

It is necessary to do the analysis in these two stages to know the operating window and boundary conditions for the operation in order to conclusively evaluate the most appropriate drill pipe configuration for the project.

OrcaFlex software version 9.5a will be used for the analysis. OrcaFlex is a non-linear time domain, finite element software program principally used for the static and dynamic modelling of systems used in offshore construction environment. These systems may include marine risers (flexible and rigid types), drill pipes, mooring systems, etc. At present, the Reelwell company are not sure of the way the pipe would be operated, either by rotating the string or by rotating the bit during the operation. One of the limitation of the model in OrcaFlex software is the perform a simulation with a rotating drill pipe which may be the case during operation. Therefore, a manual calcualtion would also be carried out to find the effects on the drill string if the company decides to rotate the string.

The OrcaFlex software would perform the following analysis:

- **Static Analysis**: OrcaFlex would calculate the static equilibrium position of the model developed. In static, wave effects, current effects and wind effects are excluded from the simulation. A hand calculation would also be carried out to confirm the results from the model developed in the software.
- **Dynamic Analysis:** OrcaFlex would carry out a time simulation response of the entire system model to wave loads, current loads, wind loads and the effects of the movement of the vessel. The results expected from this analysis would be enumerated in subsequent sub-chapter of this report.
- **Fatigue Analysis:** In OrcaFlex, the fatigue analysis is a post-processor analysis. OrcaFlex calculates the fatigue damage using many different methods. The damages to the line in our case may be obtained in damage per hour, damage per day or damage per year. This can then be collected and added for specific load cases and then presented by the software.

6.1 Force Diagram for the RDM-R Drill Pipe

In order to fully appreciate the solutions and results of this report we will need to understand the nature of the loads and forces acting on or influencing the drill pipe. We have identified these forces as shown in the free body diagram or the force diagram shown in figure 42 below. Some of these loads have been explained in chapter 4 of this report there is therefore no need to further explain them. The aforementioned forces include; wind induced loads, wave induced loads, current induced load and the forces as a result of the motion of the vessel.

Other forces that are worth mentioning are:

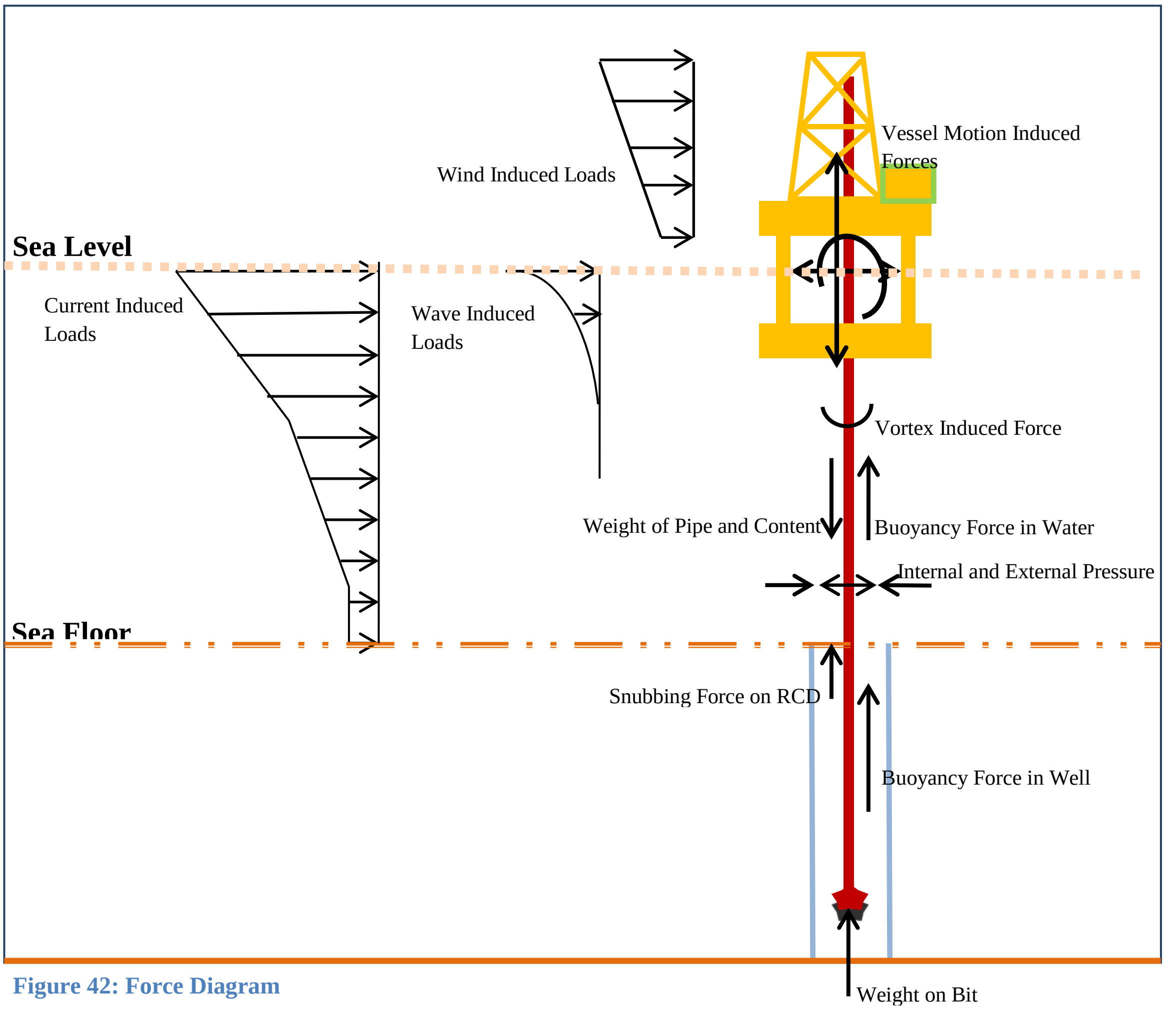

Figure 42: Force Diagram

- **Weight on Bit**: The amount of downward weight exerted on the drill bit of a drill pipe is called weight on bit. In our own word, the weight on bit is the amount of weight taken off the hook load when the drill bit rests at the bottom of the well.
- **Buoyancy Force**: Any structure immersed in a fluid experiences upward force acting against the weight of the structure. This net force that accelerates the object upwards is called the buoyancy force. According to Archimedes principle, the buoyant force on a submerged drill pipe is equal to the weight of the displaced fluid. It is important to point out that equal volume of an object, in this case, the drill pipe will feel equal buoyant forces. This fact will be used during the discussion of the results
- **Snubbing Force**: The snubbing force is a force that tries to push the drill pipe out of the well. This occurs as a result of the pressure differential on the RCD causing an upward axial force on the drill pipe. The pressure differential is the difference in pressure between the circulation fluid at the RCD level and the corresponding pressure head of water at the same level. The advantage of the snubbing force is that it reduces the hook load and hence the tensioning system.

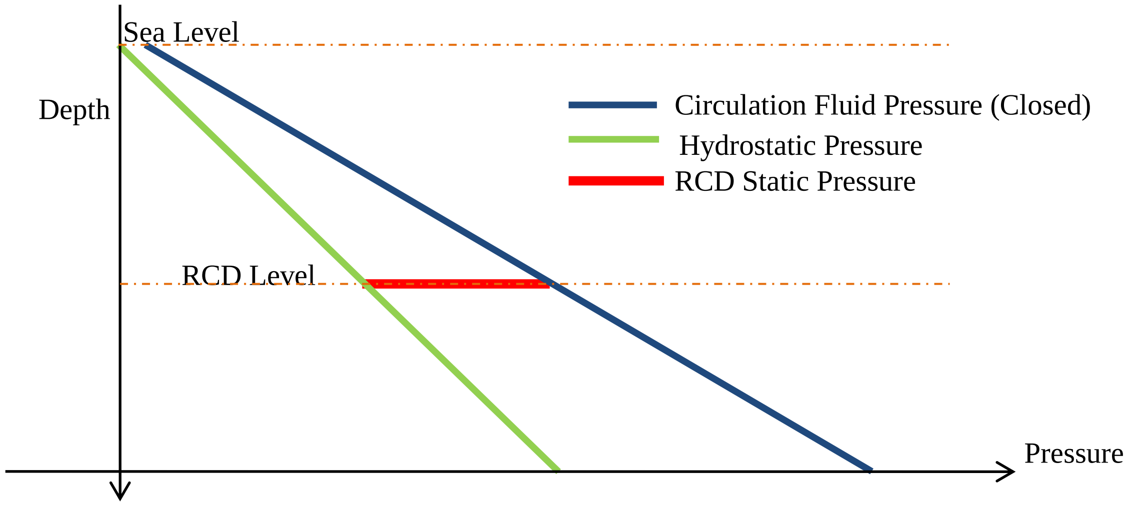

Figure 43: Snubbing Force Illustration

- **Vortex Induced Vibration Force**: As water current flows across the pipe, as shown in the figure 44 below, on the alternative sides of the pipe, upper and the bottom surface, vortices are shed (vortex shedding) at a frequency called the shedding frequency. As the shedding frequency approaches structural Eigen-frequency of the pipe, the pipe will start to oscillate. An increase in speed of current would normally correspond to an increase in the shedding frequency. At a certain range of current speeds, the vortex shedding frequency locks to the pipe Eigen-frequency and the pipe vibrates violently in a way that could cause disaster. The associated fluctuating force is predominantly in the direction across the flow as shown by the red dashed figure 8 in the figure below.

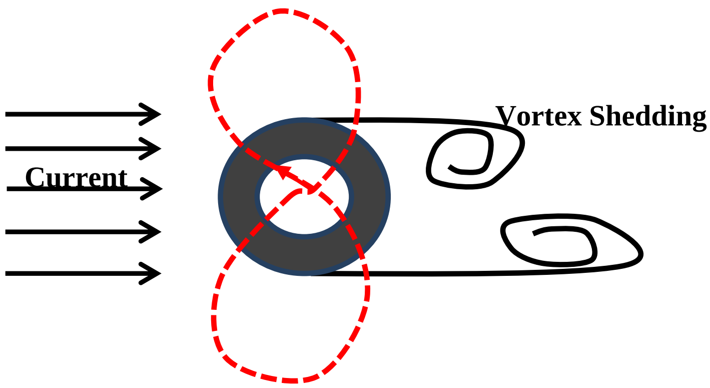

Figure 44: VIV

We would like to point it out here from our research and findings that the vortex induced vibrations (VIV) cannot cause an immediate collapse of the pipe but it is of great contribution to the structural fatigue of the pipe and should therefore be checked.

The next sub-chapter shows how the model designed in OrcaFlex software. The choice for the different components of the model is also illustrated.

6.2 Mechanical Model

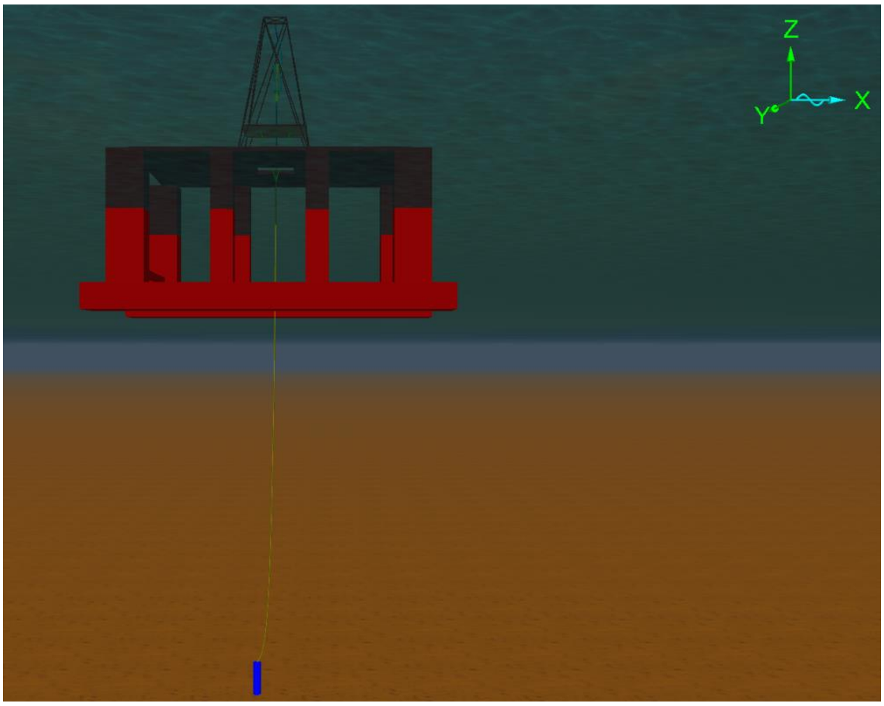

Figure 45: Shaded Graphic Model (Orcaflex Software)

The model comprises basically of a semi-submersible drill vessel, RDM-R drill pipe, links, winches, buoys, subsea stack (BOP, RCD, etc) and a model for the well design. In the next sub-chapter we would explain the characteristics of some of the essential components of the model. Since it is impossible to drill in OrcaFlex we have attempted to model the conditions in the well by using cylindrical solids filled with the proposed drilling fluid of specific gravity 1.5. The top hole is a 30" conductor installed. The next hole is also filled with the drilling fluid like the top hole but completed with a 22" surface casing. The stage where the RDM-R method will be used is the lower 2000m subsalt region. The proposed drill bit is 17.5" and it is planned to be completed with a 13.625" casing.

Figure 46 below is a window cut out from the OrcaFlex software. It shows the components of the various mechanical component making up the model.

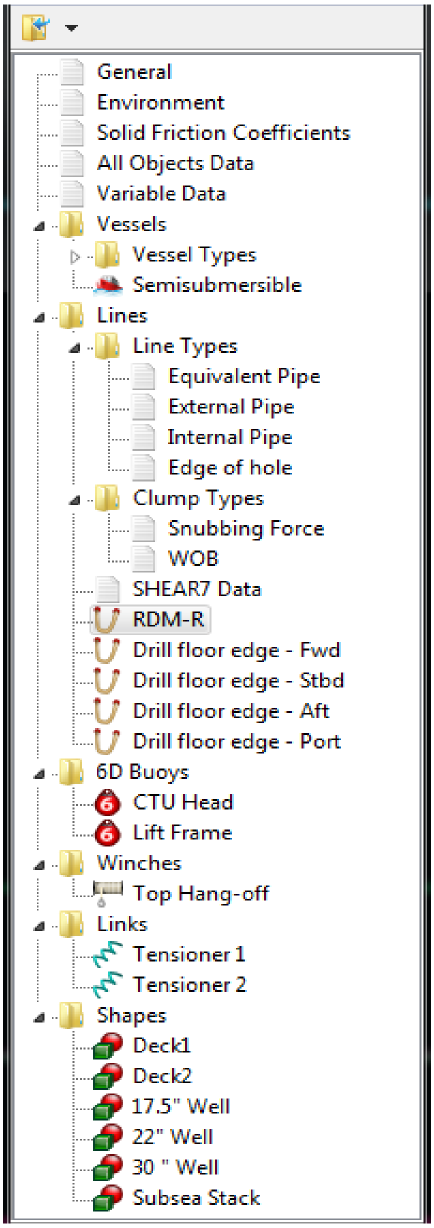

Figure 46: Model Components

6.2.1 Environment

The environment consists of the sea characteristics and general Metocean data. At the location of the field, the following are the prevailing environmental data used in the model.

- Water depth = 2000m
- Water temperature = 18^0C
- Kinematic viscosity = 1.35 * $10^6 m^2/s$
- Sea water density = $1025 kg/m^3$

6.2.1.1 Wave Condition in the Santos Basin

The wave condition in the Santos basin is mainly described by a two peaked/bimodal spectrum, the swell and the high frequency wave. The low frequency swell which originates from the south is due to extra tropical cyclone activities in the area. The high frequency wave that is related with the northerly sea is due to the local easterly winds. According to Vogel M., et al, (2010) in their paper titled

"Metocean Measurement in Northern Santos Basin", says that typical significant wave heights is between 2.2m and 0.8m with a maximum values and mean values put at 1.7m (period = 14s) and 5 m (period = 11s) respectively. On a typical day, wave period varies from 5s to 13s. The longest period registered during July, August and September of the research was 19s associated with a significant wave height of 0.5m. The paper also says that the waves that with very high period of about 24.5s and highest significant height of 7m were recorded but they are very rare events like once in 15501 observations (Vogel M., et al, 2010).

Table 6 below shows the extracted wave conditions in Santos basin from "Brazilian Offshore Wave Climate Based on NWW3 Reanalysis" written by Casia Pianca et al, (2010) and submitted to Brazilian Journal of Oceanography, paper number 58(1):53-70.

Season	**Significant Wave Height (m)**		**Wave Period(s)**
Summer	Typical Wave	1-2	10-12
	Highest Recorded	4.0	6-8
Fall	Typical Wave	1-3	10-12
	Highest Recorded	6.3	6-8
Winter	Typical Wave	2-3	10-12
	Highest Recorded	5.7	6-8
Spring	Typical Wave	1-2	6-8
	Highest Recorded	4.5	8-10

Table 6: Wave Condition in Santos Basin (Casia Pianca et al, 2010)

To model the double peaked wave conditions in the Santos basin, we will use two different wave trains. One would be the swell and the other would be a Dean wave. OrcaFlex combined the two wave trains to form a single wave density profile as shown below in figure 47

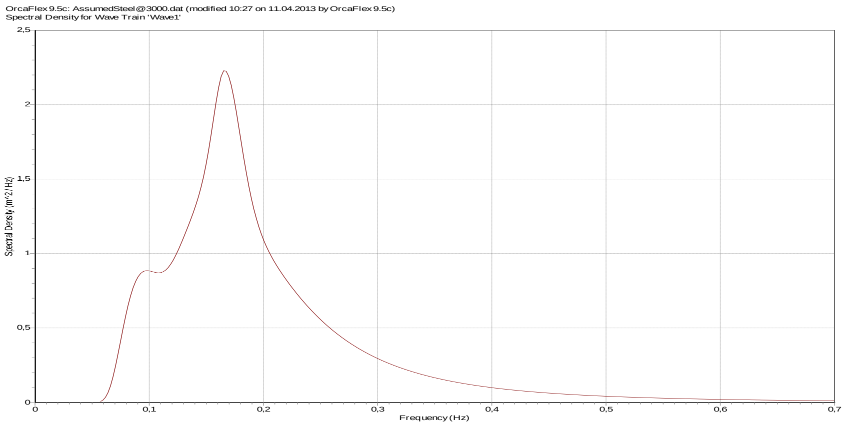

Figure 47: Wave Spectrum from OrcaFlex

6.2.1.2 Current Data

It is expected that current forces exerted on installations and pipes in deep water environment is very important to the determination of the overall environmental loads on the system. The analysis of current in the Santos basin shows that extreme events are associated with low frequency phenomena, such as meanders and eddies of the Brazil Current (Jose A. M. Lima et al, 1999).

Table 7 shows the current profile as extracted from "New Oceanographic Challenges in Brazilian Deepwater Oil Fields" written by Jose A. M. Lima et al (1999).

Depth	Current Speed (m/s)
0	-1.0
50	-0.6
100	-0.5
150	-0.4
200	-0.3
350	-0.2
400	-0.2
450	0.1
500	0.2
600	0.2
800	0.3
1000	0.5
1200	0.3
1400	0.2
1800	0.1
2000	0.05

Table 7: Current Profile (Jose A. M. Lima et al, 1999)

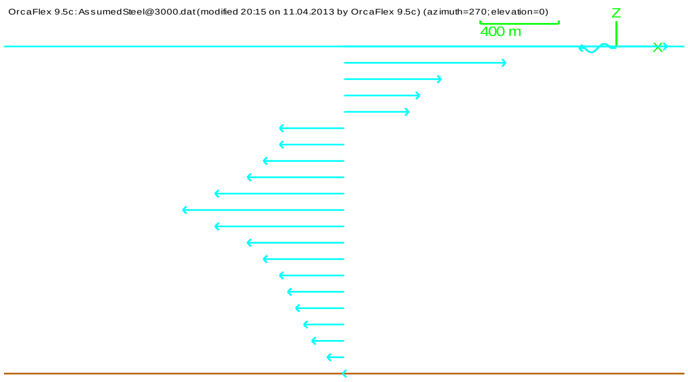

Figure 48: Current Vertical Profile Graph in 3D

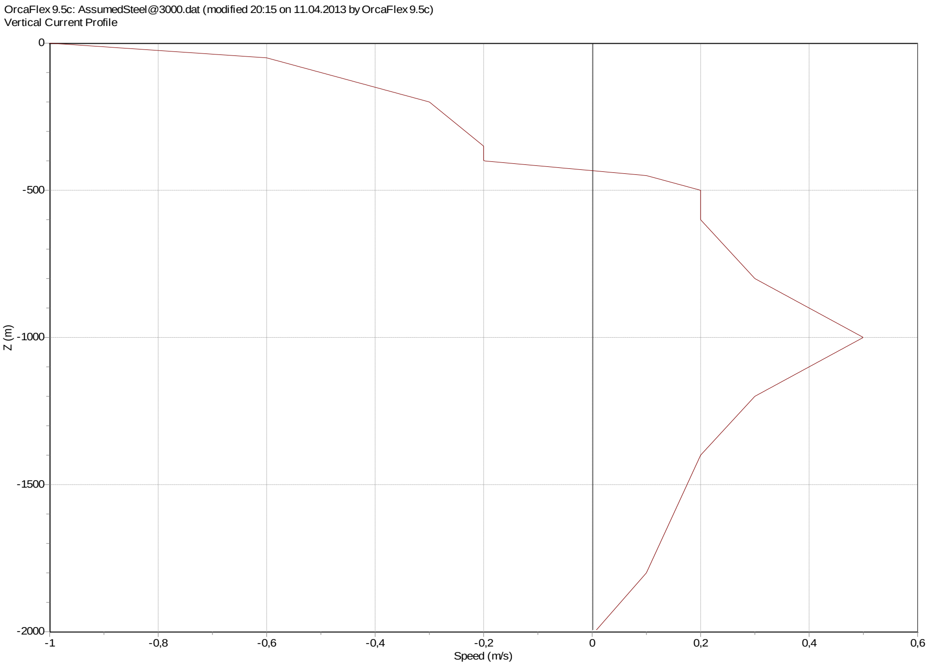

Figure 49: Current Vertical Profile Graph

6.2.1.3 Wind Data

Wind load is also very important in determining the hydrodynamic loads on the vessel. For instance in the basin, speeds up to 10m/s occurs during spring, winter and autumn due to strong southeasterly and southwesterly winds. The northeasterly winds can also get as high as 15m/s during spring and summer (Jose A. M. Lima et al, 1999).

Seasons	Wind Speed (m/s)
Summer	3.4
Fall	2.3
Winter	4.4
Spring	4.8

Table 8: Wind Data (Vogel M., et al, 2010)

In this report and for the model, the wind speed is assumed constant and wind load is included on the vessel, the drill pipe above sea bed and the buoys. The following are the properties of wind utilized:

Wind Speed = 4.4m/s

Air Density = 0.0013te/m^3

Air Kinematic Viscosity = 15 * 10^{6}m^2/s

6.2.2 Vessel

Vessels are used to model barges, ships, floating platforms, etc. They are rigid bodies whose motions has to be supplied into the model by the user. The motion of the vessel can be specified by directly specifying the Response Amplitude Operators (RAOs) for pitch, surge, roll, heave, sway and yaw. Otherwise,the use canspecify the first order wave load RAOs (OrcaFlex, 2012).

The vessel used in the model is a 40000 tonnes drilling semisubmersible. Figure 50 below shows the 2D and the 3D views of the vessel as copied from the OrcaFlex software environment.

6.2.3 Lines

In OrcaFlex, lines are linear elements used to model pipes, hoses, cables, chains or other similar items. The properties of a Line (Buoyancy, mass per unit length, diameter, bend stiffness, etc.)are inputed by dividing the line up into sections and segments as shown in figure 51 below. Each segment of the line has properties given to it for the purpose of this model.

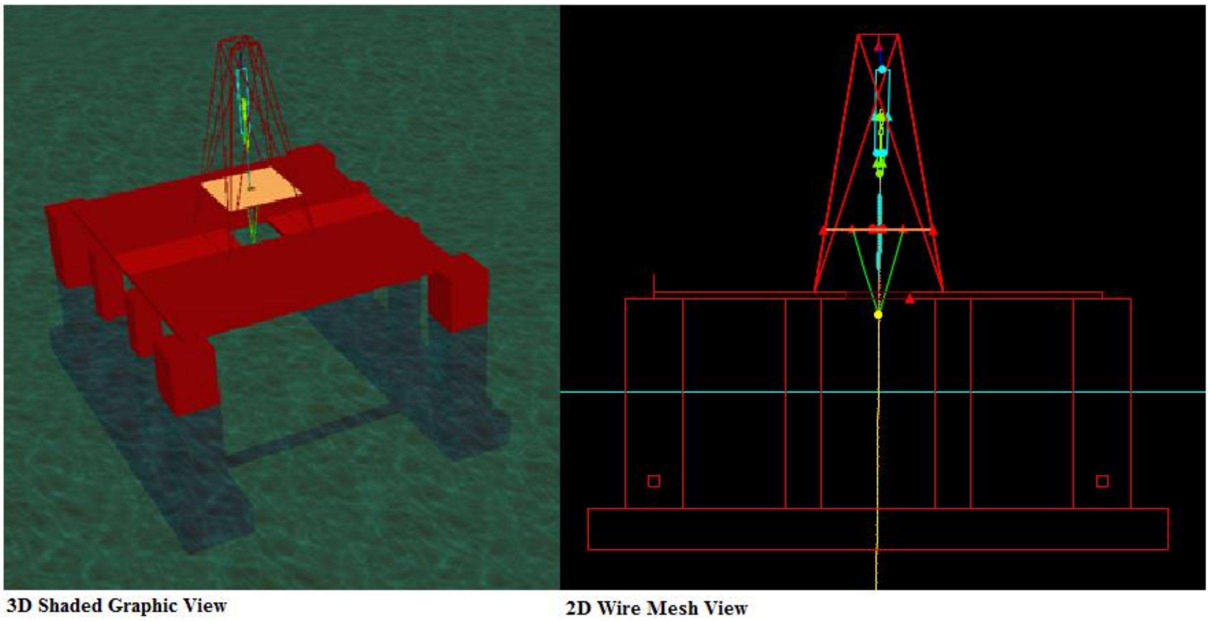

Figure 50: Drilling Vessel

There are several types of line categories, for example, homogenous line, general line, equivalent line, etc. In this model we will be using the equivalent line category because it can be use to model a pipe-in-pipe situation. The RDM-R drill pipe consists of a conventional drill pipe housing an internal pipe (pipe-in-pipe situation). To correctly model the RDM-R drill pipe, we will require a pipe category that is intended for modeling pipe-in-pipe lines. OrcaFlex calculates the single representative property (mass per unit length, geometry, stiffness etc.) of the lines and use it for the modeling.

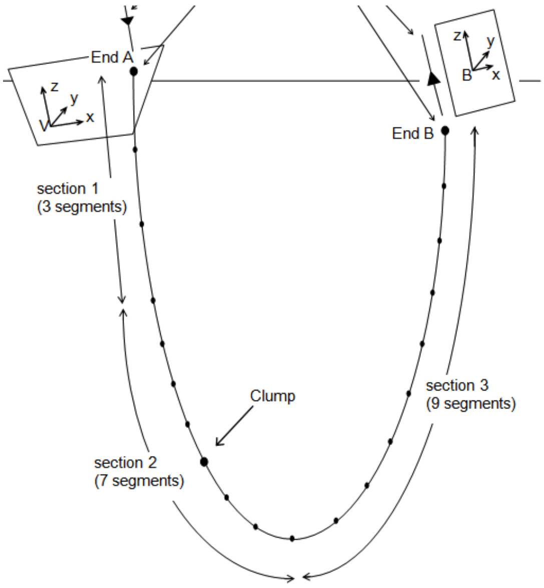

Figure 51: Line Segments and Sections (OrcaFlex, 2012)

The data required to set up an equivalent line type comprises of the following:

- Secondary Lines: These lines represent lines that are either external or internal to the carrier line. The properties of such a line can be specified to either or not contribute to the properties of the equivalent line.
  In our model, the secondary line is the inner pipe and it contributes to the properties of the equivalent line.
- A carrier line type: The carrier line houses all the internal secondary lines and the results of the equivalent line are reported for the carrier line.
  In this model, the carrier line is the outer pipe.

At present, the Reelwell Company has proposed 2 dual drill pipe configurations, that is, the Steel dual drill pipe and the Aluminum dual drill pipe. In addition to this, in the quest to further increase the mass flow rate of the circulation during drilling operation, the company is proposing using a larger steel pipe configuration than the present RDM-R drill pipe whose parameters are given below. This third pipe would be called the assumed dual drill pipe for the remaining parts of this report.

The following tables show the parameters of the 3 dual drill pipes that would be analyzed in this report.

1. **RDM-R Steel Dual Drill Pipe Parameters**

Parameters	Outer String	Inner String
Pipe Outer Diameter [mm]	168 (6 5/8”)	88.9 (3.5”)
Pipe Inner Diameter [mm]	140 (5.5”)	78
Tool Joint Outer Diameter [mm]	203 (8”)	96

Tool Joint Inner Diameter [mm]	127 (5")	76
Pipe Joint Length [m]	13.5	13.5
Pipe Weight in Air [kg/M]	40.9	13.1
Max Tension Load [ton]	270	~
Max Torque [k ft lbs]	85	~
Yield Pressure [bar]	630	400
Collapse Pressure [bar]	290	400
Young Modulus [GPa]	212	212
Poisson Ratio	0.293	0.293

2. RDM-R Aluminum Dual Drill Pipe Parameters

Parameters	Outer String	Inner String
Pipe Outer Diameter [mm]	198 (7.8")	104
Pipe Inner Diameter [mm]	172	90
Tool Joint Outer Diameter [mm]	209	113
Tool Joint Inner Diameter [mm]	150	90
Pipe Joint Length [m]	14	14
Pipe Weight in Air [kg/M]	28.5	5.8
Max Tension Load [ton]	300	~
Max Torque [k ft lbs]	100	~
Yield Pressure [bar]	525	540
Collapse Pressure [bar]	430	450
Young Modulus [GPa]	69	69
Poisson Ratio	0.33	0.33

3. RDM-R Assumed Steel Dual Drill Pipe Parameters

Parameters	Outer String	Inner String
Pipe Outer Diameter [mm]	193.68 (7 5/8")	139.70 (5 ½")
Pipe Inner Diameter [mm]	161.40 (6.35")	121.36 (4.67")
Tool Joint Outer Diameter [mm]	~	~
Tool Joint Inner Diameter [mm]	~	~
Pipe Joint Length [m]	~	~
Pipe Weight in Air [kg/M]	70.67	29.52
Max Tension Load [ton]	~	~
Max Torque [k ft lbs]	~	~

Yield Pressure [bar]	~	~
Collapse Pressure [bar]	~	~
Young Modulus [GPa]	212	212
Poisson Ratio	0.293	0.293

All other line types in the model browser are for drawing purposes and do not affect the results obtained on the RDM-R drill pipe.

6.2.4 6D-Buoys

They are rigid bodies with six degrees of freedom, three translational and three rotational. It is used to model objects whose motions is to be calculated or just for design puporses.In the model the 6D-buoys are used for drwaing purposes to enhance the model. Buoys have properties (mass, moments of inertia, moments, etc) but they are given negligible properties for this model.

6.2.5 Links

Links are massless and are used to connect or link two objects together in the model. There are two types of links available in OrcaFlex: Tethers and Spring/Damper units. Tethers are simple elastic ties that takes only tension and no compression. Spring/dampers are combined damper and a linear or non-linear spring units. The links can can take tension and compression.
In the model, links are used to model the tensioners and a spring/damper unit is used to allow for the oscillating loads in the dynamic analysis.

6.2.6 Winches

Like the links, winches have no mass and they are used to connect or link two or more objects together in the model.
In the model the winch is given a negligible property. It is therefore in the model for drawing purposes to enhance the model.

6.2.7 Shapes

Shapes are three dimensional geometric objects with adjustable properties, making them flexible to be used to model a large variety of objects in the model. One of the various types of shapes found in OrcaFlex software 9.5a is the elastic solids. An elastic solid serves as a physical barrier to the movements of lines. It can be assigned stiffness to resist penetration from the line. The force of penetration can be obtained from the OrcaFlex making it a good candidate to model the well and thereby, the clashing force between the RDM-R drill pipe and the well.

In the model, the subsea stack, the well and other member of the vessels are modeled with the shapes. The three layers of the well are model in a way to closely model what the condition in the well is. The top layer is filled with the circulating fluid and with a hole diameter of 30”. The next hole is also filled with the same fluid with a diameter of 22” as obtained in the present stage of the drilling operation. The third layer which would be handles by Reelwell AS is a 17.5” well filled with the circulation fluid. Figure 52 below shows the side cross sectional view of the well.

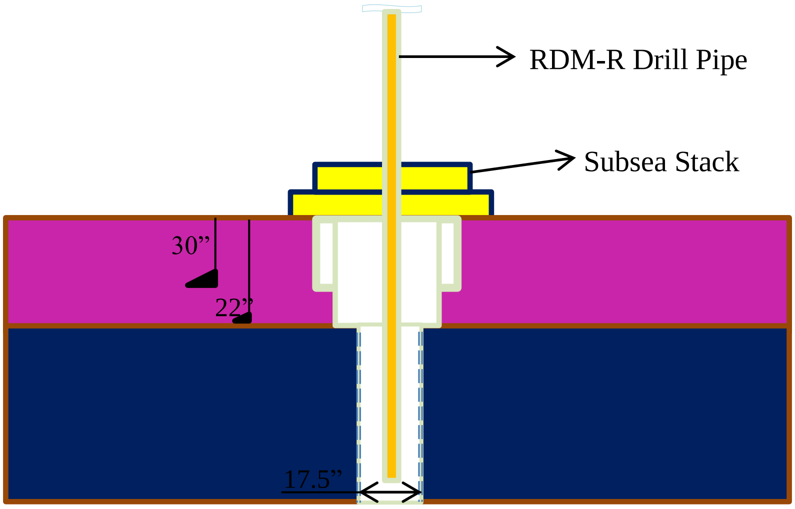

Figure 52: Cross Section through the Well

6.3 Expected Results from OrcaFlex Simulation

There are numerous results that could be obtained from OrcaFlex. As the purpose of this report is to find the effects of hydrodynamic forces on the RDM-R dual drill pipe, all results that are collated and reported in this report are on the RDM-R pipe. For further work, the results from the motions of the tensioner may also be extracted for the tensioner design. The three most important result types in OrcaFlex are:

- **Time History Results:** Time History graph represents a plot of single variable against time. In the model result, the tension time history results will show a plot of how the tension in the lines changes with the period of simulation.
- **Range Graphs Result:** This shows the values a specified variable took as a function of the arc length of the drill line. The result from the range graphs is the most important result that would be obtained from the OrcaFlex dynamic analysis to this report. It will show us the plot of the effective tension in lines against the arc length of the line. This makes it possible to observe the area of the line that is subjected to the maximum loading.
- **The X-Y Graph:** It shows the vessel movement envelope. This is not very important for the course of this report and its presentation would not be part of this report.

The kinds of result that a user may like to see in OrcaFlex are relatively different. For this report the following are the result which I will be looking at:

1. **Effective Tension**: The effective tension is available at mid-segment points and line ends. Positive value denotes tension and negative value denotes compression. The effective tension is important for this report because it is the governing parameter for buckling of the drill pipe as an Euler strut. It relates to the wall tension with the following relations:

$$P_e = P_w + (P_i A_i - P_0 A_0)$$

Where;

P_e = Effective Tension

P_w = Wall Tension

P_i = Internal Pressure

P_i = External Pressure

A_i = Internal Cross Sectional Area

A_0 = External Cross Sectional Area

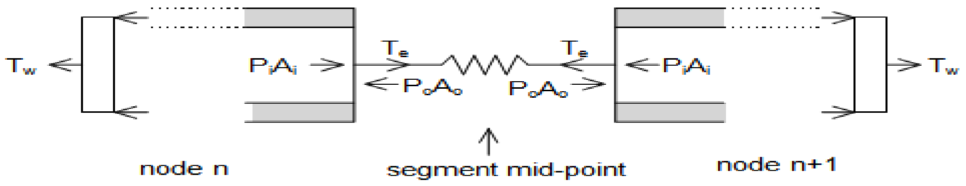

Figure 53: Tension and Pressure Forces (OrcaFlex, 2012)

2. **Wall Tension**: This is important to find out the local buckling of the drill pipe. The wall tension is available at mid-segment points and at line ends. The reported wall tension in this report is the total wall tension and it is actually the tension in the walls of the drill pipe.
3. **API RP 2RD Stress**: Available at mid-segment points and line ends. API RP 2RD Stress is a Von-Mises type stress. The Von-Mises stress combines all principal stresses in the pipe to obtain an average stress that is used for yield criterion. This is important for us in this report to compare with the maximum limiting yield stresses as stated in the parameters of the drill pipe categories.
4. **Solid Contact Force**: The solid contact force reports the clashing of the drill pipe with the walls of the well, in this case, the elastic solid. This is important to measure the clashing force of the pipe with the well to examine it is tolerable with the maximum compressive force on the pipe.

Chapter 7: Analysis Results and Discussion

7.1 Overview of Results

We have presented the results of our findings on the subject matter in this chapter. The RDM-R drill pipe is a product of the Reelwell Company and the results in this chapter of the report is for the project undertaken by the Company in the BG subsalt well in Santos basin, Brazil. All input data were referenced from the said site. The presentation of the results would be in two stages, the manual results and the results obtained from OrcaFlex Software. This is done in order to check the results obtained from the OrcaFlex software static analysis against the static hand calculations. As could be seen from appendix A, the axial load results from the hand calculations and the static results from OrcaFlex are approximately the same.

OrcaFlex Software performed the static and the dynamic analysis on the mechanical model as shown in figure 45 of chapter 6. Due to the relatively subtle wave conditions in the Santos Basin site of the project the difference in the dynamic analysis stresses on the string is about 10% more than the loading during static analysis. This would not have been the case if the same operation were carried out in the North where extreme weather condition is observed and JONSWAP wave spectrum would have been applied. The wave condition in the Santos basin is a double peaked wave. In the model, we used a combination of two wave trains to obtain the doubly peaked waves nature of the site, a combination of swell and normal wave. This necessitated the used of two wave spectrums, the Gaussian Swell spectrum and the Dean's wave spectrum. The combination of these wave trains can be found in figure 48.

The following are the purposes of carrying out the dynamic analysis:

- To obtain the forces and tensions in the riser at the hook/hang-off point (End A).
- To determine the the position of the maximum, minimum stresses and deflections.
- To obtain the API-RP-2RD stress and compare it with the API-RP-2RD limiting stress.
- To obtain the solid contact force or the clashing force with the RCD and the BOP walls.
- All the above analysis and results are based on the prevailing environmental conditions as enumerated in chapter 6.

The simulation was done in two stages, at 3000m total depth (TVD) and at 5000m TVD. Total vertical depth (TVD) is the total vertical depth of the pipe. As explained earlier, at the present stage of the project the well has been drilled up to 3000m TVD by conventional method. The Reelwell Company will start drilling from 3000m TVD to 5000m TVD using riserless drilling with RDM-R method. This is the reason why the simulations are done in the aforementioned two stages to know the window of forces between which the drill string would be made to operate.

7.2 Discussion of Results

7.2.1 Static Results

The static results show the reports on some properties of interest at conditions where there are no waves, currents nor wind forces acting on the string or the vessel. The simulation period was slated at 30s for the model to attain equilibrium position and calculations of these properties are made at equilibrium. One of the limitations of OrcaFlex Software is in its inabilities to go beyond the mud line. What we have done as an approximate model is to calculate the properties below the mud line and lump it on the string above the mud line. This is the reason why the tension and forces appears wavy in the extracted figures below.

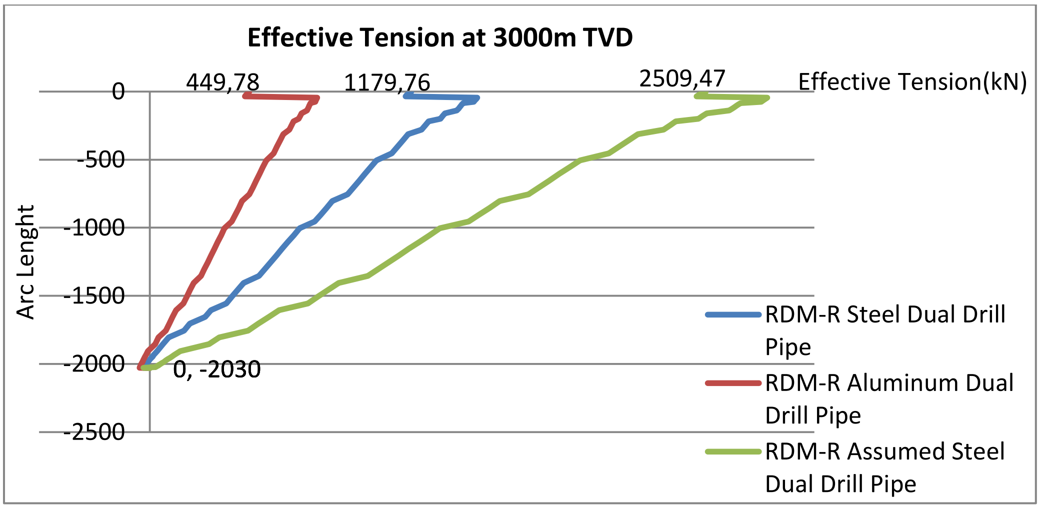

Figure 54: Effective Tension at 3000m TVD

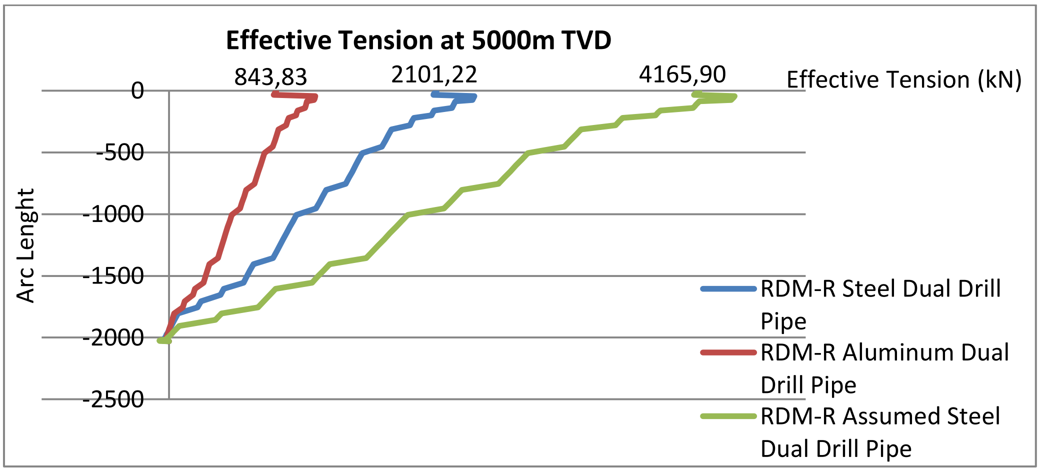

Figure 55: Effective Tension at 5000m TVD

OrcaFlex Software solves the model with a finite element method by dividing the string into sections and nodes. What we have done is to lump the properties equally on every node above the mud line and below the sea level. This is why at 3000m and 5000m below the sea level the graph shows a 2030m length of the string.

A drastic drop in both the effective tension and the wall tension is noticed in figures 54 through to figure 57. This is because the two properties are functions of the pressure differentials between the external and internal pipe's environment. At water level the difference in pressure becomes higher as the fluid changes from water to air. The density of air is negligible compare to the density of the fluid which invariably causes the sharp drop in the value of the properties as we go towards the hook position.

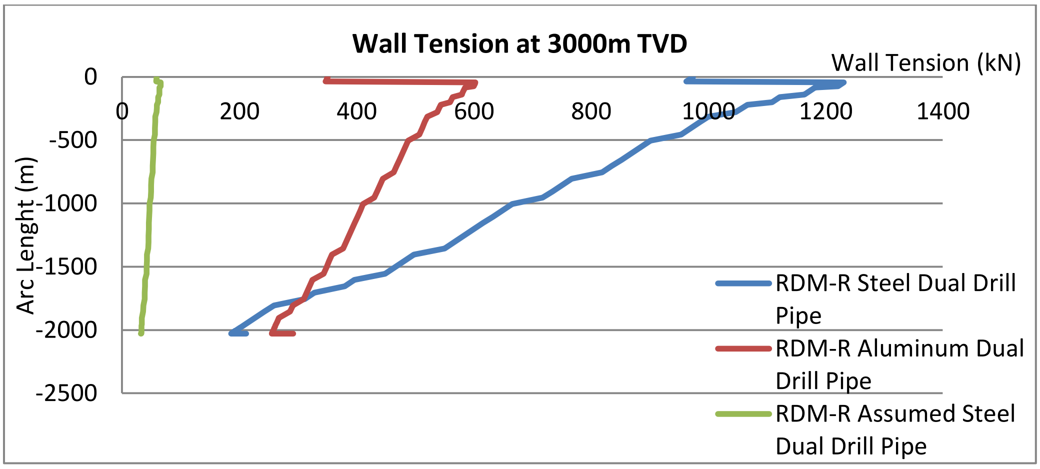

Figure 56: Wall Tension at 3000m TVD

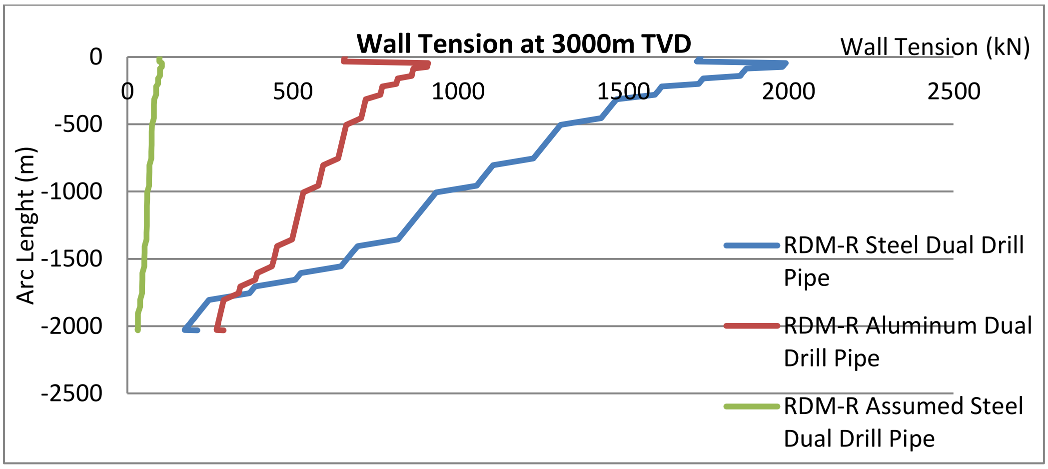

Figure 57: Wall Tension at 5000m TVD

The effective tension is the same as the top tension or the measurement at the hook point. This is approximately equal to the manual calculations in appendix A. The aluminum DDP has the smallest effective wall tension because of its relatively small material density and large external volume that created a large buoyancy force. The buoyancy force reduces to a large extent the hook load. In chapter 6 of this report we showed the relationship between the effective tension and wall tension. We believe that because of the high fluid content density coupled with the large internal area for the assumed steel pipe might have caused it to have the smallest wall tension value. This might have been over exaggerated because of the approximated fluid content's density used for the simulation.

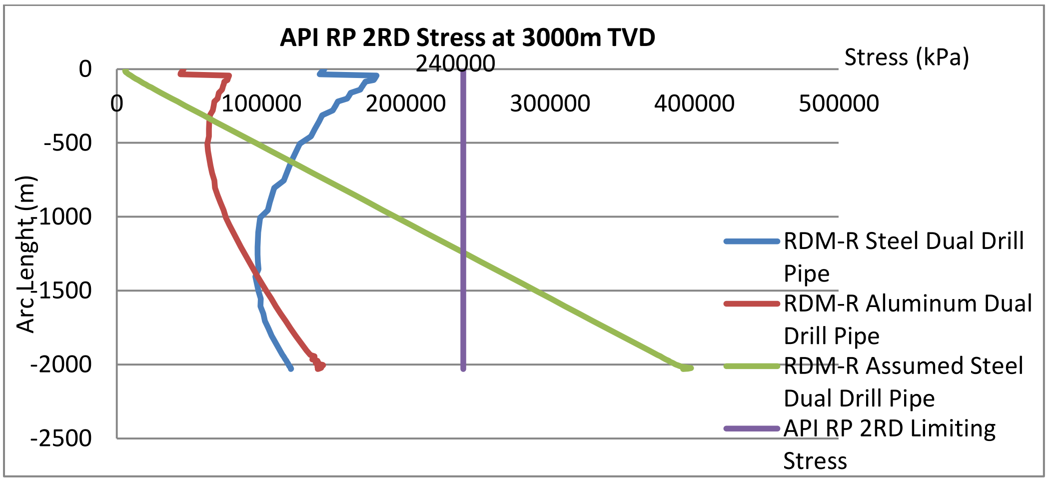

Figure 58: API RP 2RD Stress at 3000m TVD

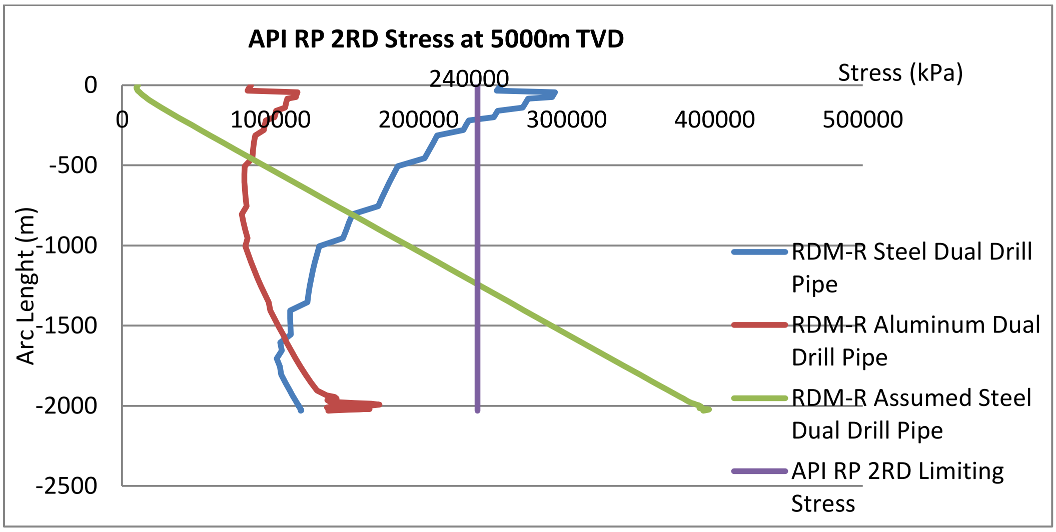

Figure 59: API RP 2RD Stress at 5000m TVD

Figures 58 and 59 shows the API RP 2RD stresses for the pipes. The API RP 2RD stress is a Von-Mises type of stress. The Von-Mises stress combines all principal stresses acting in the pipe to obtain an average stress that is used for yield criterion. The stresses are drawn against the API RP 2RD limiting stress as shown above. We would like to point out here that the limiting stress that is used as a standard API RP 2RD limiting stress by Orcaflex Software and as such used in this analysis is a lower grade material compare to the grade of material that is used for the RDM-R DDPs. The limiting stress value as recorded for this lower grade material was put at 240 MPa against the 817 MPa for the RDM-R steel DDP and 400 MPa for the RDM-R aluminum DDP but interpretation of the result would be based on what the situation is in the simulation.

At 3000m below water line the steel DDP and the aluminum DDP Von-Mises stress values are less than the limiting stress value. This shows that the material is below its yield point when subjected to the said conditions. As length of the string increases however, the steel DDP surpasses the limiting stress. This means that at some point before 5000m TVD the material will enter yield region.

The assumed steel DDP Von-Mises stress value surpasses the limiting stress value at 1000m TVD and 3000m TVD. As the length of the string exceeds 1000m the pipe material will enter the material yield region. Its behavior in the Von-Mises stress may be due to the high content density used to compensate for the equivalent pipe dimensions. The effect of this is that the hoop's stress, $\sigma_{\theta\theta}$ dominated the axial stresses, σ_{zz} and the radial stresses, σ_{rr} in the Von-Mises stress at every section of the pipe. And as the hoop's stress increases with depth the Von-Mises stress increased linearly as the depth increases.

As would be expected, the clashing force during static is the same in all cases.

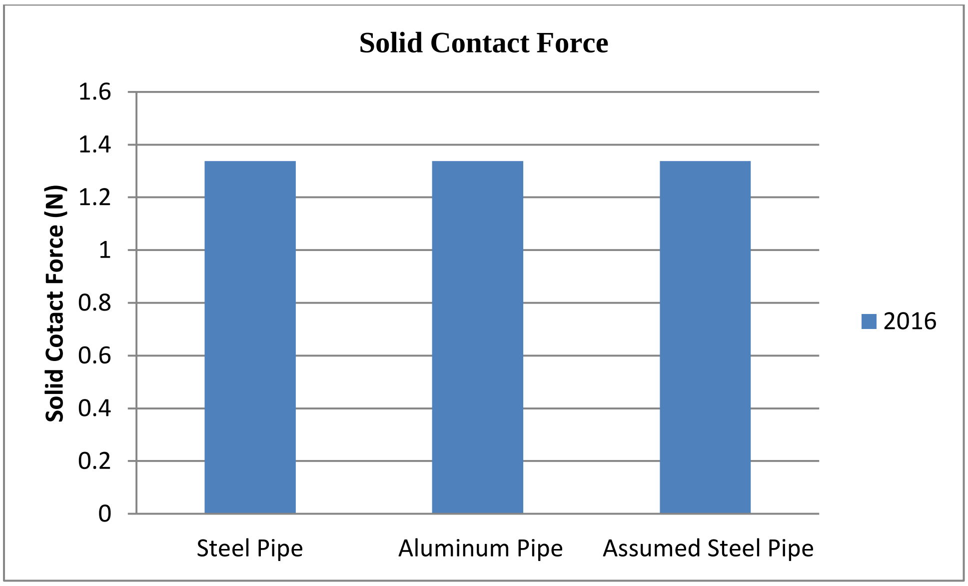

7.2.2 Dynamic Results

In this section of the report we have reported the effective tension, the wall tension, the API RP 2RD stress and the clashing force at 3000m and 5000m below sea level. These properties of the lines are as explained above for the case of the static conditions. In addition to the environmental condition during the static simulation, the dynamic analysis adds the current effect, wave effect, wind effects and the influence of vessel motions and RAOs. As could be seen, the results from the dynamic simulations add an approximate of 10% in addition to the results from static simulation for the effective tension and the wall tension properties.

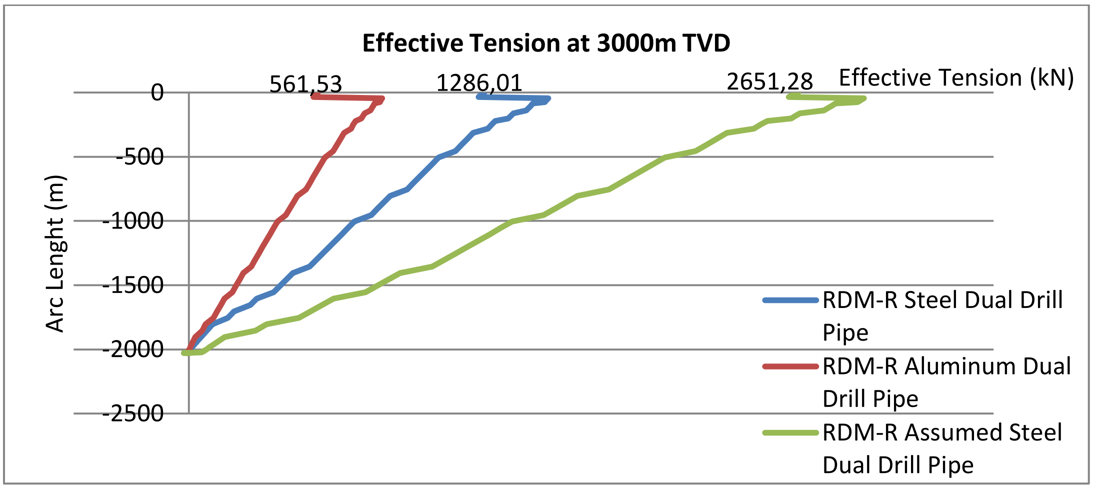

Figure 60: Effective Tension at 3000m TVD

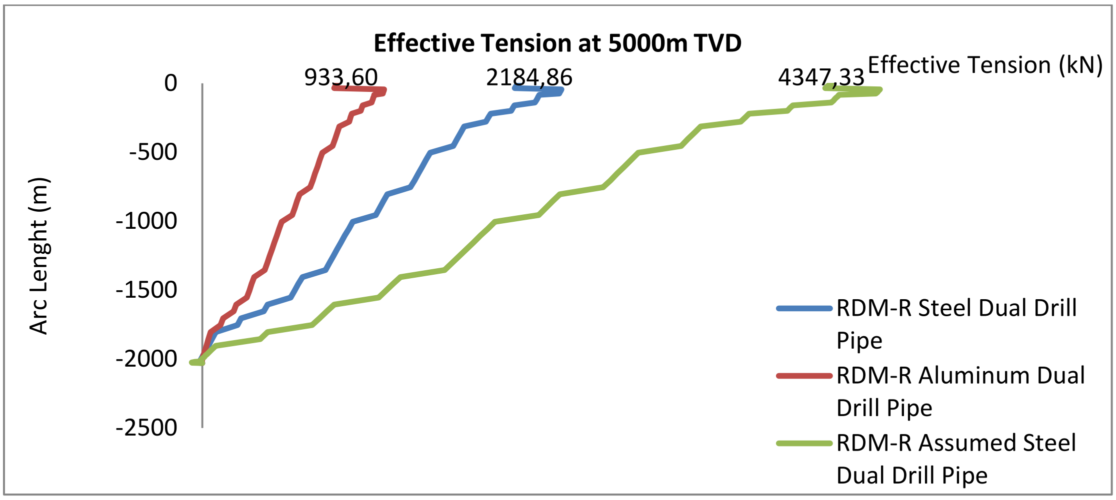

Figure 61: Effective Tension at 5000m TVD

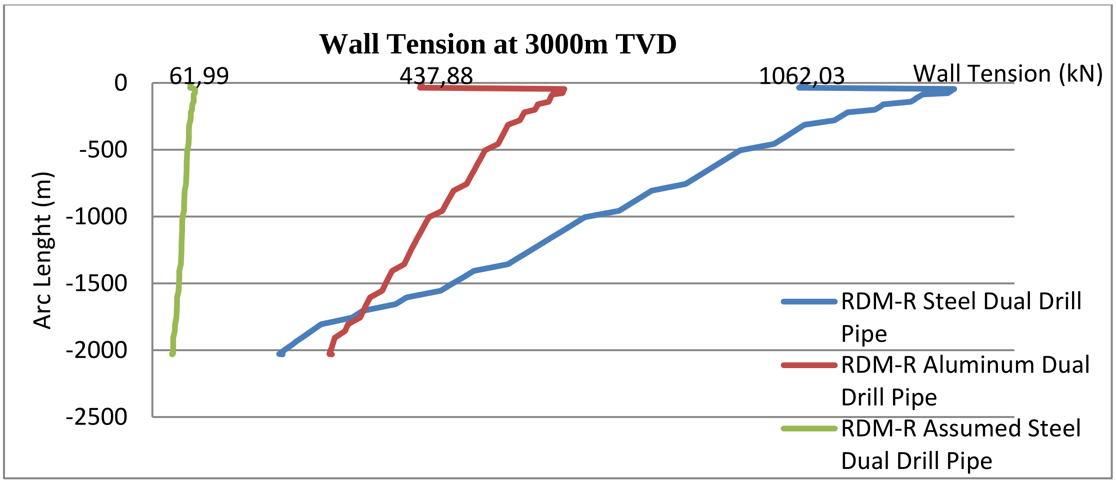

Figure 62: Wall Tension at 3000m below Sea Level

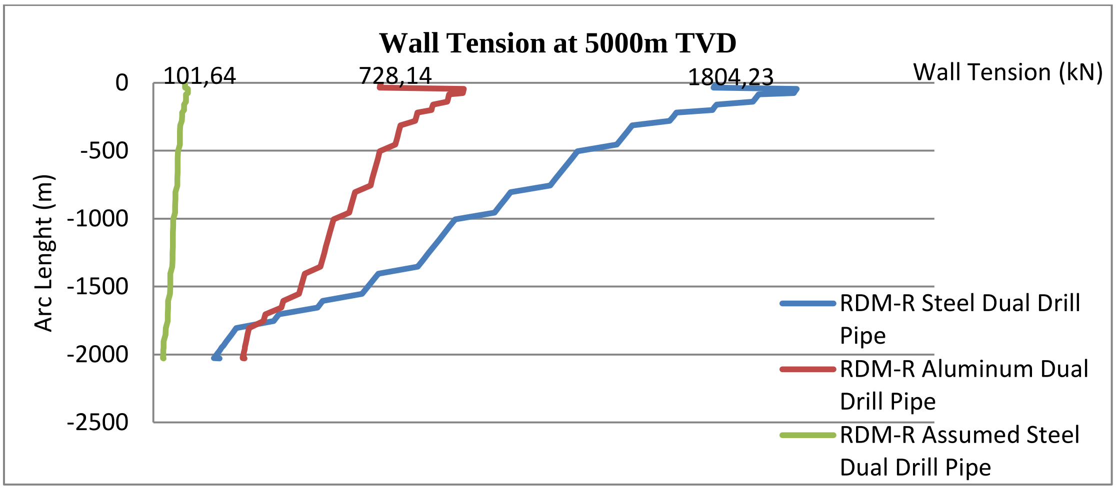

Figure 63: Wall Tension at 5000m below Sea Level

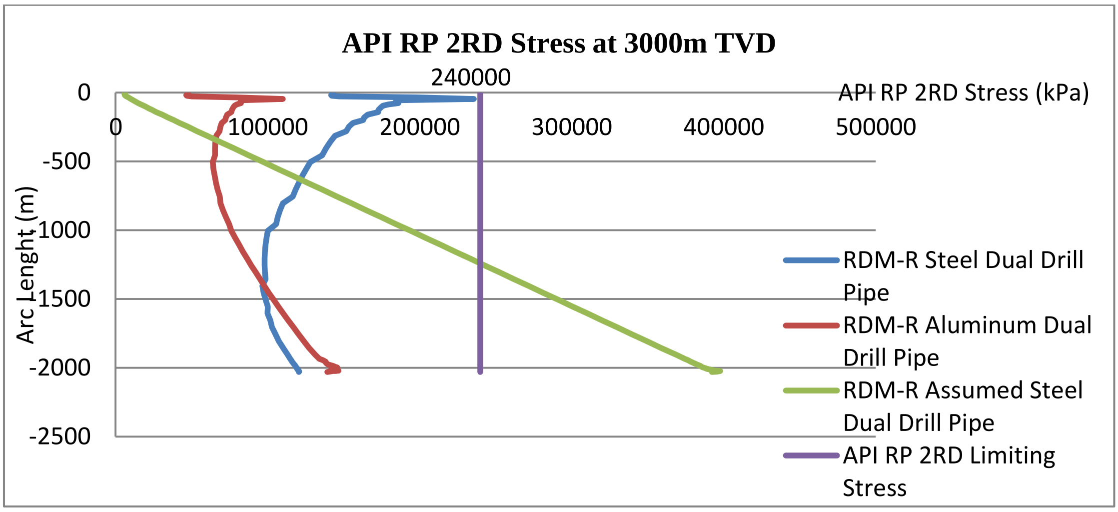

Figure 64: API RP 2RD Stress at 3000m below Sea Level

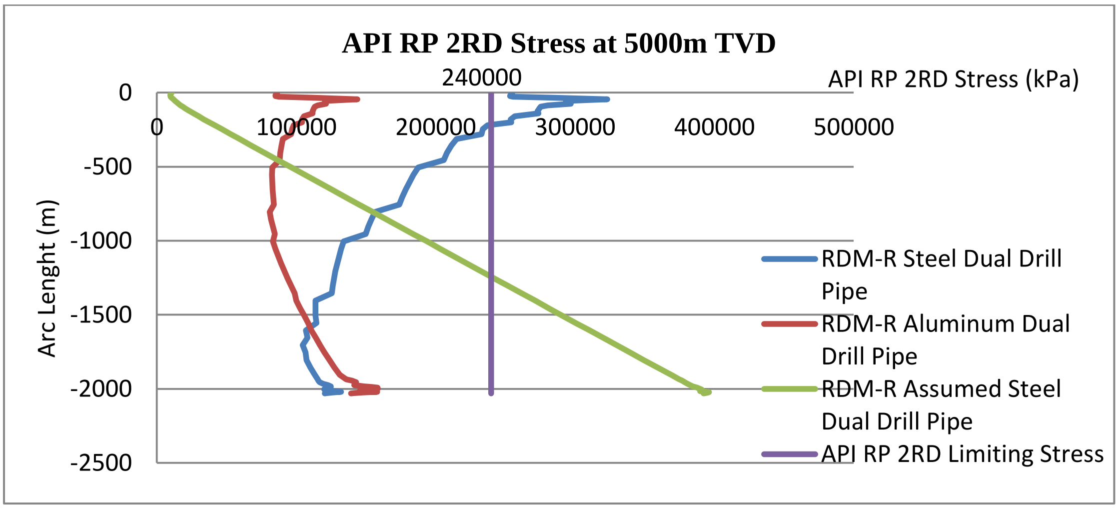

Figure 65: API RP 2RD Stress at 5000m below Sea Level

Figure 66 and figure 67 shows the clashing force during the dynamic simulation of the model. The clashing force reports the contact force between the lines and the wall of the subsea stack. This is done to serve as an input for the design of the RCD. The subsea stack is assumed to be 10m above the mud line. The top 2m is assumed as the height of the RCD and 8m for the rest of the subsea stack as shown in previous chapter. This is why we have chosen to plot only the sections where contact may occur, that is, between arc length 2010 and 2030. The forces observed are as shown below. The contact force should be checked against the limiting force of impact or lateral force that the pipe can be exposed to before it collapse or fails. The analysis was carried out at a position just above the subsea stack. This may not be the case during operation due to vessel moving off-position horizontally. When this happens, the contact force may record even greater value and it should be checked.

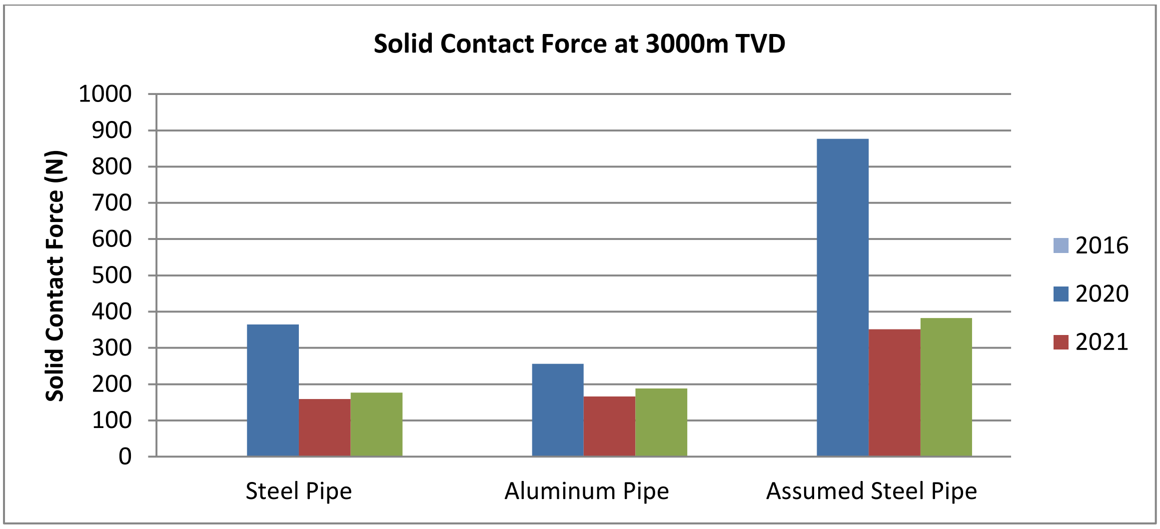

Figure 66: clashing Force Report at 3000m below Sea Level

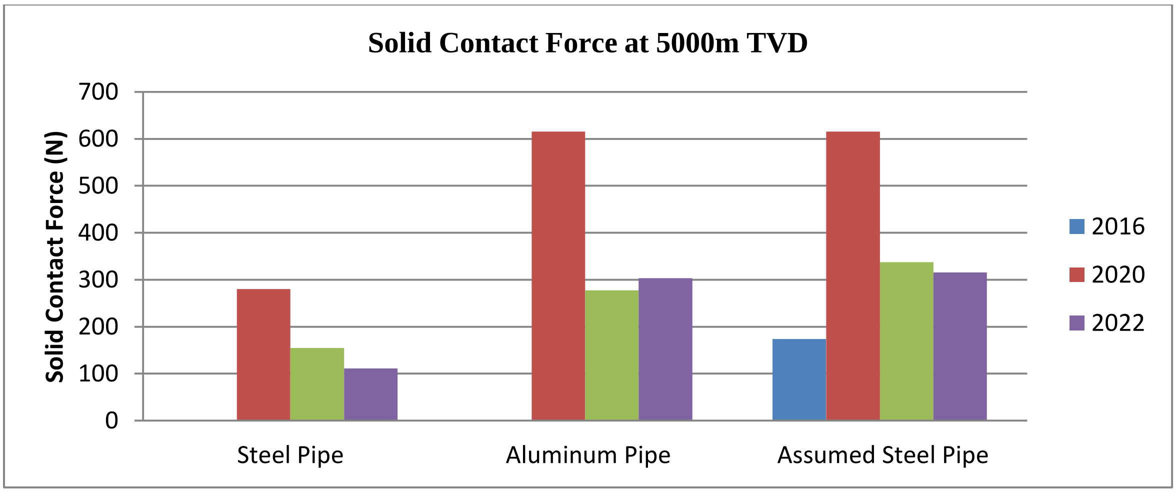

Figure 67: clashing Force Report at 5000m below Sea Level

7.2.3 Oscillating Dynamic Load for Top Drive Design

The drill string is exposed to varying load during operation and as a result of the varying nature of the environmental loads and the dynamic behavior of the drill vessel. The string itself is suspended from the top drive system mounted on the mast or derrick of the vessel for rotation during drilling operation. The top drive system is a mechanical device operated electrically or hydraulically to provide torque to the drill string. Some of the things that need to be considered when selecting a top drive system for a particular project are the power rating on the motor for drill pipe rotation and the safe working load (SWL) of the tool. There are different designs of the top drive system with different SWL capacity. The purpose of this section is to show the expected varying loads with time to determine the optimum top drive system that could be employed for the project.

	Maximum (kN)	Constant Tension (kN)	Minimum (kN)
Steel	1300	1180	1140
Aluminum	560	450	320
Assumed Steel	2650	2510	2360

Table 9: Load Varying at 3000m

	Maximum (kN)	Constant Tension (kN)	Minimum (kN)
Steel	2200	2150	2000
Aluminum	950	840	870
Assumed Steel	4340	4180	3980

Table 10: Load Variation at 5000m

Appendix D shows the distribution of the load with time for the environment conditions stated in the previous chapter. This varying load may be an input for the system's heave motion compensator. The heave compensating system facilitates a constant tension in the string. There is need to maintain a constant tension in the string to avoid excessive compression that could lead to buckling.

7.2.4 Magnus Effects on Rotating Drill String

When the drill pipe is rotated in current of water, a force is generated sidewise of the vertical pipe. This force is called the lift force. The lift force is generated by virtue of the drag of the pipe against the motions of the water that makes the streamline asymmetry over the pipe causing more concentration on one side of the pipe as shown in figure 68 below.

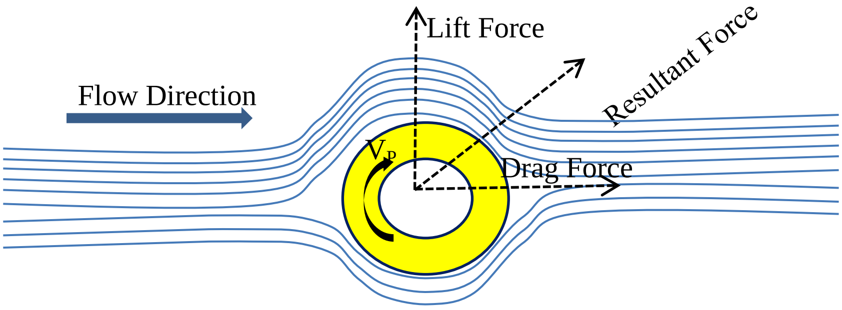

Figure 69: Magnus Effect on Rotating Pipe

High concentration of the streams means a relatively higher velocity and low pressure. There is always a motion in the direction of lower pressure which, in this case, is the lift force as shown in figure 68 above. In order to adjust to the change in pressure across it, the pipe will move in the direction of the resultant force between the lift force and the drag force as shown in figure 68. This motion due to the resultant force is called the Magnus effect and it is a function of the velocity of the water current and the speed of pipe rotation.

The resultant force, F acting on the pipe is then:

$F = \sqrt{{F_L}^2 + {F_D}^2}$ at an angle, θ

Where:

Lift Force, $F_L = C_L A \frac{\rho {V_C}^2}{2}$

Drag Force, $F_D = C_D A \frac{\rho {V_C}^2}{2}$

$\tan\theta = \frac{C_D}{C_L}$

C_L, C_D = Experimental Values for lift coefficient and drag coefficient of a rotating cylinder of infinite length in a position perpendicular to the direction of flow.

Current Velocity = V_C

Peripheral Velocity of Pipe = V_P

Fluid Density = ρ

Projected Area of Pipe = A

Therefore, $F = \sqrt{{F_L}^2 + {F_D}^2} = \frac{\rho A {V_C}^2}{2}\sqrt{{C_L}^2 + {C_D}^2}$

The values of lift coefficients are shown in table 11. These values are functions of the ratio of the water current velocity and the peripheral speed of the pipe. The corresponding drag coefficients are obtained from experiment. The angle for the resultant force is calculated from the formulae given above and values are reported in the table.

$\frac{V_P}{V_C}$	C_L	C_D	$\tan\theta$	θ
0	0	1.2	∞	90.0
2	4.0	2.8	0.7000	35.0
4	11.0	5.0	0.455	24.5
6	13.8	5.0	0.362	19.9
8	15.0	5.0	0.333	18.4
10	15.5	5.0	0.323	17.9
12	16.0	5.0	0.285	15.9

Table 11: Lift and Drag Coefficients (National Academy of Science, 1960)

Assuming the speed of rotation of the pipe is between 120 RPM (1.06 m/s) to about 150 RPM (1.32 m/s) and the current speed is slated at 0.6 m/s typical of the Santos Basin, the calculated resultant force as a result of Magnus effect is approximately 354 kN for the steel DDP, 417 kN for the aluminum DDP and 409 kN for the assumed steel acting at angle 35^0 to the direction of current.

In conclusion to this sub-chapter, the string would only be rotated at a high speed when the pipe has penetrated to an appreciable depth, we can assume therefore that approximately half of the calculated force will be felt by the vessel in the direction of the resultant force (National Academy of Science, 1960).

7.2.5 Fatigue Analysis

Due to exposure to oscillating environmental loads and the random movement of the vessel the slender drill string would be exposed to fatigue. According to DNV-OS-F201 (2010), fatigue analysis on riser should consider the following relevant cyclic loads:

- VIV
- First order wave effects
- Second order floater motion
- pressure and thermally induced cyclic stresses
- Collisions

The contribution of the first order wave to fatigue damage is most significant and that is what we would concentrate on discussing and addressing. The contributors to the drill string-wave fatigue loading include the content density, environmental conditions, water depth, drill vessel and its motion characteristics. For the explanation of the fatigue damage, the S-N curves fatigue assessment will be used in reference to DNV-OS-F201 (2010) and DNV-RP-C203 (2010).

To use S-N curves for fatigue check in the pipe the following must be considered:

1. Short-term distribution of nominal stress range
2. Selection of appropriate S-N curve
3. Thickness correction factor
4. Stress concentration factor (SCF)
5. Accumulated fatigue damage (D_{fat}) over all short term conditions.

Fatigue capacity is given in terms of S-N curves to show the number of stress cycles to failure (N) for a specified constant stress range (S). Expressed as:

$N = \bar{a}S^{-m}$ ($\bar{a}$ and *m* are empirical constants established by experiments).

In fatigue damage calculations, the applied stress range is obtained by application of a stress concentration factor (*SCF*) and thickness correction to the nominal stress range. Expressed as follows:

$$S = S_o \cdot SCF \cdot \left(\frac{t}{t_{ref}}\right)^k$$

Where:

S_o Nominal stress range

t Thickness through which a crack will most likely grow.

t_{ref} Reference thickness.

= 25 mm for welded connections other than tubular joints.

= 32 mm for tubular joints

= 25 mm for bolts

k Thickness exponent (a function of the actual structural design) on fatigue strength

= 0.10 for tubular butt welds made from one side

= 0.25 for threaded bolts subjected to stress variations in the axial direction

$\left(\frac{t}{t_{ref}}\right)^k$ Thickness correction factor

Figure 68 below shows some S-N curves for welded, tubular and other types of joints obtained from DNV-RP-C203 (2010).

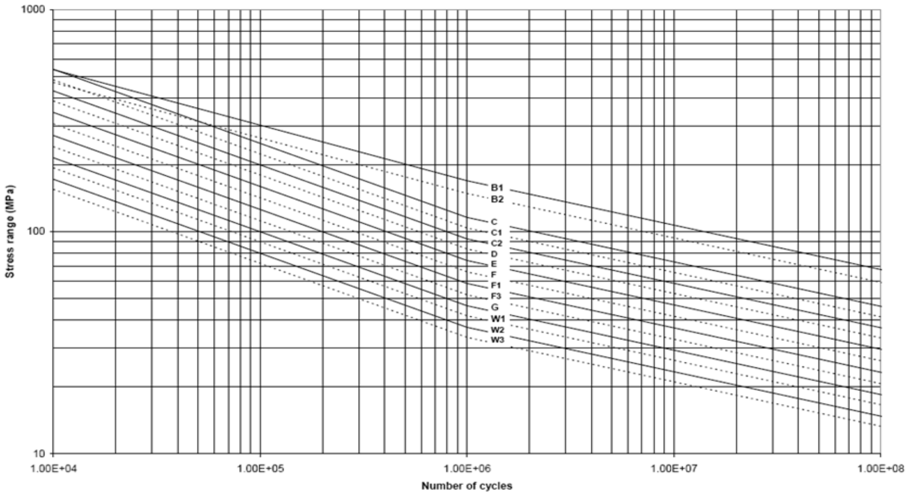

Figure 68: S-N Curves for Seawater Environment with Cathodic Protection (DNV-RP-C203, 2010)

7.2.5.1 Stress Concentration Factor

This is the ratio of the hot spot stress to the local nominal stress. The spot in the structure where a fatigue crack may initiate is called the hot spot.

7.2.5.2 Accumulated Fatigue Damage (D_{fat})

The fatigue criterion to be satisfied is:

$$D_{fat} \cdot DFF \leq 1.0$$

where:

D_{fat} Accumulated fatigue damage defined from Palmgren-Miner rule

DFF Design fatigue

According to Palmgren-Miner rule,

$$D_{fat} = \sum_i \frac{n(S_i)}{N(S_i)}$$

Where;

$n(S_i)$ The number of stress cycles with range S_i

$N(S_i)$ The number of stress cycles to failure.

7.2.5.3 Fatigue Analysis Procedure

The general approach for calculation of wave induced fatigue damage is given below:

- The wave environment scatter diagram is subdivided into a number of representative blocks.
- Within each block, a single sea-state is selected to represent all the sea states within the block. This representative sea state has the highest probability of occurrence within the block.
- The fatigue damage is estimated for each selected short-term sea state for all the blocks.
- The fatigue damage over all the blocks is summed up, taken into consideration directional probabilities, to obtain the weighted fatigue damage from all sea states.

- The fatigue life is the reciprocal of this weighted fatigue damage.

Due to unavailability of comprehensive wave data from the site the fatigue damage would not be carried out in this report. I recommend that at list a 10 years return wave be used to completely ascertain the damage due to accumulated fatigue on the line.

7.2.6 Equivalent Pipe Properties

The Appendix C of this report contains the pipe properties calculations for the equivalent pipe. The equivalent pipe is used to model the pipe in pipe situation of the dual drill strings. What OrcaFlex does is to calculate the combined properties of the outer and inner pipes, that is, the members and sums it into one single representative pipe member with single properties like mass, stiffness, geometry, etc. This single pipe is the equivalent pipe that is used for the simulation.

The disadvantage of this method is that the equivalent pipe has a smaller internal diameter that reduces the volume of the fluid content. What we have done is to calculate the total volume of the supposed volume of fluid and calculate a density higher than the fluid density to compensate for the loss in the fluid content weight. This may not be totally correct because the wall tension is a function of the pressure differentials between the internal and the external sides of the pipe. As we have increased the content's density the difference becomes very high that it affects the results of the effective wall tension. In addition to this, the fluids content inertial force too may affect the dynamic behavior of the equivalent pipe which may give results lower than the expected results. There are indications that the new version of the OrcaFlex Software can be used to model a better pipe in pipe situation, I recommend that subsequent works on this same subject matter should consider this.

7.2.7 RDM-R and CRD on Axial Loads

The idea behind riserless drilling is to totally eliminate the high cost marine riser. Aside from high cost, the marine riser has also been unsuccessful in many deep water applications due to its weight, size, hydrodynamic behavior and other reasons as mentioned in previous chapters. A typical 21" marine drilling riser may reach up to 50" and may weigh up to 500 lb/ft (743.76 kg/m) with the weights of other attachments included (Leach et al, 2002).

The above statement by Leach and the group forms the basis of our argument in comparing the top drive load requirement or the axial load requirements on the vessel for the dual drill string and the marine riser. We would compare graphically and show why RDM-R by the Reelwell AS Company is the better alternative compare to the conventional riser drilling (CRD) for the Santos Basin project. The Reelwell Company has stated that, theoretically the RDM-R method has been proven to be an effective method for deep and ultra-deep waters drilling without any need for high expensive 5th or 6th generation drilling vessel, this section of the report will also buttress this fact with the graphical representation of the top drive axial load requirement for the RDM-R method and the CRD method that uses marine riser. These axial loads would be compared against the top drive axial load capacities of some chosen drilling rigs that can operate in water depth above 2000m.

The following data are used for the drill string and marine riser in CRD:

Marine Riser + Accessories =	743.8	kg/m^3
Mud weight density =	12.52	ppg (1500 kg/m^3)
Seawater density =	8.6	ppg (1025 kg/m^3)
Height above the sea level =	10	m.
Marine riser outer diameter =	21	inches (0.5334 m)
Marine riser inner diameter =	19.5	inches (0.4953 m)
Material Density =	7850	kg/m^3
Drill string =	6 5/8	inches (0.1683 m)
Weight of Riser and Attachment =	500	lb/ft (743.76 kg/m)
Drill string Weight in air =	40.9	kg/m
Sea depth =	2000	m

Rig Name	Rig Generation	Max Water Depth[1] (m)	Variable Deck Load Capacity[1] (ton)	Liquid Mud Capacity[1] (m3)	Top Tension Capacity[1] (ton)	**Top Drive Capcity[1] (tons)**	Day Rate[2] ($)
Saipem's Scarabeo 5	4th	2000	3400	380	880	**650**	> 400k
Transocean's Sedco Energy	5th	2286	6000	715	1088	**750**	> 500k
Odfjell's Deepsea Stavanger	6th	3000	7500	760	1450	**900**	> 600k

Table 12: Drilling Rig Capacity and Day Rates *1 = Extracted from company's website*
2 = Extracted from E&P Magazine, March 19, 2013

Table 12 above shows the various load capabilities and day rates for different generations of drilling rig. The data are obtained and used as typical characteristics of a particular generation of the rig, values of these characteristics may change depending on the rig type and make. As would be noticed from the table, all chosen generations of rig have the ability to be utilized in water depth in excess of 2000m. This is so because the Santos Basin Project is in water depth greater than 2000m, therefore, the water depth capacity of the any rig for the project must be able to operate in an environment in excess of 2000m water depth.

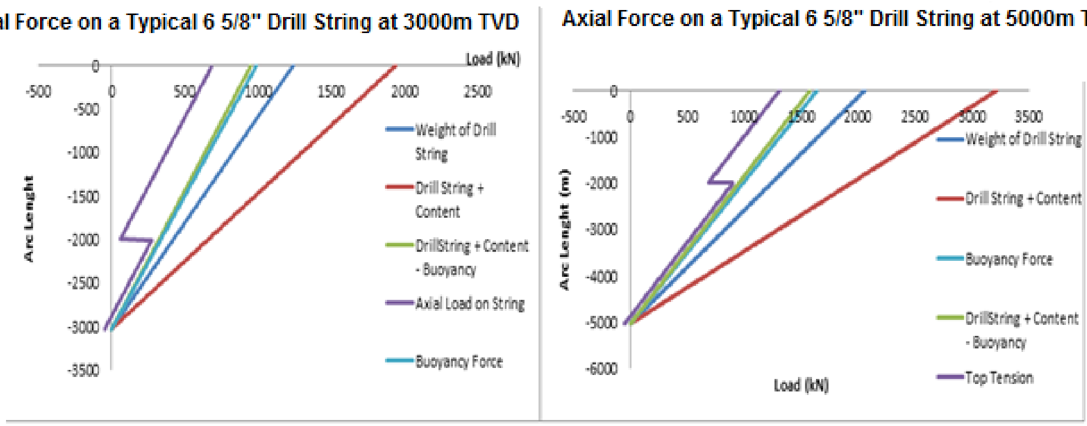

Figure 69: Axial Load on a Typical Conventional Drill String

Figure 69 above shows the axial loads or the top tension on a typical 6 5/8 string at 3000m and 5000m under static conditions. This load is very important in identifying the hook load requirement on the top drive assembly as will soon be discussed in the top drive design for the RDM-R dual string. The top drive is a mechanical element that suspends the drill string and serves the purpose of allowing vertical movement of the pipe in dynamic conditions. It facilitates the drilling process by serving as a compensator for heave motions. Figure 70 below shows the axial force on the marine riser at 2000m water depth. The liquid mud capacity can only be handled by nothing less than the 5th generations or 6th generation drill rigs. This is one of the reasons, amongst others, why it is impossible to extend the use of a lower generation rigs with conventional riser drilling in deep and ultra-deep water environment.

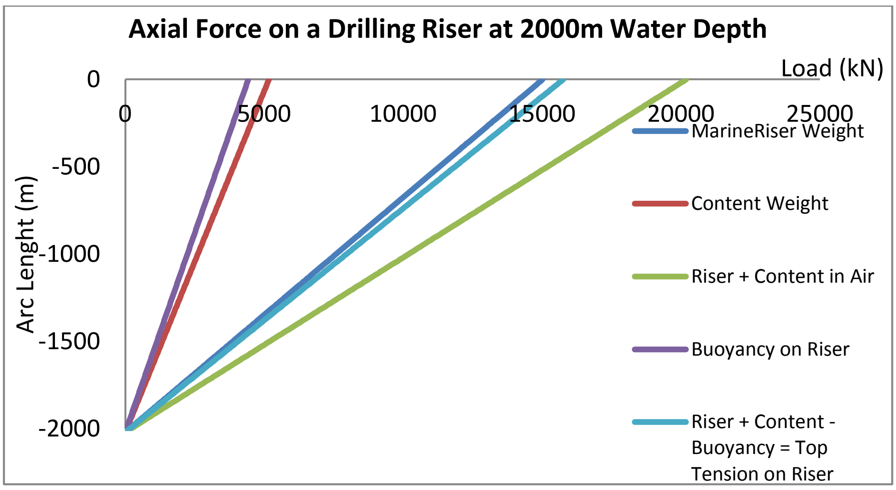

Figure 70: Axial Force on Marine Riser at 2000m below Sea level

The top tension rating is in excess of 1500 tons. It is clear that for the water depth under consideration even the stated 6th generation drill rig cannot handle the axial load at the tensioner end. We should point out that they are some 6th generation drill rigs, few and expensive, that could operate at this depth and with such enormous force.

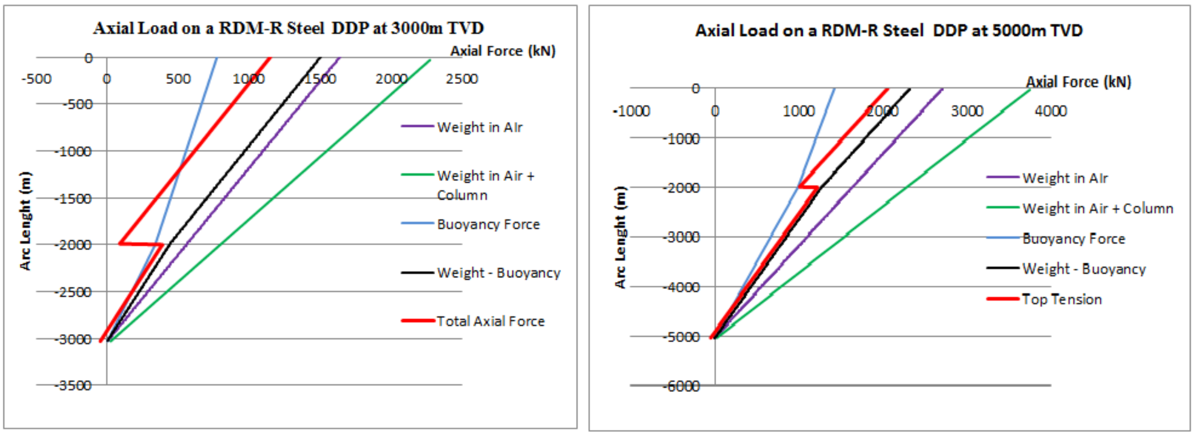

Figure 71: Axial Forces on RDM-R Steel DDP

Figures 71 through to figure 73 shows the manually calculated axial forces on the categories of string These includes the steel DDP, the aluminum DDP and the assumed steel DDP at 3000m and 5000m below sea level.

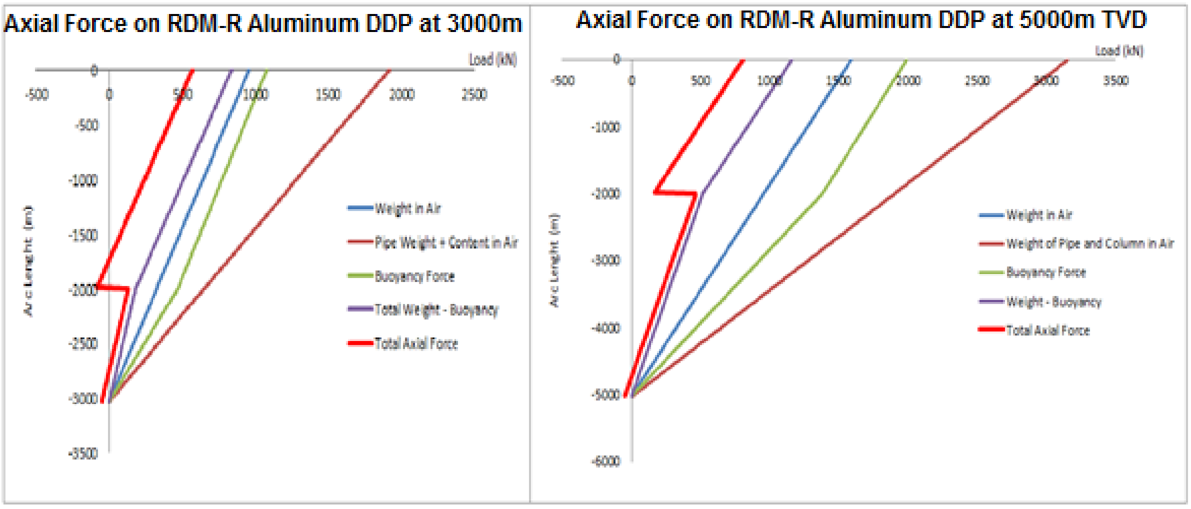

Figure 72: Axial Forces on RDM-R Aluminum DDP

Figure 74 and 75 below show the axial loads and the top tension requirement of the RDM-R DDPs and the marine riser at 3000m below sea level. Figure 76 and 77 below also show the top tensions at 5000m below sea level. Included in the figures are the top drive capacities of the drill rigs as extracted from table 9. We included the rigs' capacities to show their limits against the actual top drive axial loads requirements of the dual strings and the marine riser. The aim of reporting and discussing the figures from figure 74 to figure 77 is to buttress the fact that the application of the marine riser may have reached its limit both technologically and economically. Although 6th generation rigs have been reported to operate in water depth in excess of 10000 feet but with the increase in the top tension requirements as water depth increases may pose even bigger challenges that makes the extension of this marine riser technology beyond its present use.

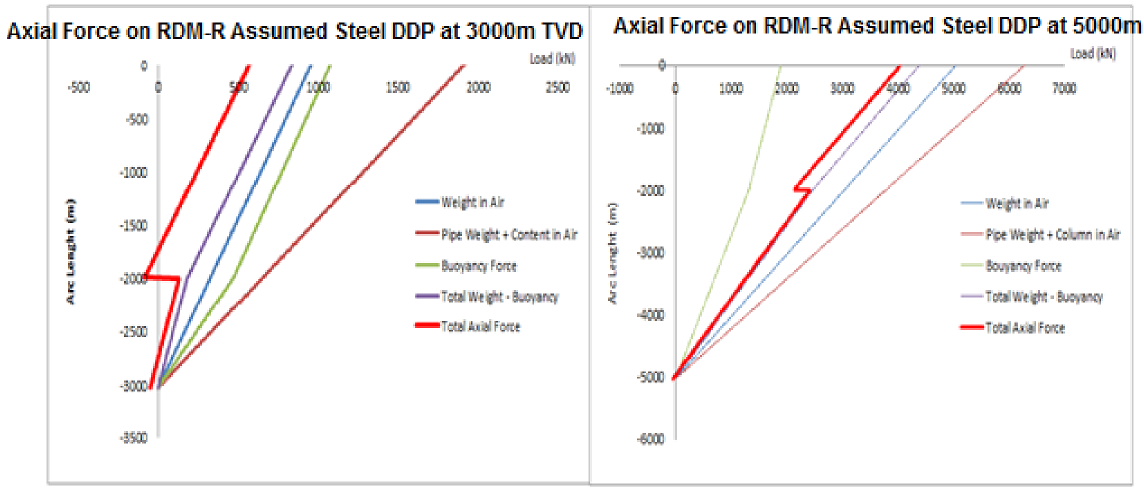

Figure 73: Axial Forces on RDM-R Assumed Steel DDP

The figures also show different contributors to the top tension for the dual strings. It can be seen from these that the RDM-R strings is an effective method in ultra-deep waters on a 4th generation drill rigs. As TVD increases the top tension also increases. Therefore, a higher generation rig may be required when the TVD is in excess of 3500m for the RDM-R assumed steel pipe. For the RDM-R steel pipe, at TVD of about 3800m a higher generation rig may be required while for the RDM-R aluminum pipe in excess of about 4200m.

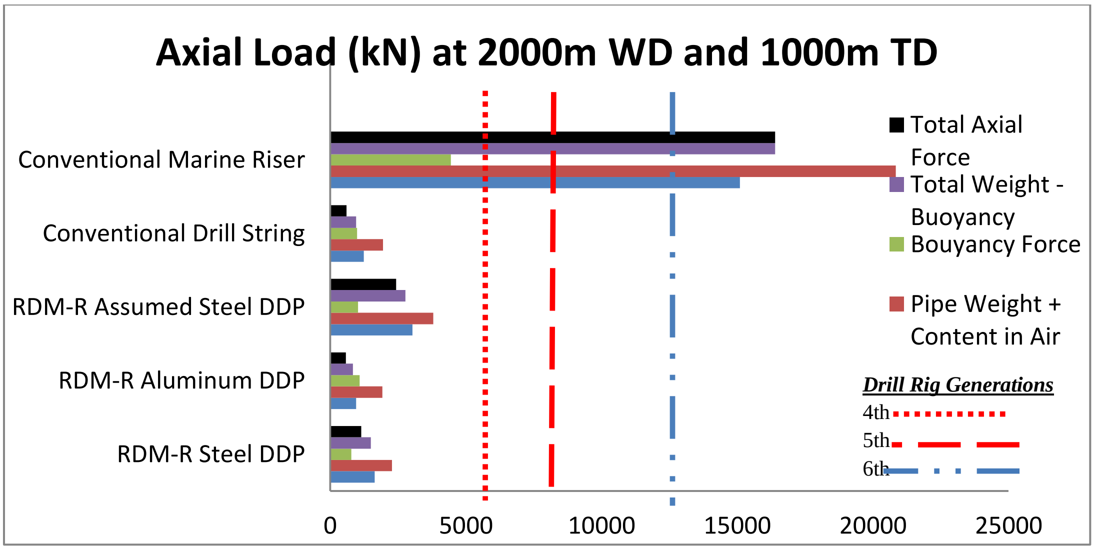

Figure 74: Top Drive Capacity Comparison at 3000m below Water Level

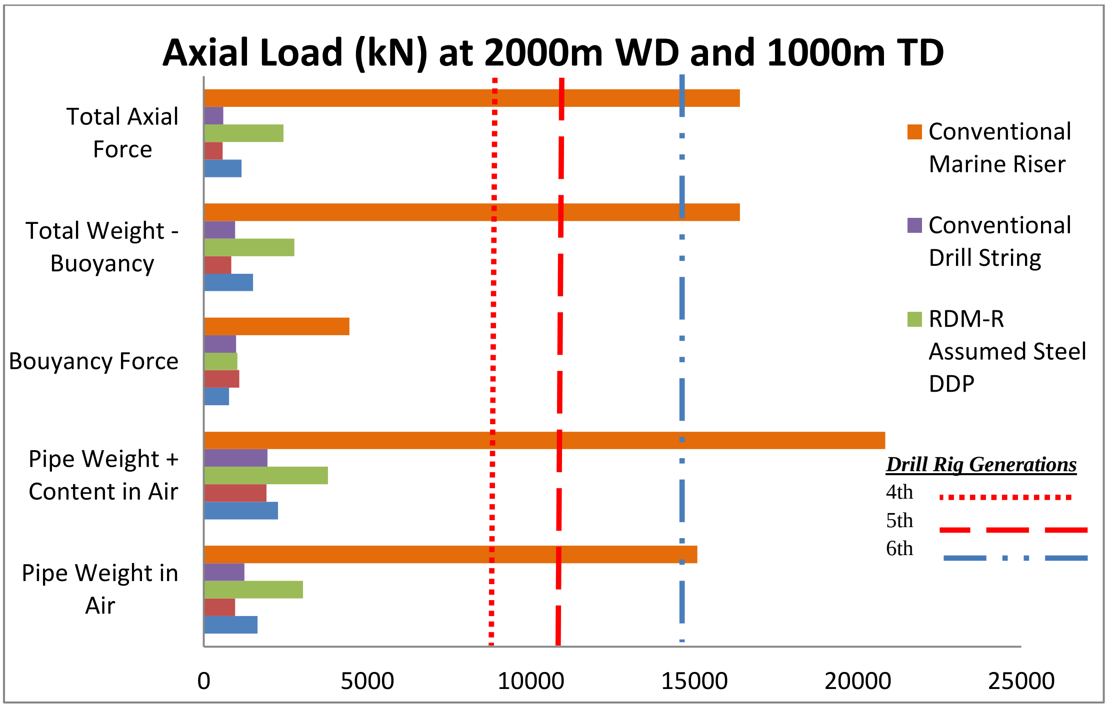

Figure 75: Top Drive Capacity Comparison at 3000m below Water Level

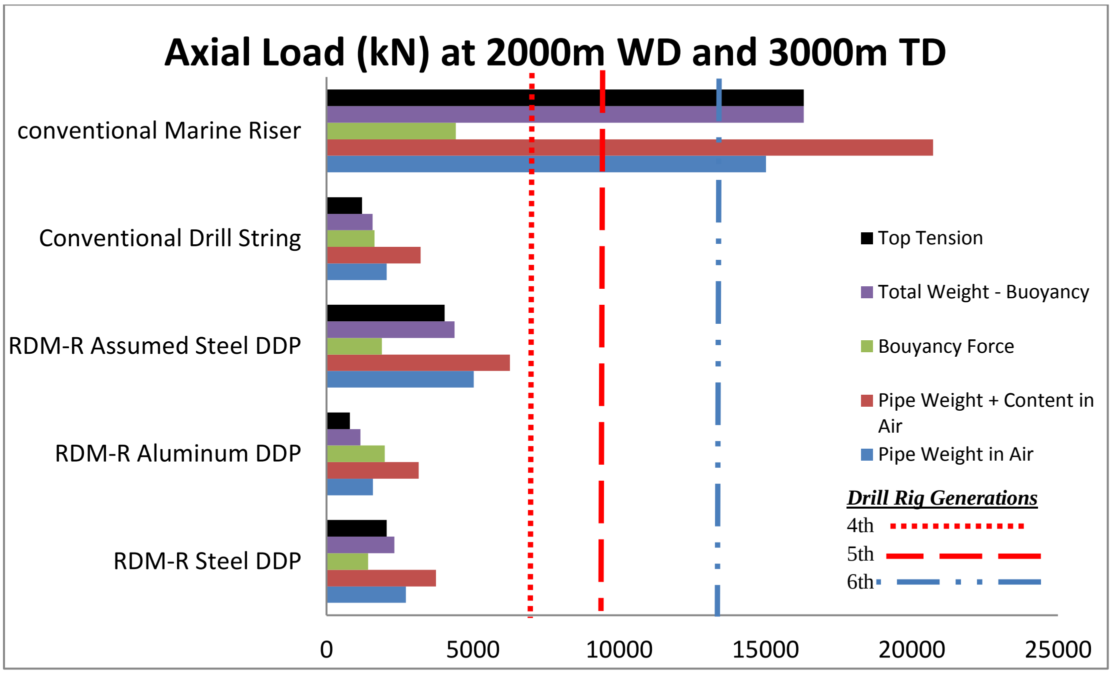

Figure 76: Top Drive Capacity Comparison at 5000m below Sea Level

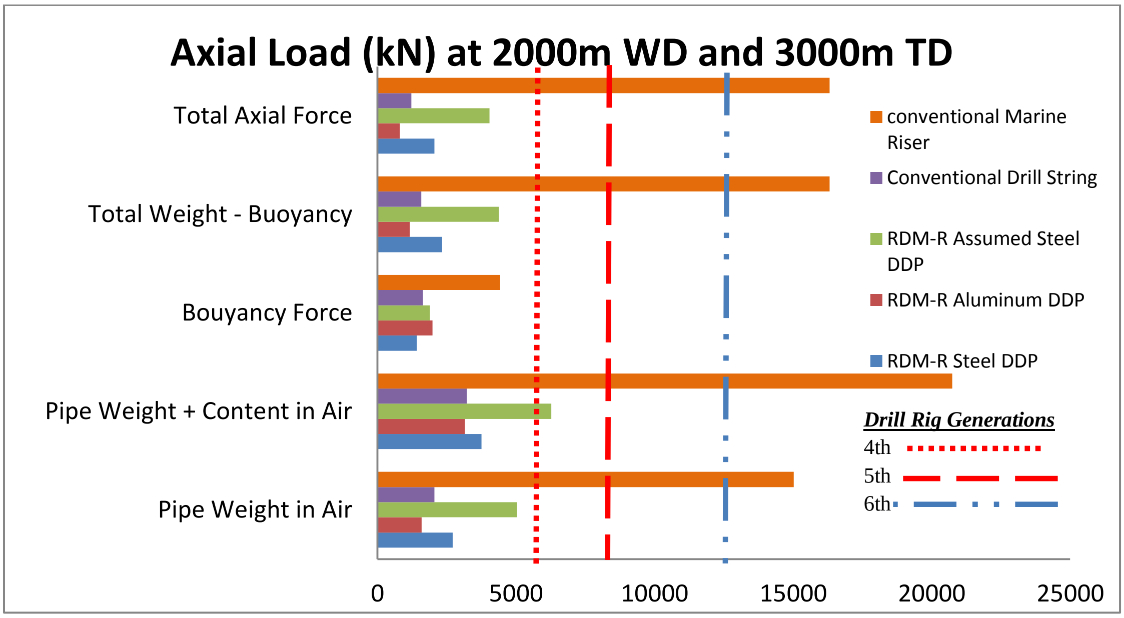

Figure 77: Top Drive Capacity Comparison at 5000m below Water Level

The aluminum dual string has a lower top tension basically because of its material density and the large external area or volume. The top tension is a function of the pipe's weight, the weight of the content and buoyancy force. The buoyancy force depends largely on the external area of the pipe in contact with the fluid content. This force reduces the hook load on the vessel and as such it is an advantage if it can be increased by any factor. The assumed RDM-R steel pipe has buoyancy force in the same range as the aluminum pipe but the material density is relatively too large that it annuls the effects of the buoyancy force. Increasing only the volume so as to increase the positive effects of buoyancy as done in the assumed dual pipe case may not necessary reduces the top tension as we thought. The density of the material also contributes immensely to the pipe's weight and consequently the hook load.

In all, the aluminum dual string has the minimum top tension at the conditions considered. If the top tension is therefore the only factor determining the choice of the string for this project, the aluminum string is the best choice but all other factors should be considered and this would be discussed in the concluding part of this report.

Chapter 8: Conclusion and Recommendation

8.1 Summary

This report has focused on hydrodynamic analysis on RDM-R dual drill pipes (DDPs) in open water. The RDM-R DDP is a product of the Reelwell Company and the analysis data herein was based on the project undertaken by the Reelwell Company for BG Brazil in their presalt well located in Santos Basin, Brazil. The different configurations of the DDPs analyzed were the steel DDP, the aluminum DDP and the assumed steel DDP. OrcaFlex software version 9.5a was used to carry out the simulation. The analysis was carried out at 3000m and 5000m depth from sea level to know the operating window and boundary conditions for the operation in order to conclusively evaluate the most appropriate DDP configuration for the project.

Based on the above summary and the results as presented in Chapter 7, we have made the following conclusions:

8.2 Conclusion

1. Based on the results obtained from the hydrodynamic analysis on the DDPs, the operation in the Santos Basin, all things being equal, is feasible.

2. Due to the relatively subtle wave and current conditions in the Santos Basin site of the project the difference in the dynamic analysis axial force on the string is about 10% more than the loading during static analysis.
3. Rotating the entire pipe induced heavy loads on the pipe as a result of the Magnus effect. The load is approximately 177 kN in the steel DDP analysis, 208 kN in the aluminum DDP and 204 kN in the assumed steel DDP.

4. The aluminum DDP showed great potentials at all the conditions considered. An aluminum pipe designed to equal dimensions as the steel pipe weighs about 35% less than the steel pipe. From the results obtained, there are indications that the Von-Mises stress in the aluminum pipe is increasing more rapidly with depth. This should be checked if there is any need to go further than the depth considered.

5. From the results, the steel DDP may be used for operations in less than 4000m TVD but may not reach the target of 5000m TVD because the Von-Mises stress at that level exceeds the API-RP-2RD limiting stress as obtained from the Orcaflex Software.

6. The behavior of the assumed steel DDP in the Von-Mises stress as calculated by Orcaflex Software is as a result of the hoop's stress, $\boldsymbol{\sigma_{\theta\theta}}$ dominated the axial stresses, $\boldsymbol{\sigma_{ZZ}}$ and the radial stresses $\boldsymbol{\sigma_{rr}}$ in the Von-Mises stress at every section of the pipe. And as the hoop's stress increases with depth the Von-Mises stress increased linearly as the depth increases. This result would undergo another run for verification when the newest version of Orcaflex

Software (Orcaflex 9.6) is available. Orcaflex 9.6 is said to have the capacity to model the pipe in pipe situation more appropriately.

7. The pipes were checked for burst and collapse at all the conditions considered with respect to DNV-OS-F201 standards. The drill pipes satisfied the conditions based on the standard. The calculations and results can be obtained from appendix B of this report.

8. Given the same environmental condition as used in this analysis, a 4th generation drilling rig may be utilized for the operation in Santos Basin with any of the proposed DDPs.

9. Extrapolating the axial loads of the strings and comparing it with the capacities of the drill rigs showed that a higher generation rig than the 4^{th} generation rig may be required when the TVD is in excess of 7500m for the RDM-R assumed steel pipe. For the RDM-R steel pipe, at TVD of about 15000m a higher generation rig may be required while for the RDM-R aluminum pipe in excess of about 30000m.

10. As seen in figures 70, at 2000m water depth only the 5^{th} and 6^{th} generation rigs can handle the liquid mud capacity requirement for a CRD method that uses a marine riser. This is one of the reasons, amongst others, why it may be impossible to extend the use of a lower generation rigs with conventional riser drilling in deep and ultra-deep water environment.

8.3 Recommendations

1. We recommend that manual calculations of the stresses and forces should be carried out at the hot spots of the pipe. These may include the point of connection with the top drive, point of connection with the RCD and areas of the pipe above sea level.
2. Due to unavailability of comprehensive wave data from the Santos Basin site of the project the fatigue damage could not be carried out in this report. We recommend that at least a 10 years return wave be used to completely ascertain the damage due to accumulated fatigue on the pipe. Fatigue failure that may arise as a result of vortex induced vibrations should also be studied.
3. As Orcaflex Software cannot rotate the pipe, to include the effects of rotating the pipe we recommend that an equivalent current velocity which will take care of the Magnus resultant force be used for the Orcaflex simulation.
4. If possible, a motor should be used to rotate the drill bit rather than rotating the entire string because rotating the entire string may increase the lateral force on the string (Magnus effects).
5. Good positioning of the vessel may reduce the lateral force on the pipe at the RCD level.

6. We suggest another test run to verify the results in this report using the new version of the Orcaflex Software.
7. Simulation test may also be carried out in a wave tank to ascertain the sensitivities of the DDP to the environmental variables.

References

1. gCaptain. As retrieved from http://gcaptain.com/hyundai-heavy-unveils-hd12000/ on February 25, 2013.
2. Lim E.F.H. and Ronalds B.F. (2000). Evolution of Production Semisubmersible. SPE 63036. A paper presented at the 2000 SPE Annual Technical Conference and Exhibition held in Dallas, Texas, USA.
3. Rigzone. How Does a Drillship Work? As retrieved from http://www.rigzone.com/training/insight.asp?insight_id=306&c_id=24 on February 25, 2013.
4. Petrocenter. Offshore Drilling Rig. As retrieved from http://www.petrocenter.com/wd/offshore%20drilling%20rig.htm on February 25, 2013.
5. Reelwell Drilling Method. (2012). Demo 2000 Riserless Drilling. A presentation at the 11th Transatlantic Science Week, Houston, Texas, USA.
6. Society of Petroleum Engineers. (2012). As retrieved from http://petrowiki.org/images/1/1a/Devol2615_1.png on February 26, 2013.
7. Mustang Engineering. (2012). 2012 Deep-water Solutions and Records for Concept Selection. As retrieved from http://www.mustangeng.com/AboutMustang/Publications/Publications/Deepwater%20Poster%20Final.pdf on March 3, 2013.
8. Kenneth P. Malloy, SPE, Stress Engineering Services, C. Rick Stone, SPE, and George H. Medley, Jr., SPE, Signa Engineering, Don Hannegan,SPE, Weatherford International, Oliver Coker, SPE, ConocoPhillips, Don Reitsma, SPE, @Balance, Helio Santos, SPE, and Joseph Kinder, SPE, Secure Drilling, Johan Eck-Olsen, SPE, StatoilHydro, JihnMcCaskill, SPE, Expro Group, James May, SPE, Smith Services, Kenneth Smith, SPE, and Paul Sonneman, SPE, Chevron Energy Technology.: "Managed-Pressure Drilling: What It Is and What It Is Not" IADC/SPE 122281, Presented at IADC/SPE Managed Pressure Drilling and Underbalanced Operations Conference and Exhibition Held in San Antonio, Texas, 12-13 February 2009.
9. Lopes, C.A. and Bourgoyne, A.T. Jr. (1997). Paper Number 8465-MS. Feasibility Study of a Dual Density Mud System for Deepwater Drilling Operations. Paper presented at the Offshore Technology Conference, Houston, Texas, USA.
10. Wikipedia. As retrieved from http://en.wikipedia.org/wiki/File:Oil_Rig_NT8.jpg on February 19, 2013.
11. Jonggeun C. (1998). Paper Number 55056. Analysis of Riserless Drilling and Well-Control Hydraulics. SPE Drill. & Completion, Vol. 14, No. 1.
12. Medley, G.H. Jr., Maurer, W.C., and Garkasi, A.Y. (1995). Paper Number 30500-MS. Use of Hollow Glass Spheres for Underbalanced Drilling Fluids. Paper presented at the SPE Annual Technical Conference and Exhibition, Dallas, Texas, USA.

13. IADC-UBO and MPD Glossary. http://www.iadc.org/iadc-committees/iadcunderbalanced-operations-managed-pressure-drilling-committee/completeddocuments/
14. Marine Wiki. As retrieved from http://www.marinewiki.org/index.php/Jack-up_units on February 21, 2013.
15. Kenneth P. Malloy. (2007) Stress Engineering Services. “Managed pressure drilling-What is it anyway”.
16. Energy Bulletin. As retrieved from http://www.energybulletin.net/stories/2010-06-29/despite-gulf-disaster-deepwater-oil-all-we-have-left on February 4, 2013.
17. The Oildrum. As retrieved from http://www.theoildrum.com/node/9169 on February 6, 2013.
18. Jonggeun C. (1998). Paper Number 55056. Analysis of Riserless Drilling and Well-Control Hydraulics. SPE Drill. & Completion, Vol. 14, No. 1.
19. Leach. C.K., Hakulia C., and Fossil B. (2002). Design of a Drilling Rig for 10.000 ft Water Depth Using a Pressured Riser. Paper SPE 74533 presented at the L.DC/SPE Drilling Conference held in Texas, USA.
20. Lopes, C.A. and Bourgoyne, A.T. Jr. (1997). Paper Number 8465-MS. Feasibility Study of a Dual Density Mud System for Deepwater Drilling Operations. Paper presented at the Offshore Technology Conference, Houston, Texas, USA.
21. Medley, G.H. Jr., Maurer, W.C., and Garkasi, A.Y. (1995). Paper Number 30500-MS. Use of Hollow Glass Spheres for Underbalanced Drilling Fluids. Paper presented at the SPE Annual Technical Conference and Exhibition, Dallas, Texas, USA.
22. Reelwell AS. (2012). A presentation at the 11th Transatlantic Science Week, Houston, Texas, USA.
23. D. Hannegan, Weatherford Intl. Inc. SPE 101855. Case Studies – Offshore Managed Pressure Drilling. A paper presented at the SPE Annual Technical Conference in Texas, USA.
24. Steve Nas, Julmar Shaun Toralde and Chad Wuest. (2009). SPE 119875. Offshore Managed Pressure Drilling Experiences in Asian Pecific. A paper Presented at SPE/IADC Drilling Conference and Exhibition held in Amsterdam, Netherlands.
25. Weatherford International LTD. (2006). Controlled Pressure Drilling and Testing Services – Return Flow Control Drilling.
26. Kenneth P. M. (2007). “Managed pressure drilling-What is it anyway”. As retrived from http://www.worldoil.com/March-2007-Managed-pressure-drilling-What-is-it-anyway.html on March 6, 2013.
27. Kjell K. F. (2011). University of Stavanger Lecture notes. Managed Pressure Drilling – what is it?
28. Weatherford International LTD. (2010). MPD - Application Answers. Constant Bottomhole Pressure. Well Design to Energize Assets. As retrieved from

http://www.weatherford.com/ECMWEB/groups/web/documents/weatherfordcorp/wft021445.pdf. on March 13, 2013.

29. World Oil Magazine. (2007). Managed Pressure Drilling - What is it anyway? As retrived from http://www.worldoil.com/March-2007-Managed-pressure-drilling-What-is-it-anyway.html on March 13, 2013.
30. SPE International. Dual Gradient Drilling Systems. As retrieved from http://petrowiki.org/Dual_gradient_drilling_systems on March 13, 2013.
31. Offshore. (2012). Detachable Artificial Mud Lift System. As retrieved from http://www.offshore-mag.com/articles/print/volume-61/issue-10/news/detachable-artificial-mud-lift-system-has-applications-for-all-depths.html on March 14, 2013.
32. Rohani M. R. (2011). Managed-Pressure Drilling; Techniques and Options for Improving Operational Safety and Efficiency. Sharif University of Technology, Tehran, Iran.
33. Ian C. Coker. (2004). Texas A&M.: "Managed Pressure Drilling Applications Index" Paper no 16621. A paper presented at Offshore Technology Conference in Houston, Texas, U.S.A.
34. Philip Frink. (2006). Blade Energy Parterners. "Managed pressure drilling—What's in a name?"
35. Paco Vieira, Maurizio Arnone, and Fabian Torres, and Fernando Barragan: "Roles of Managed Pressure Drilling Technique in Kick Detection and Well Control—The Beginning of New Conventional Drilling Way" SPE/IADC Paper Number 124664. A paper presented at SPE/IADC Middle East Drilling Technology Conference and Exhibition held in Manama, Bahrain.
36. Bill Rehm, Jerome Sshubert, ArashHaghshenas, Amir SamanPaknejad, Jim Hughes (editors).: Managed Pressure Drilling Gulf Drilling Series. ISBN: 1-933762-24-1 (978- 1-933762-24-1:alk. paper).
37. Robert Goodwin, George H. Medley, and Patrick B.B. Reynolds. (2008). Understanding MPD Complexity Level. As retrieved from http://www.epmag.com/Production-Drilling/Understanding-MPD-complexity-levels_11972 on March 20, 2013.
38. Hannegan, D.M. (2007). "Managed Pressure Drilling: A new way of looking at drilling hydraulics… Overcoming conventional drilling challenges", SPE Distinguished Lecturer Series.
39. Chustz, M.J., Smith, L.D., Dell, D. (2008). "Managed Pressure Drilling Success Continues on Auger TLP" A Paper presented at the IADC/SPE, Orlando, Florida, USA.
40. Arnone, M. (2010). "Managed Pressure Drilling Weatherford System Overview", A paper presented at the Weatherford MENA in Egypt.
41. Erdem Tercan. (2010). A Master Thesis submitted to The Graduate School of Natural and Applied Sciences of Middle East Technical University.

42. Malloy, K.P., McDonald, P. (2008). “A Probabilistic Approach to Risk Assessment of Managed Pressure Drilling in Offshore 191 Applications” A Joint Industry Project DEA 155, Technology Assessment and Research Study 582 Contract 0106CT39728 Final Report.
43. Nas, S., Torolde, J.S., Wuest, C., “Offshore Managed Pressure Drilling Experiences in Asia Pacific”, presented at the SPE/IADC Drilling Conference and Exhibition held in Amsterdam, The Netherlands, 119875, 17–19 March 2009.
44. Putra R. Science Business. (2013). Drilling to Earth’s Mantle May Now be Possible.
45. Stave R., Farestveit R., Høyland S., Rochmann P.O., and Rolland N.L. (2005). OTC 17665. Demonstration and Qualification of a Riserless Dual Gradient System. A paper presented at the 2005 Offshore Technology Conference held in Houston, TX, U.S.A.
46. Carter G., Bland B., and Pinckard M. OTC 17673. Riserless Drilling—Applications of an Innovative Drilling Method and Tools. A paper presented at the 2005 Offshore Technology Conference held in Houston, TX, U.S.A.
47. BG Brasil. (2012). WE Technology Project – Riserless Drilling.
48. Dave Smith, Warren Winters, Brian Tarr, Robert Ziegler, Iskandar Riza and Malik Faisal. (2010). SPE 130308-MS. Deepwater Riserless Mud Return System for Dual Gradient Tophole Drilling. A paper presented at the OTC held in Texas, USA.
49. Robert A. D. Function Wave Theory .Center for Applied Coastal Research University of Delaware, Newark DE 19716 USA. As retrieved from http://www.coastal.udel.edu/faculty/rad/streamless.html on September 10, 2012.
50. DNV-OS-F201 (2010): Dynamic Risers. Det Norske Veritas, Norway.
51. DNV-OS-F101 (2012) . Submarine Pipeline System. Det Norske Veritas, Norway.
52. API RP 2RD (2006). Design of Risers for Floating Production Systems (FPSs) and Tension-Leg Platforms (TLPs). American Petroleun Institute.
53. OrcaFlex Manual Version 9.6a. Orcina Ltd. Daltongate Ulverston Cumbria LA12 7AJ UK.
54. Gudmestad, O.T. (2012). Marine Operations Class Notes (Unpublished), University of Stavanger, Norway.
55. Karunakaran, D. (2012). Riser Technology 1 Class Notes (Unpublished), University of Stavanger, Norway.
56. Casia Pianca, Mazzini P. L. F. and Siegle E. (2010). Brazilian Offshore Wave Climate Based on NWW3 Reanalysis. Submitted to Brazilian Journal of Oceanography, paper number 58(1):53-70.
57. Michael Vogel, Belmiro M, Jose Antonio, Adriene F, and Paul Williams. (2010). Metocean Measurement at Northern Santos Basin-Brazil. OTC 20947. A paper presented at the OTC held in Texas, USA.
58. Jose A.M. Lima and Anna M. Scofano. (1999). OTC 10750. New Oceanographic Challenges in Brazilian Deepwater Oil Fields. A paper presented at the OTC held in Texas, USA.

59. National Academy of Science - National Research Cuncil, Washinton D.C., USA. (1960). Experimental Drilling in Deep Water. As retrieved from http://books.google.no/books?id=njgrAAAAYAAJ&printsec=frontcover&dq=experimental+drilling+in+deep+water&hl=en&sa=X&ei=jc2KUbCeDOLA7Aaz94CoAQ&redir_esc=y on May 6, 2013.

Appendix A: Manual Calculations of Axial/Hook Loads

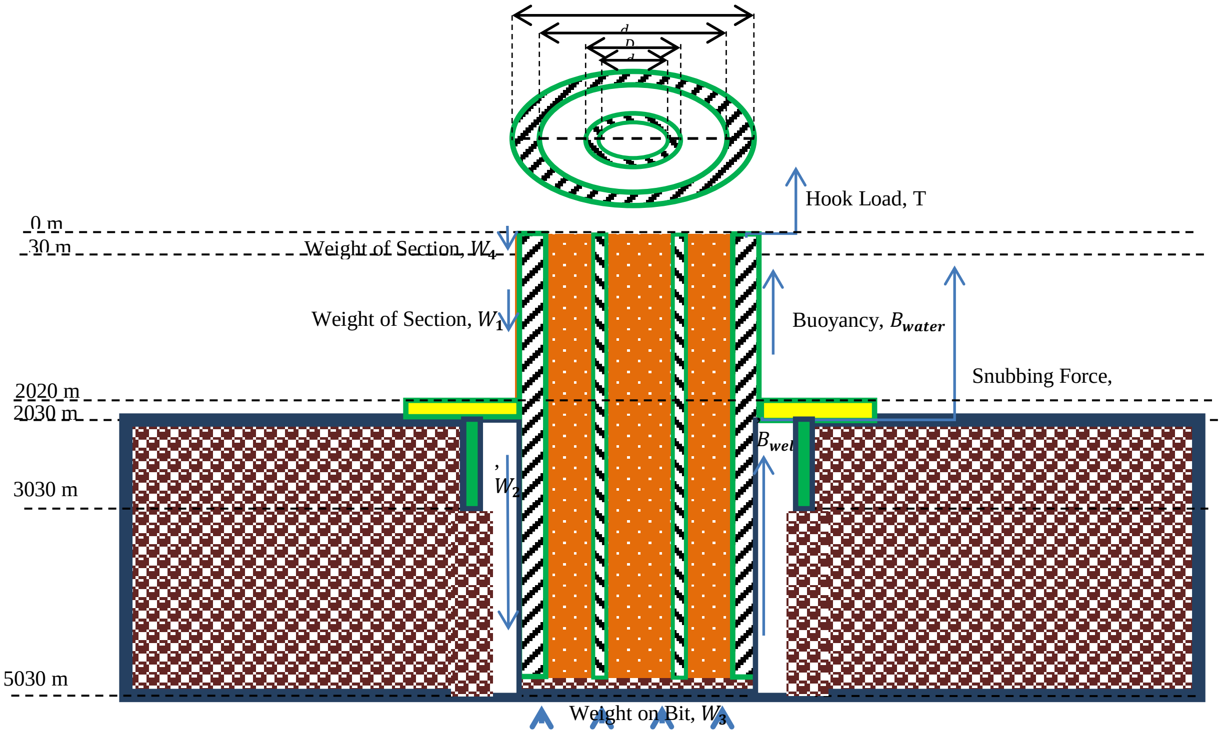

Figure 78: Free Body Diagram

	Dual Drill Pipe parameters	Steel DDP	Al DDP*
Outer string	- Pipe outer diameter [mm] - Pipe inner diameter [mm] - Tool joint outer diameter [mm] - Tool joint inner diameter [mm] - Pipe joint length [m] - Pipe weight [kg/m] in air - Max tension load [ton] - Max torque [k ft lbs] - Yield pressure [bar] - Collapse pressure [bar]	168 (6 5/8”) 140 (5.5”) 203 (8”) 127 (5”) 13.5 40.9 270 85 630 290	198 (Al) (7.8”) 172 (Al) 209 (steel) 150 (steel) 14 28.5 300 100 525 430
Inner string	- Pipe outer diameter [mm] - Pipe inner diameter [mm] - Tool joint outer diameter [mm] - Tool joint inner diameter [mm] - Pipe joint length [m] - Pipe weight [kg/m] in air - Yield pressure [bar] - Collapse pressure [bar]	88.9 (3.5”) 78 96 76 13.5 13.1 400 400	104 (Al) 90 (Al) 113 (Al) 90 (Al) 14 5.8 540 450

Table 13: RDM-R Dual Drill Pipe Parameter

A1 Hand Calculation for RDM-R Steel Pipe.

Mass of Pipe in air, W_p = Weight of Outer Pipe + Weight of Inner Pipe

= 40.9 + 13.1

= 54 kg/m

Area Covered by Mud, $A_m = \frac{\pi d_o{}^2}{4} - \frac{\pi(D_i{}^2 - d_i{}^2)}{4}$

= 0.01397 m^2

Mass of mud (SG = 1.5) column per unit meter, $W_m = \rho A_m$

= 1.5 * 1000 * 0.01397

= 21 kg/m

Filled Weight, $W_T = W_p + W_m$

= 54 + 21

= 75 kg/m

Height of pipe from sea level to top drive = 30m

W_p = 75 * 30

= 2250 kg

$Q_{air} = W_p$ * 9.81

= 22.07 kN

$W_1 = W_p L_{water}$

Where L_{water} is the distance depth from sea level to the RCD = 1990 m

$W_1 = (54 + 21)1990$

= 149250 Kg

$Q_1 = W_1 * 9.81$

= 1464.14 kN

External area of pipe, $A_p = \frac{\pi D_o{}^2}{4}$

= 0.02217 m^2

Buoyancy force in water, $B_{water} = \rho_w g A_p L$

*= 1000 * 9.81 * 0.02217 * 1990*

= 432.7 kN

$Q_{water} = Q_1 - B_{water}$

= 1464.14 – 432.7

= *1031.44 kN*

$W_2 = (W_p + W_p)L_{well}$

Where L_{well} = 3010 m

$W_2 = (54 + 21)3010$

W_2 = 225750 kg

$Q_2 = W_2 * 9.81$

= 2214.6 kN

Buoyancy force in well, $B_{well} = \rho_m g A_p L_{well}$

= 1.5 *1000 * 9.81 * 0.02217 * 3010

= 981.83 KN

$Q_{well} = Q_2 - B_{well}$

= 2214.6 – 981.83

= 1232.77 kN

Snubbing Force Calculations in Static Conditions at 2000 m

Hydrostatic pressure, $P_h = \rho_w gh$

= 196.2 bar

Open/Dual pressure with mud (SG = 1.5) = $\rho_m gh$

= 1.5 * 1000 * 9.81 * 2000

= 294.3 bar

Pressure in the RCD, $P_{RCD} = 294.3 - 196.2$

= 98.1 bar

Snubbing force, $F_3 = P_{RCD} * A_p$

= 217.49 kN

Weight on bit, $W_3 =$ 50 kN (Assumed)

In static equilibrium:

$T + W_3 + F_3 = Q_{air} + Q_{water} + Q_{well}$

T + 50 + 217.49 = 22.07 + 1031.44 + 1232.77

T = 2018.79kN

Total weight of pipe and column, $W_T = Q_{air} + Q_1 + Q_2$ = 22.07 + 1464.14 + 2214.6

W_T = 3700.81 kN

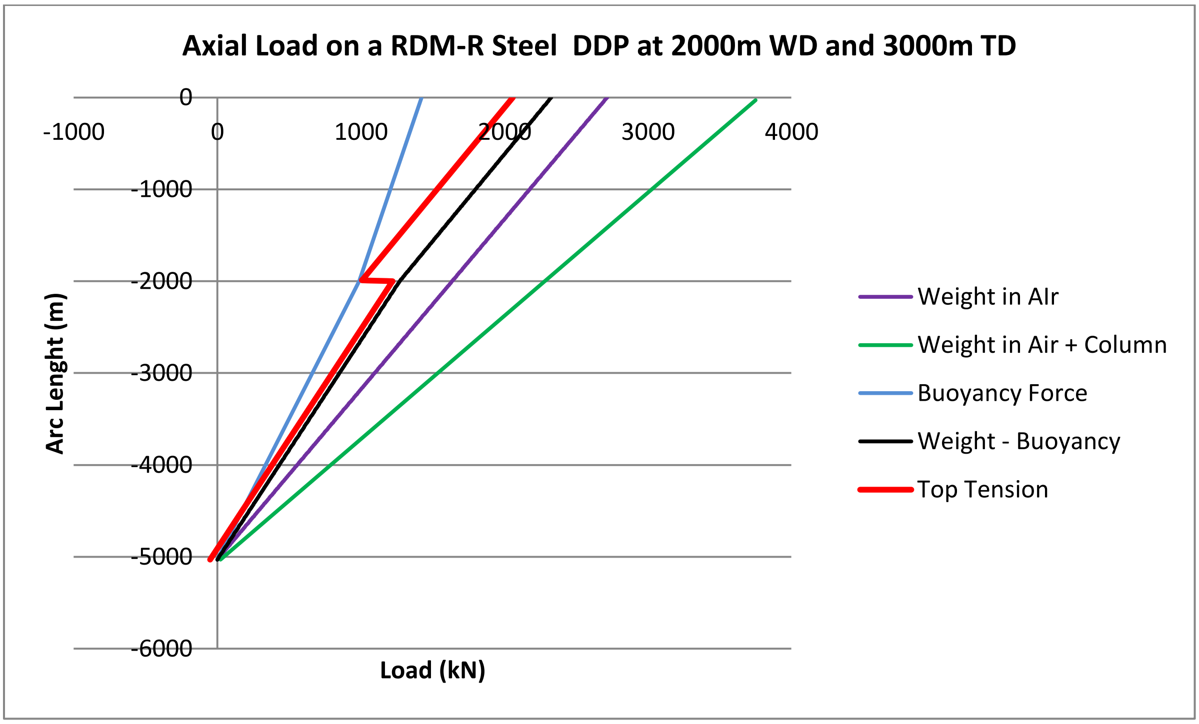
Axial Load on a RDM-R Steel DDP at 2000m WD and 3000m TD
0
-1000
0
1000
2000
3000
4000
-1000
-2000
-3000
-4000
-5000
-6000
Arc Lenght (m)
Load (kN)
Weight in AIr
Weight in Air + Column
Buoyancy Force
Weight - Buoyancy
Top Tension

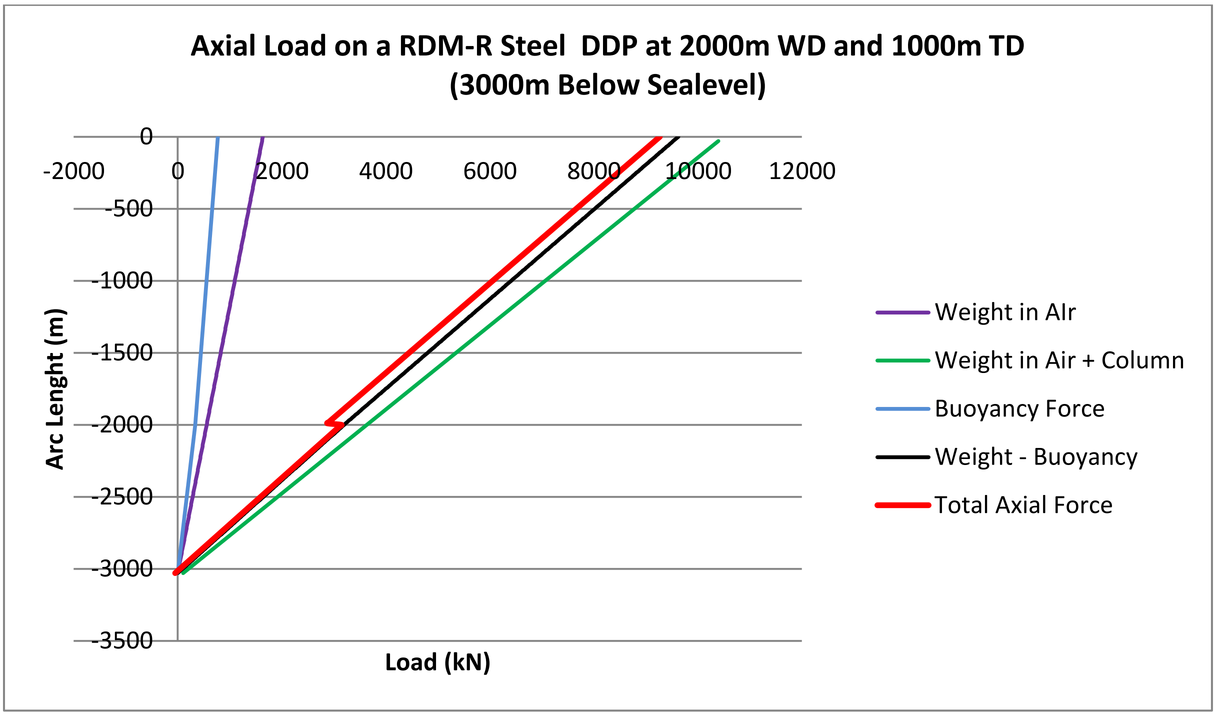
Axial Load on a RDM-R Steel DDP at 2000m WD and 1000m TD
(3000m Below Sealevel)
0
-2000
0
2000
4000
6000
8000
10000
12000
-500
-1000
-1500
-2000
-2500
-3000
-3500
Arc Lenght (m)
Load (kN)
Weight in AIr
Weight in Air + Column
Buoyancy Force
Weight - Buoyancy
Total Axial Force

A2 Hand Calculation for RDM-R Aluminum Dual Drill Pipe.

Mass of Pipe in air, W_p = Weight of Outer Pipe + Weight of Inner Pipe

= 28.5 + 5.8

= 31.6 kg/m

Area Covered by Mud, $A_m = \frac{\pi {d_o}^2}{4} - \frac{\pi({D_i}^2 - {d_i}^2)}{4} = 0.0211\ m^2$

Mass of mud (SG = 1.5) column per unit meter, $W_m = \rho A_m$

= 1.5 * 1000 * 0.0211

= 31.65 kg/m

Filled Weight, $W_T = W_p + W_m$

= 31.6 + 31.65

= 63.26 kg/m

Height of pipe from sea level to top drive = 30m

W_p = 63.26 * 30

= 1897.72 kg

$Q_{air} = W_p$ * 9.81

= 18.62 kN

$W_1 = W_p L_{water}$

Where L_{water} is the distance depth from sea level to the RCD = 1990 m

*W_1 = 63.26 * 1990*

= 125887Kg

*$Q_1 = W_1$ * 9.81*

= 1234.96 kN

External area of pipe, $A_p = \frac{\pi {D_o}^2}{4}$

= $0.031m^2$

Buoyancy force in water, $B_{water} = \rho_w g A_p L$

*= 1000 * 9.81 * 0.031 * 1990*

= 601.09 kN

$Q_{water} = Q_1 - B_{water}$

= 1234.96 – 601.09

= 633.87 kN

$W_2 = (W_p + W_m)L_{well}$

Where L_{well} = 3010 m

$W_2 = (31.60 + 31.65)3010$

W_2 = 190382.5 kg

$Q_2 = W_2 * 9.81$

= 1867.65 kN

Buoyancy force in well, $B_{well} = \rho_m g A_p L_{well}$

= 1.5 *1000 * 9.81 * 0.031 * 3010

= 1373.06 kN

$Q_{well} = Q_2 - B_{well}$

= 1867.65 – 1373.06

= 497.59 kN

Snubbing Force Calculations in Static Conditions at 2000 m

Hydrostatic pressure, $P_h = \rho_w gh$

= 196.2 bar

Open/Dual pressure with mud (SG = 1.5) = $\rho_m gh$

= 1.5 * 1000 * 9.81 * 2000

= 294.3 bar

Pressure in the RCD, $P_{RCD} = 294.3 - 196.2$

= 98.1 bar

Snubbing force, $F_3 = P_{RCD} * A_p$

= 304.11 kN

Weight on bit, $W_3 =$ 50 kN(Assumed)

In static equilibrium:

$T + W_3 + F_3 = Q_{air} + Q_{water} + Q_{well}$

T + 50 + 304.11 = 18.62 + 633.87 + 497.57

T = 795.95 kN

Total weight of pipe and column, $W_T = Q_{air} + Q_1 + Q_2$

= 18.62 + 1234.96 + 1867.65

W_T = 3121.65 kN

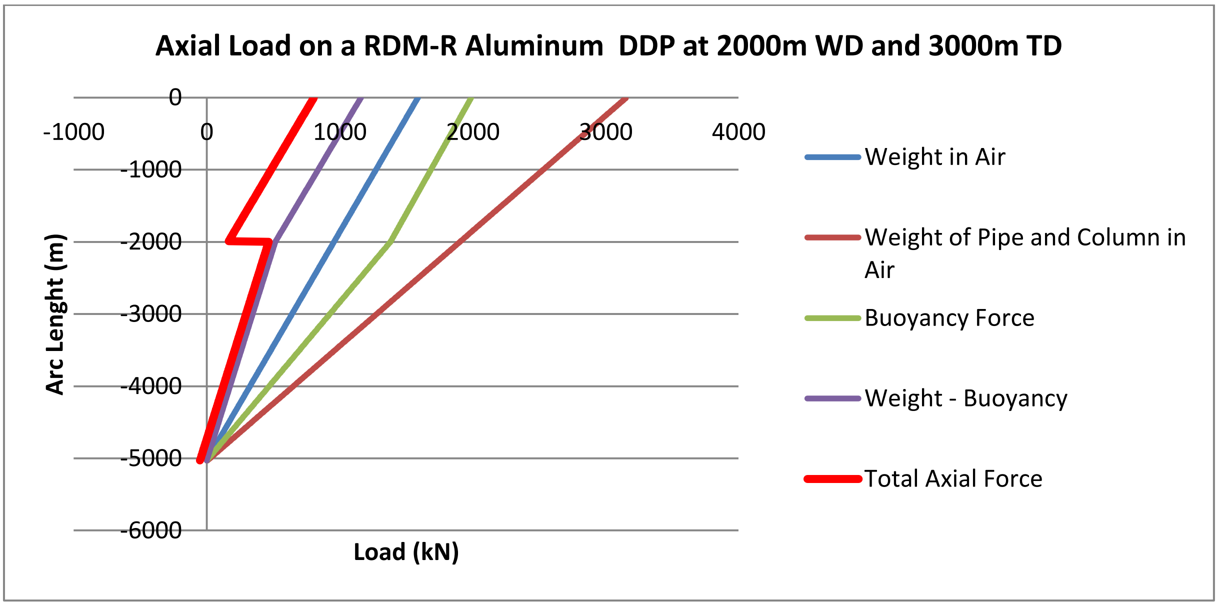
Axial Load on a RDM-R Aluminum DDP at 2000m WD and 3000m TD
0
-1000
0
1000
2000
3000
4000
-1000
-2000
-3000
-4000
-5000
-6000
Arc Lenght (m)
Load (kN)
Weight in Air
Weight of Pipe and Column in Air
Buoyancy Force
Weight - Buoyancy
Total Axial Force

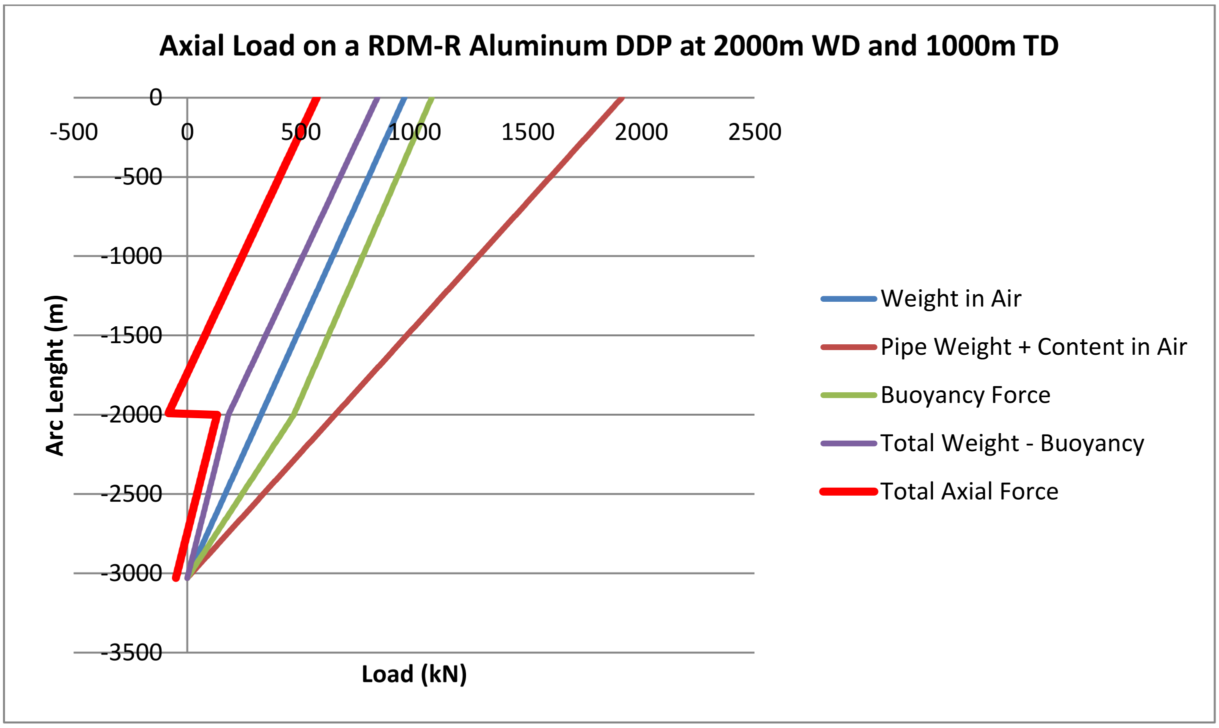
Axial Load on a RDM-R Aluminum DDP at 2000m WD and 1000m TD
0
-500
0
500
1000
1500
2000
2500
-500
-1000
-1500
-2000
-2500
-3000
-3500
Arc Lenght (m)
Load (kN)
Weight in Air
Pipe Weight + Content in Air
Buoyancy Force
Total Weight - Buoyancy
Total Axial Force

A3 Hand Calculation for Assumed Steel Dual Drill Pipe.

Parameters	**Outer String**	**Inner String**
Pipe Outer Diameter (mm)	193.68 [7 $^{5}/_{8}$ "]	139.70[5 $^{1}/_{2}$ "]
Pipe Inner Diameter	161.40[6.35"]	121.36[4.67"]
Density (kg/m^3)	7850	7850
Pipe Weight (kg/m) in Air	70.67	29.52

Pipe Weight (kg/m) in Air = Density * Area = 7850* $\frac{\pi}{4}(D^2 - d^2)$

Outer String: Pipe Weight (kg/m) in Air = 7850 * $\frac{\pi}{4}(0.19368^2 - 0.1614^2)$ = 70.67 kg/m^3

Inner String: Pipe Weight (kg/m) in Air = 7850 * $\frac{\pi}{4}(0.1397^2 - 0.12136^2)$ = 29.52 kg/m^3

Mass of Pipe in air, W_p = Weight of Outer Pipe + Weight of Inner Pipe

= 70.67 + 29.52 = 100.19 kg/m

Area Covered by Mud, $A_m = \frac{\pi d_o^2}{4} - \frac{\pi(D_i^2 - d_i^2)}{4} = 0.0167\ m^2$

Mass of mud (SG = 1.5) column per unit meter, $W_m = \rho A_m$

= 1.5 * 1000 * 0.0167 = 25.05 kg/m

Filled Weight, $W_T = W_p + W_m$

= 100.19 + 25.05 = 125.24 kg/m

Height of pipe from sea level to top drive = 30m

W_p = 125.24 * 30 = 3757.17 kg

$Q_{air} = W_p$ * 9.81 = 36.86 kN

$W_1 = W_p L_{water}$

Where L_{water} is the distance depth from sealevel to the RCD = 1990 m

*W_1 = 125.24 * 1990 = 249227.6 Kg*

*$Q_1 = W_1$ * 9.81= 2444.92 kN*

External area of pipe, $A_p = \frac{\pi D_o^2}{4}$ = 0.0295 m^2

*Buoyancy force in water, $B_{water} = \rho_w g A_p L$ = 1000 * 9.81 * 0.0295 * 1990 = 575.90 kN*

$Q_{water} = Q_1 - B_{water}$ = 2444.92 – 575.9 = 1869.02 kN

$W_2 = (W_T)L_{well}$

Where L_{well} = 3010 m

W_2 = (125.24)3010

W_2 = 376972.4 kg

$Q_2 = W_2 * 9.81$ = 3698.10 kN

Buoyancy force in well, $B_{well} = \rho_m g A_p L_{well}$

= 1.5 *1000 * 9.81 * 0.0295 * 3010 = 1306.62 KN

$Q_{well} = Q_2 - B_{well}$

= 3698.10 – 1306.62 = 2391.48 kN

Snubbing Force Calculations in Static Conditions at 2000 m

Hydrostatic pressure, $P_h = \rho_w gh$

= 196.2 bar

Open/Dual pressure with mud (SG = 1.5) = $\rho_m gh$

= 1.5 * 1000 * 9.81 * 2000 = 294.3 bar

Pressure in the RCD, $P_{RCD} = 294.3 - 196.2$ = 98.1 bar

Snubbing force, $F_3 = P_{RCD} * A_p$

= 289.40 kN

Weight on bit, $W_3 =$ 50 kN(Assumed)

In static equilibrium:

$T + W_3 + F_3 = Q_{air} + Q_{water} + Q_{well}$

T + 50 + 289.40 = 36.86 + 1869.02 + 2391.48

T = 3957.97 kN

Total weight of pipe and column, $W_T = Q_{air} + Q_1 + Q_2$ = 36.86 + 2444.92 + 3698.10

W_T = 6179.88 kN

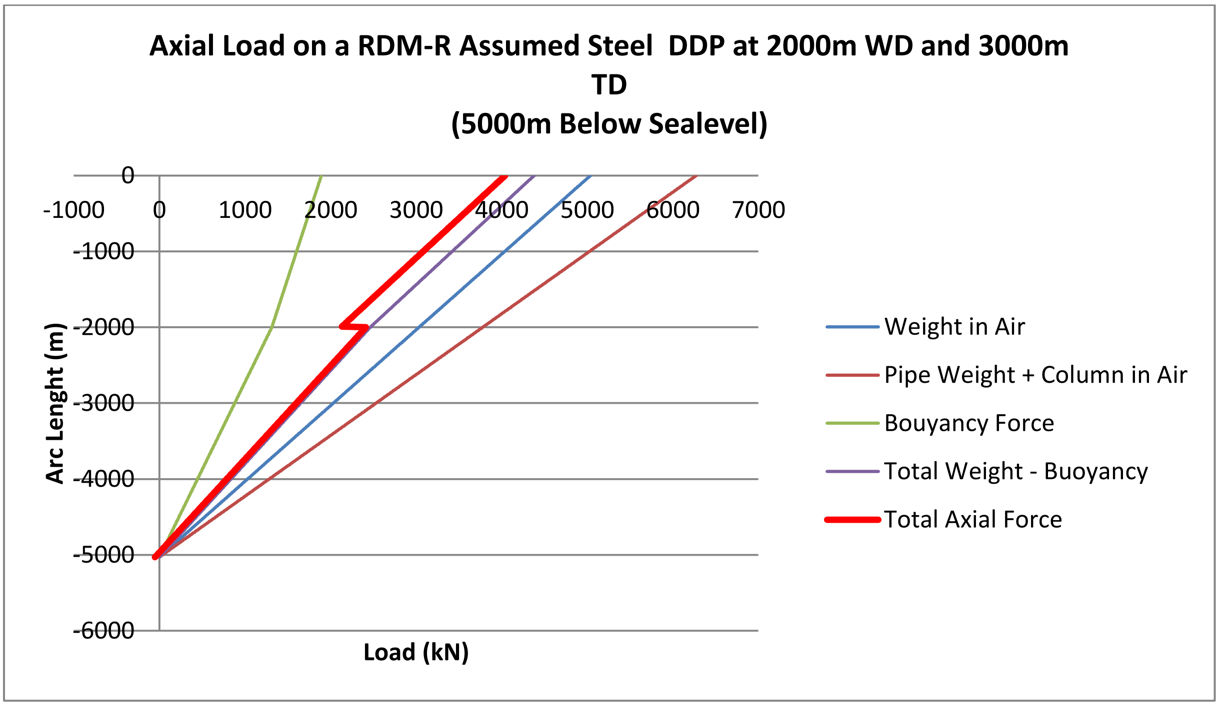
Axial Load on a RDM-R Assumed Steel DDP at 2000m WD and 3000m TD
(5000m Below Sealevel)
0
-1000
0
1000
2000
3000
4000
5000
6000
7000
-1000
-2000
-3000
-4000
-5000
-6000
Arc Lenght (m)
Load (kN)
Weight in Air
Pipe Weight + Column in Air
Bouyancy Force
Total Weight - Buoyancy
Total Axial Force

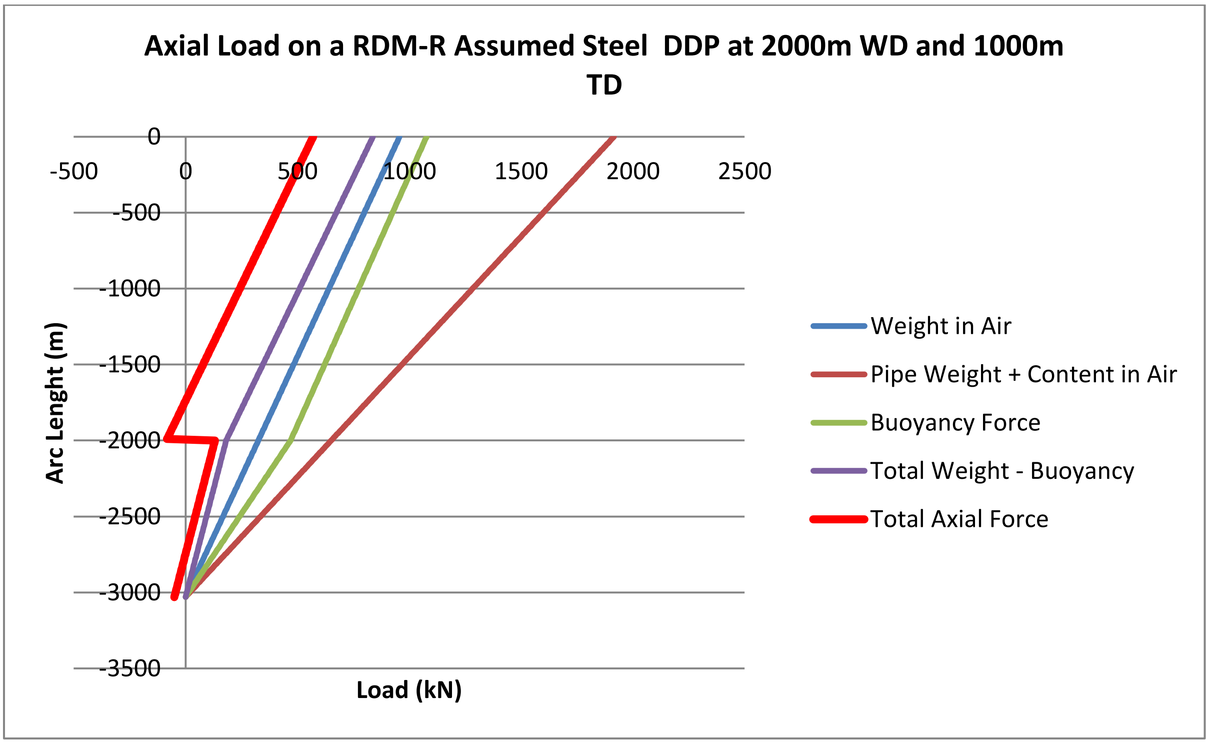
Axial Load on a RDM-R Assumed Steel DDP at 2000m WD and 1000m TD
0
-500
0
500
1000
1500
2000
2500
-500
-1000
-1500
-2000
-2500
-3000
-3500
Arc Lenght (m)
Load (kN)
Weight in Air
Pipe Weight + Content in Air
Buoyancy Force
Total Weight - Buoyancy
Total Axial Force

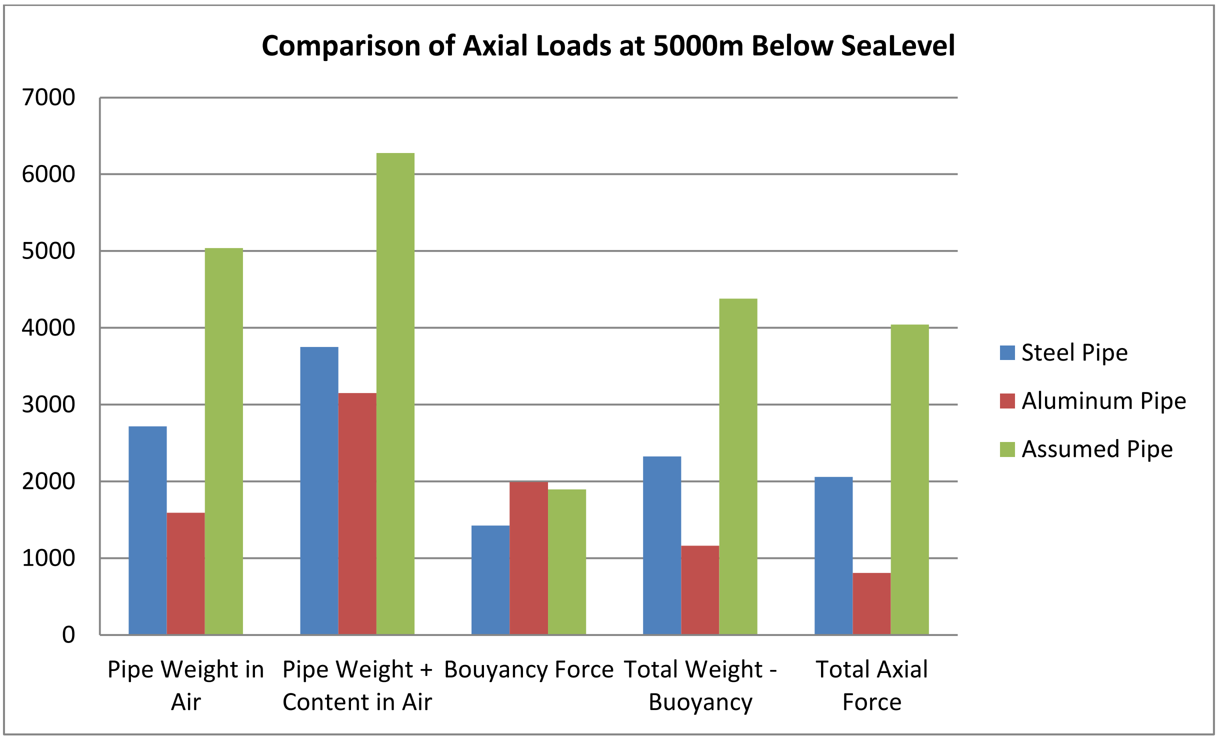
Comparison of Axial Loads at 5000m Below SeaLevel
7000
6000
5000
4000
3000
2000
1000
0
Pipe Weight in Air
Pipe Weight + Content in Air
Bouyancy Force
Total Weight - Buoyancy
Total Axial Force
Steel Pipe
Aluminum Pipe
Assumed Pipe

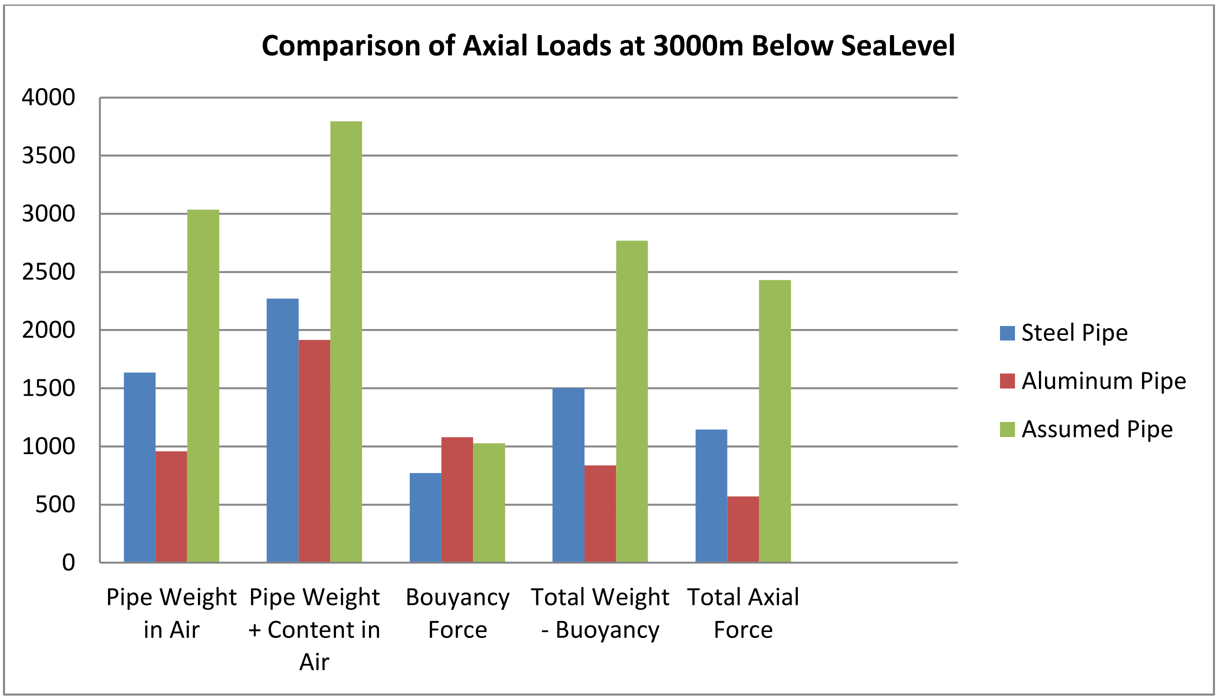
Comparison of Axial Loads at 3000m Below SeaLevel
4000
3500
3000
2500
2000
1500
1000
500
0
Pipe Weight in Air
Pipe Weight + Content in Air
Bouyancy Force
Total Weight - Buoyancy
Total Axial Force
Steel Pipe
Aluminum Pipe
Assumed Pipe

A4 Hand Calculation for Conventional Marine Riser and Drill String

Drill Pipe (6 5/8") Weight in Air = 40.9 kg/m

Area Covered by Mud, $A_m = \frac{\pi {d_i}^2}{4} = 0.0154\ m^2$

Mass of mud (SG = 1.5) column per unit meter, $W_m = \rho A_m$

$= 1.5 * 1000 * 0.0154 = 23.1\ kg/m$

Filled Weight, $W_T = W_p + W_m$

$= 40.9 + 23.1 = 64\ kg/m$

Height of pipe from top drive (TVD) = 5030m

$W_p = 64 * 5030 = 321920$ kg

$Q_{air} = W_p * 9.81 = 3158.04$ kN

External area of Drill pipe, $A_p = \frac{\pi {D_0}^2}{4} = 0.0222\ m^2$

Buoyancy force in mud, $B_{mud} = \rho_m g A_p L = 1500 * 9.81 * 0.0222 * 5030 = 1643.17\ kN$

$Q_{string} = Q_{air} - B_{mud} = 3158 – 1643.17 = 1514.83\ kN$

Snubbing Force Calculations in Static Conditions at 2000 m

Hydrostatic pressure, $P_h = \rho_w gh$

= 196.2 bar

Open/Dual pressure with mud (SG = 1.5) = $\rho_m gh$

= 1.5 * 1000 * 9.81 * 2000 = 294.3 bar

Pressure in the RCD, $P_{RCD} = 294.3 - 196.2$ = 98.1 bar

Snubbing force, $F_3 = P_{RCD} * A_p$

= 217.78 kN

Weight on bit, $W_3 =$ 50 kN(Assumed)

In static equilibrium:

$T + W_3 + F_3 = Q_{string}$

T + 50 + 217.78 = 1514.83

T = 1247.05 kN

Marine Riser Weight in Air = 743.76 kg/m (Leach et al, 2002).

Area Covered by Mud, $A_m = \frac{\pi(D_i^2 - d_e^2)}{4} = 0.1705\ m^2$

Mass of mud (SG = 1.5) column per unit meter, $W_m = \rho A_m$

$$= 1.5 * 1000 * 0.1705 = 255.76\ kg/m$$

Filled Weight, $W_T = W_p + W_m$

$$= 743.76 + 255.76 = 999.52\ kg/m$$

Height of pipe from sea level to top drive = 2030m

W_p = 999.52 * 2030 = 2029025.60 kg

$Q_{air} = W_p$ * 9.81 = 19904.74 kN

External area of Drill pipe, $A_p = \frac{\pi D_0^2}{4} = 0.2235\ m^2$

Buoyancy force in water, $B_{water} = \rho_w g A_p L$ *= 1500 * 9.81 * 0.2235 * 2030 = 6676.27 kN*

$Q_{riser} = Q_{air} - B_{water}$ *= 19904.74 – 6676.27 = 13228.47 kN*

In static equilibrium:

$T = Q_{riser}$

T = 13228.47 kN

Appendix B: Failure Modes Check

B1 Burst Check

1.1 Burst Check for RDM-R Steel Dual Drill Pipe

Parameter	Equation	Value	Unit
Outer Diameter, D	~	168	mm
Specific Minimum Yield Stress, SMYS	~	718.75	MPa
Specific Minimum Tensile Stress, SMTS	~	791.67	MPa
Yield Stress Temperature Derating Factor, $f_{y,temp}$	~	0	MPa
Tensile Strength Temperature Derating Factor, $f_{u,temp}$	~	0	MPa
Material Strength Factor, α_u	~	0.96	~
Material Resistance Factor, γ_m	~	1.15	~
Safety class resistance factor, γ_{sc}	~	1.26	~
Water Depth, d	~	2000	m
Starting Elevation of Circulation Fluid, h_0	~	30	m
Circulation Fluid Density, ρ_i	~	1500	Kg/m3
Seawater Density, ρ_e	~	1025	Kg/m3
Maximum Surface Design Pressure, P_d	~	0	MPa
Yield Stress, f_y	$(SMYS - f_{y,temp})\alpha_u$	690	MPa
Tensile Strength, f_u	$(SMTS - f_{u,temp})\alpha_u$	760	MPa
Height of Internal Fluid Column, h	$d + h_0$	2030	m
Local Internal Design Pressure, P_{ld}	$P_d + \rho_i * g * h$	29.87	MPa
Local Incidental Pressure, P_{li}	$P_{id} + 0.1P_d$	29.87	MPa
Local External Pressure, P_e	$\rho_e * g * h$	19.91	MPa
Minimum Required Wall Thickness Without Allowance and Tolerance, t_1	$\frac{D}{\frac{4}{\sqrt{3}}\frac{\min(f_y:\frac{f_u}{1.15})}{\gamma_m\gamma_{sc}(P_{li}-P_e)}+}$	1.57	mm
Burst Resistance, P_b	$\frac{2}{\sqrt{3}}\frac{2t}{D-t}\min(f_y:\frac{f_u}{1.15})$	138.75	MPa

Burst Criteria (According to $DNV - OS - F201$) $\underset{OK}{\Rightarrow}$ $(P_{li} - P_e) \leq \frac{P_b(t_1)}{\gamma_m\gamma_{sc}}$

COMMENT = OK

1.2 Burst Check for RDM-R Aluminum Dual Drill Pipe

Parameter	Equation	Value	Unit
Outer Diameter, D	~	198	mm
Specific Minimum Yield Stress, SMYS	~	98.96	MPa
Specific Minimum Tensile Stress, SMTS	~	114.58	MPa
Yield Stress Temperature Derating Factor, $f_{y,temp}$	~	0	MPa
Tensile Strength Temperature Derating Factor, $f_{u,temp}$	~	0	MPa
Material Strength Factor, α_u	~	0.96	~
Material Resistance Factor, γ_m	~	1.15	~
Safety class resistance factor, γ_{sc}	~	1.26	~
Water Depth, d	~	2000	m
Starting Elevation of Circulation Fluid, h_0	~	30	m
Circulation Fluid Density, ρ_i	~	1500	Kg/m3
Seawater Density, ρ_e	~	1025	Kg/m3
Maximum Surface Design Pressure, P_d	~	0	MPa
Yield Stress, f_y	$(SMYS - f_{y,temp})\alpha_u$	95	MPa
Tensile Strength, f_u	$(SMTS - f_{u,temp})\alpha_u$	110	MPa
Height of Internal Fluid Column, h	$d + h_0$	2030	m
Local Internal Design Pressure, P_{ld}	$P_d + \rho_i * g * h$	29.87	MPa
Local Incidental Pressure, P_{li}	$P_{id} + 0.1P_d$	29.87	MPa
Local External Pressure, P_e	$\rho_e * g * h$	19.91	MPa
Minimum Required Wall Thickness Without Allowance and Tolerance, t_1	$\frac{D}{\frac{4}{\sqrt{3}}\frac{\min(f_y;\frac{f_u}{1.15})}{\gamma_m\gamma_{sc}(P_{li}-P_e)}+}$	0.131	mm
Burst Resistance, P_b	$\frac{2}{\sqrt{3}}\frac{2t}{D-t}\min(f_y;\frac{f_u}{1.15})$	10.64	MPa

Burst Criteria (According to $DNV - OS - F201$) $\underset{OK}{\Rightarrow}$ $(P_{li} - P_e) \leq \frac{P_b(t_1)}{\gamma_m\gamma_{sc}}$

COMMENT = OK

1.3 Burst Check for Assumed RDM-R Steel Dual Drill Pipe

Parameter	Equation	Value	Unit
Outer Diameter, D	~	193.675	mm
Specific Minimum Yield Stress, SMYS	~	718.75	MPa
Specific Minimum Tensile Stress, SMTS	~	791.67	MPa
Yield Stress Temperature Derating Factor, $f_{y,temp}$	~	0	MPa
Tensile Strength Temperature Derating Factor, $f_{u,temp}$	~	0	MPa
Material Strength Factor, α_u	~	0.96	~
Material Resistance Factor, γ_m	~	1.15	~
Safety class resistance factor, γ_{sc}	~	1.26	~
Water Depth, d	~	2000	m
Starting Elevation of Circulation Fluid, h_0	~	30	m
Circulation Fluid Density, ρ_i	~	1500	Kg/m3
Seawater Density, ρ_e	~	1025	Kg/m3
Maximum Surface Design Pressure, P_d	~	0	MPa
Yield Stress, f_y	$(SMYS - f_{y,temp})\alpha_u$	690	MPa
Tensile Strength, f_u	$(SMTS - f_{u,temp})\alpha_u$	760	MPa
Height of Internal Fluid Column, h	$d + h_0$	2030	m
Local Internal Design Pressure, P_{ld}	$P_d + \rho_i * g * h$	29.87	MPa
Local Incidental Pressure, P_{li}	$P_{id} + 0.1P_d$	29.87	MPa
Local External Pressure, P_e	$\rho_e * g * h$	19.91	MPa
Minimum Required Wall Thickness Without Allowance and Tolerance, t_1	$\frac{D}{\frac{4}{\sqrt{3}}\frac{\min(f_y:\frac{f_u}{1.15})}{\gamma_m\gamma_{sc}(P_{li}-P_e)}+}$	1.81	mm
Burst Resistance, P_b	$\frac{2}{\sqrt{3}}\frac{2t}{D-t}\min(f_y:\frac{f_u}{1.15})$	138.73	MPa

Burst Criteria (According to $DNV - OS - F201$) $\underset{OK}{\Rightarrow}$ $(P_{li} - P_e) \leq \frac{P_b(t_1)}{\gamma_m\gamma_{sc}}$

COMMENT = OK

B2 Collapse Check

2.1 Collapse Check for RDM-R Steel Dual Drill Pipe

Parameter	Equation	Value	Unit
Outer Diameter, D	~	168	mm
Thickness, t	~	14	mm
Yield Stress, f_y	$(SMYS - f_{y,temp})\alpha_u$	690	MPa
Tensile Strength, f_u	$(SMTS - f_{u,temp})\alpha_u$	760	MPa
Water Depth, d	~	2000	m
Starting Elevation of Circulation Fluid, h_0	~	30	m
Circulation Fluid Density, ρ_i	~	1500	Kg/m3
Seawater Density, ρ_e	~	1025	Kg/m3
Local External Pressure, P_e	$\rho_e * g * h$	19.91	MPa
Height of Internal Fluid Column, h	$d + h_0$	2030	m
Minimum Internal Pressure, P_{min}	$\rho_i * g * h$	29.87	MPa
Material Resistance Factor, γ_m	~	1.15	~
Safety class resistance factor, γ_{sc}	~	1.26	~
Young's modulus of pipe material, E	~	200	GPa
Poisson Ratio, ϑ	~	0.29	~
The initial departure from circularity of pipe and pipe ends of pipe (Ovality), f_0	$\frac{D_{max} - D_{min}}{D}$	1	~
Manufacturing process reduction factor, α_{fab}	~	1	~
Elastic collapse pressure, $p_{el}(t)$	$\frac{2 \cdot E \cdot \left(\frac{t}{D}\right)^3}{1-\vartheta^2}$	252.73	MPa
Plastic collapse pressure, $p_p(t)$	$2\frac{t}{D} \cdot f_y \cdot \alpha_{fab}$	115	MPa
Resistance for external pressure, $p_c(t)$	$p_c(t) = y - \frac{b}{3}$	-561.73	MPa
b	$-p_{el}(t)$	-252.73	
c	$-\left[p_p(t)^2 + p_{el}(t) \cdot p_p(t) \cdot f_0 \cdot \frac{D}{t}\right]$	-3.61*10[5]	
d	$p_p(t)^2 * p_{el}(t)$	3.34*10[6]	
u	$\frac{1}{3}\left(-\frac{1}{3}b^2 + c\right)$	-1.27*10[5]	
v	$\frac{1}{2}\left(\frac{2}{27}b^3 - \frac{1}{3}bc + d\right)$	-1.41*10[7]	
φ	$\cos^{-1}\left(\frac{-v}{\sqrt{-u^3}}\right)$	71.85	
y	$-2\sqrt{-u}\cos\left(\frac{\varphi}{3} + \frac{60\pi}{180}\right)$	-646.00	

Collapse Criteria (According to $DNV - OS - F201$) $\underset{OK}{\Rightarrow}$ $(p_e - p_{min}) \leq \frac{p_c(t_1)}{\gamma_m \gamma_{sc}}$

COMMENT = OK

2.2 Collapse Check for RDM-R Aluminum Dual Drill Pipe

Parameter	Equation	Value	Unit
Outer Diameter, D	~	198	mm
Thickness, t	~	13	mm
Yield Stress, f_y	$(SMYS - f_{y,temp})\alpha_u$	95	MPa
Tensile Strength, f_u	$(SMTS - f_{u,temp})\alpha_u$	110	MPa
Water Depth, d	~	2000	m
Starting Elevation of Circulation Fluid, h_0	~	30	m
Circulation Fluid Density, ρ_i	~	1500	Kg/m^3
Seawater Density, ρ_e	~	1025	Kg/m^3
Local External Pressure, P_e	$\rho_e * g * h$	19.91	MPa
Height of Internal Fluid Column, h	$d + h_0$	2030	m
Minimum Internal Pressure, P_{min}	$\rho_i * g * h$	29.87	MPa
Material Resistance Factor, γ_m	~	1.15	~
Safety class resistance factor, γ_{sc}	~	1.26	~
Young's modulus of pipe material, E	~	69	GPa
Poisson Ratio, ϑ	~	0.33	~
The initial departure from circularity of pipe and pipe ends of pipe (Ovality), f_0	$\frac{D_{max} - D_{min}}{D}$	1	~
Manufacturing process reduction factor, α_{fab}	~	1	~
Elastic collapse pressure, $p_{el}(t)$	$\frac{2 \cdot E \cdot \left(\frac{t}{D}\right)^3}{1 - \vartheta^2}$	438.31	MPa
Plastic collapse pressure, $p_p(t)$	$2\frac{t}{D} \cdot f_y \cdot \alpha_{fab}$	12.47	MPa
Resistance for external pressure, $p_c(t)$	$p_c(t) = y - \frac{b}{3}$	-287.59	MPa
b	$-p_{el}(t)$	-438.31	
c	$-\left[p_p(t)^2 + p_{el}(t) \cdot p_p(t) \cdot f_0 \cdot \frac{D}{t}\right]$	$-8.34*10^4$	
d	$p_p(t)^2 * p_{el}(t)$	$6.81*10^4$	
u	$\frac{1}{3}\left(-\frac{1}{3}b^2 + c\right)$	$-4.91*10^4$	
v	$\frac{1}{2}\left(\frac{2}{27}b^3 - \frac{1}{3}bc + d\right)$	$-9.18*10^6$	
φ	$\cos^{-1}\left(\frac{-v}{\sqrt{-u^3}}\right)$	32.46	
y	$-2\sqrt{-u}\cos\left(\frac{\varphi}{3} + \frac{60\pi}{180}\right)$	-433.70	

Collapse Criteria (According to $DNV-OS-F201$) $\underset{OK}{\Rightarrow}$ $(p_e - p_{min}) \le \frac{p_c(t_1)}{\gamma_m \gamma_{sc}}$ COMMENT = OK

2.3 Collapse Check for RDM-R Assumed Steel Dual Drill Pipe

Parameter	Equation	Value	Unit
Outer Diameter, D	~	193.675	mm
Thickness, t	~	16.14	mm
Yield Stress, f_y	$(SMYS - f_{y,temp})\alpha_u$	690	MPa
Tensile Strength, f_u	$(SMTS - f_{u,temp})\alpha_u$	760	MPa
Water Depth, d	~	2000	m
Starting Elevation of Circulation Fluid, h_0	~	30	m
Circulation Fluid Density, ρ_i	~	1500	Kg/m^3
Seawater Density, ρ_e	~	1025	Kg/m^3
Local External Pressure, P_e	$\rho_e * g * h$	19.91	MPa
Height of Internal Fluid Column, h	$d + h_0$	2030	m
Minimum Internal Pressure, P_{min}	$\rho_i * g * h$	29.87	MPa
Material Resistance Factor, γ_m	~	1.15	~
Safety class resistance factor, γ_{sc}	~	1.26	~
Young's modulus of pipe material, E	~	200	GPa
Poisson Ratio, ϑ	~	0.29	~
The initial departure from circularity of pipe and pipe ends of pipe (Ovality), f_0	$\frac{D_{max} - D_{min}}{D}$	1	~
Manufacturing process reduction factor, α_{fab}	~	1	~
Elastic collapse pressure, $p_{el}(t)$	$\frac{2 \cdot E \cdot \left(\frac{t}{D}\right)^3}{1 - \vartheta^2}$	267.92	MPa
Plastic collapse pressure, $p_p(t)$	$2\frac{t}{D} \cdot f_y \cdot \alpha_{fab}$	115	MPa
Resistance for external pressure, $p_c(t)$	$p_c(t) = y - \frac{b}{3}$	-571.23	MPa
b	$-p_{el}(t)$	-267.92	
c	$-\left[p_p(t)^2 + p_{el}(t) \cdot p_p(t) \cdot f_0 \cdot \frac{D}{t}\right]$	$-3.73*10^5$	
d	$p_p(t)^2 * p_{el}(t)$	$8.25*10^6$	
u	$\frac{1}{3}\left(-\frac{1}{3}b^2 + c\right)$	$-1.87*10^5$	
v	$\frac{1}{2}\left(\frac{2}{27}b^3 - \frac{1}{3}bc + d\right)$	$-1.63*10^7$	
φ	$\cos^{-1}\left(\frac{-v}{\sqrt{-u^3}}\right)$	78.37	
y	$-2\sqrt{-u}\cos\left(\frac{\varphi}{3} + \frac{60\pi}{180}\right)$	-732.03	

Collapse Criteria (According to $DNV-OS-F201$) $\underset{OK}{\Rightarrow}$ $(p_e - p_{min}) \leq \frac{p_c(t_1)}{\gamma_m \gamma_{sc}}$

COMMENT = OK

Appendix C: Pipe Properties Calculations

C1 Pipe Properties for RDM-R Steel Pipe

Calculation Input

Pipe Outer Diameter, D_0 = 168 mm

Pipe Inner Diameter, D_i = 108 mm

Modulus of Elastcity, E = 200 GPa

Poisson Ratio, ϑ= 0.293

Calculation Outputs

Wall Thickness = $\frac{D_0 - D_i}{2}$ = 30 mm

Cross sectional Area, A_Z = $\frac{\pi(D_0^2 - D_i^2)}{4}$ = 0.013 m^2

Moment of Inertia, $I_x = \frac{\pi(D_0^4 - D_i^4)}{64}$ = $3.24*10^{-5}$ m^4

Modulus of Rigidity, G = $\frac{E}{2(1+\vartheta)}$ = 77.34 GPa

Polar Moment of Inertia, $J_{zz} = \frac{\pi(D_0^4 - D_i^4)}{32}$ = $6.48*10^{-5}$ m^4

Bending Stiffness, K_B= EI_x = 6.49 MNm^2

Axial Stiffness, K_A= EA_Z = 2.60 GN

Torsional Stiffness, K_T= GJ_{zz} = 5.01 MNm

C2 Pipe Properties for RDM-R Aluminum Pipe

Calculation Input

Pipe Outer Diameter, D_0 = 198 mm

Pipe Inner Diameter, D_i = 137 mm

Modulus of Elastcity, E = 69 GPa

Poisson Ratio, ϑ= 0.33

Calculation Outputs

Wall Thickness = $\frac{D_0 - D_i}{2}$ = 30.5 mm

Cross sectional Area, A_Z = $\frac{\pi(D_0^2 - D_i^2)}{4}$ = 0.016 m^2

Moment of Inertia, $I_x = \frac{\pi(D_0^4 - D_i^4)}{64}$ = $9.3*10^{-4}$ m^4

Modulus of Rigidity, G = $\frac{E}{2(1+\vartheta)}$ = 25.94 GPa

Polar Moment of Inertia, $J_{zz} = \frac{\pi(D_0^4-D_i^4)}{32}$ = 1.86*10^{-3} m^4

Bending Stiffness, K_B= EI_x = 2.49 MNm^2

Axial Stiffness, K_A= EA_Z = 0.111 GN

Torsional Stiffness, K_T= GJ_{zz} = 4.825 MNm

C3 Pipe Properties for RDM-R Assumed Steel Pipe

Calculation Input

Pipe Outer Diameter, D_0 = 194 mm

Pipe Inner Diameter, D_i = 81 mm

Modulus of Elastcity, E = 200 GPa

Poisson Ratio, ϑ= 0.293

Calculation Outputs

Wall Thickness = $\frac{D_0-D_i}{2}$ = 56.5 mm

Cross sectional Area, A_Z = $\frac{\pi(D_0^2-D_i^2)}{4}$ = 0.0244 m^2

Moment of Inertia, I_x= $\frac{\pi(D_0^4-D_i^4)}{64}$ = 6.74*10^{-5} m^4

Modulus of Rigidity, G = $\frac{E}{2(1+\vartheta)}$ = 77.34 GPa

Polar Moment of Inertia, $J_{zz} = \frac{\pi(D_0^4-D_i^4)}{32}$ = 1.35*10^{-4} m^4

Bending Stiffness, K_B= EI_x = 1.348 MNm^2

Axial Stiffness, K_A= EA_Z = 0.488 GN

Torsional Stiffness, K_T= GJ_{zz} = 1.044 MNm

Appendix D: Oscillating Load Report - Input for Top Drive Design

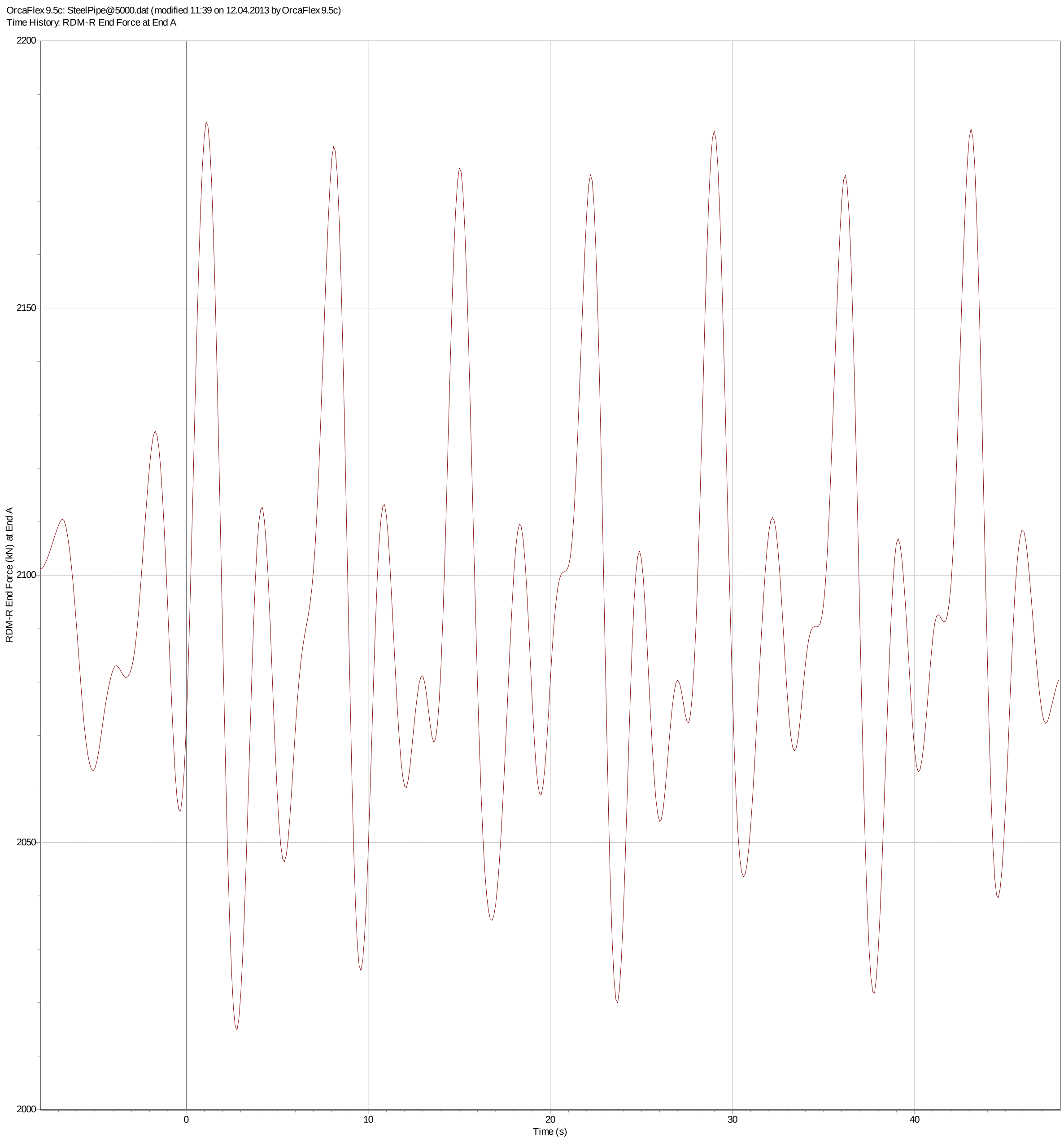
OrcaFlex 9.5c: SteelPipe@5000.dat (modified 11:39 on 12.04.2013 by OrcaFlex 9.5c)
Time History: RDM-R End Force at End A
RDM-R End Force (kN) at End A
2200
2150
2100
2050
2000
0
10
20
30
40
Time (s)

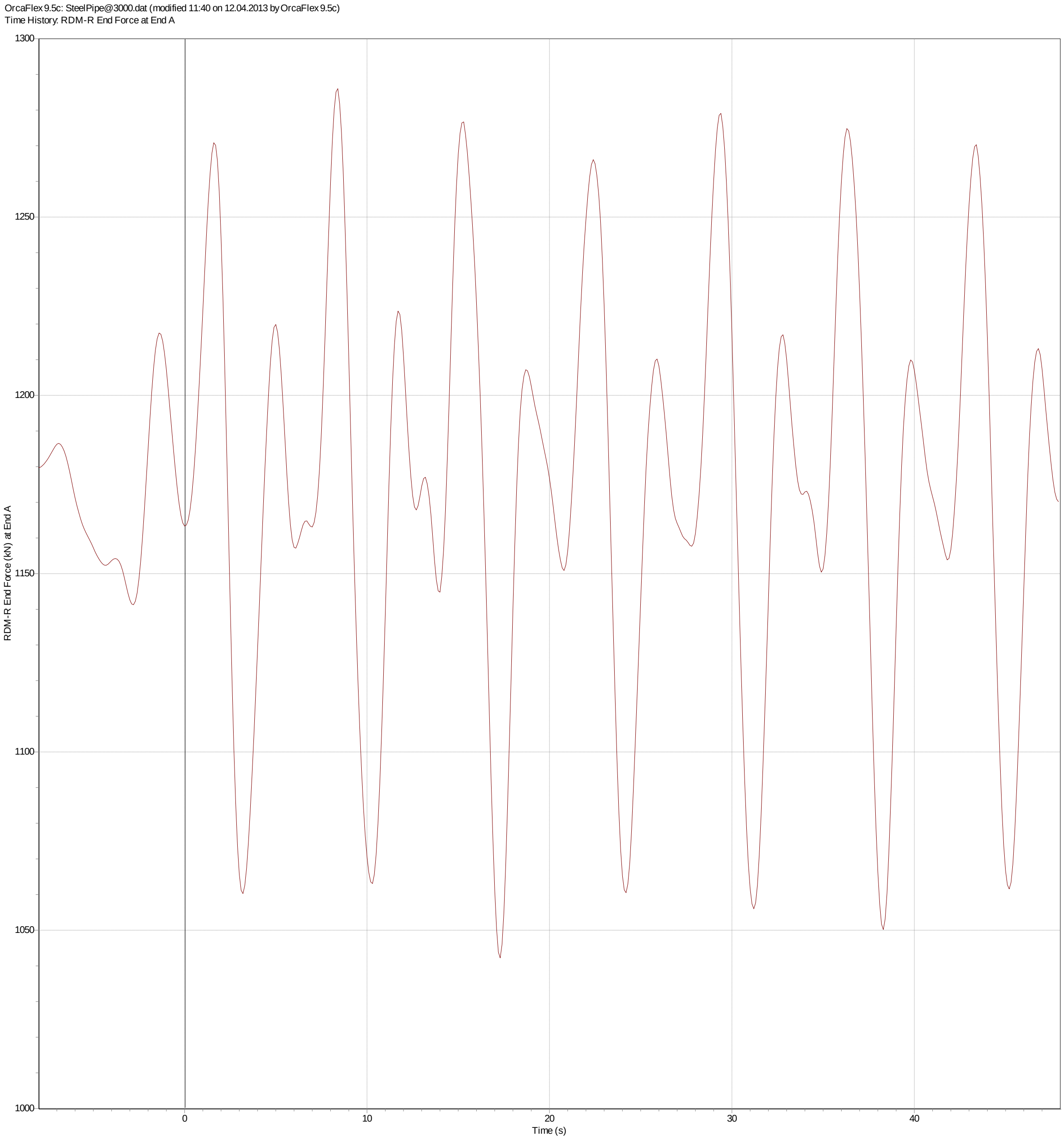
OrcaFlex 9.5c: SteelPipe@3000.dat (modified 11:40 on 12.04.2013 by OrcaFlex 9.5c)
Time History: RDM-R End Force at End A
RDM-R End Force (kN) at End A
Time (s)
1300
1250
1200
1150
1100
1050
1000
0
10
20
30
40

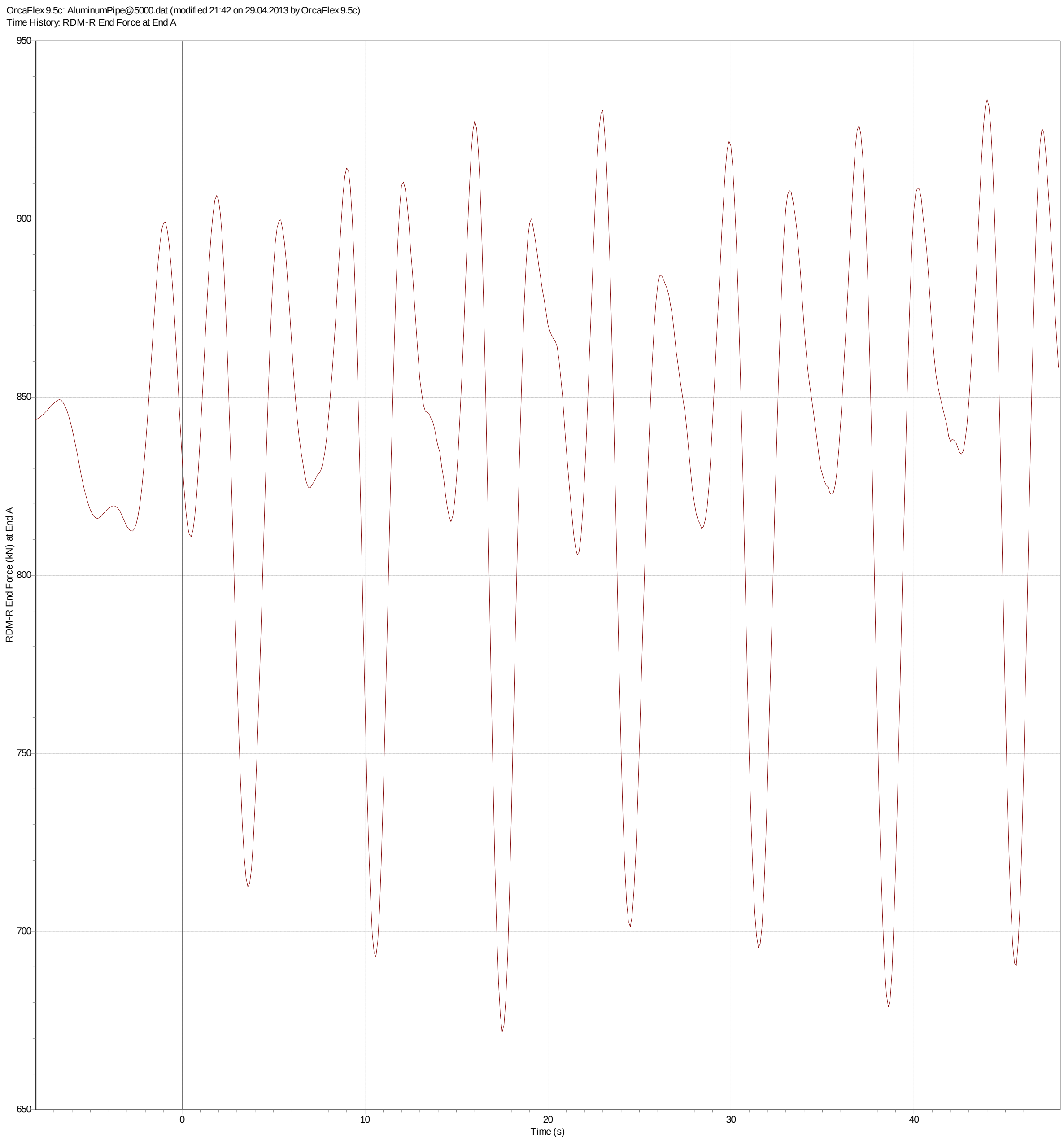
OrcaFlex 9.5c: AluminumPipe@5000.dat (modified 21:42 on 29.04.2013 by OrcaFlex 9.5c)
Time History: RDM-R End Force at End A
RDM-R End Force (kN) at End A
Time (s)
950
900
850
800
750
700
650
0
10
20
30
40

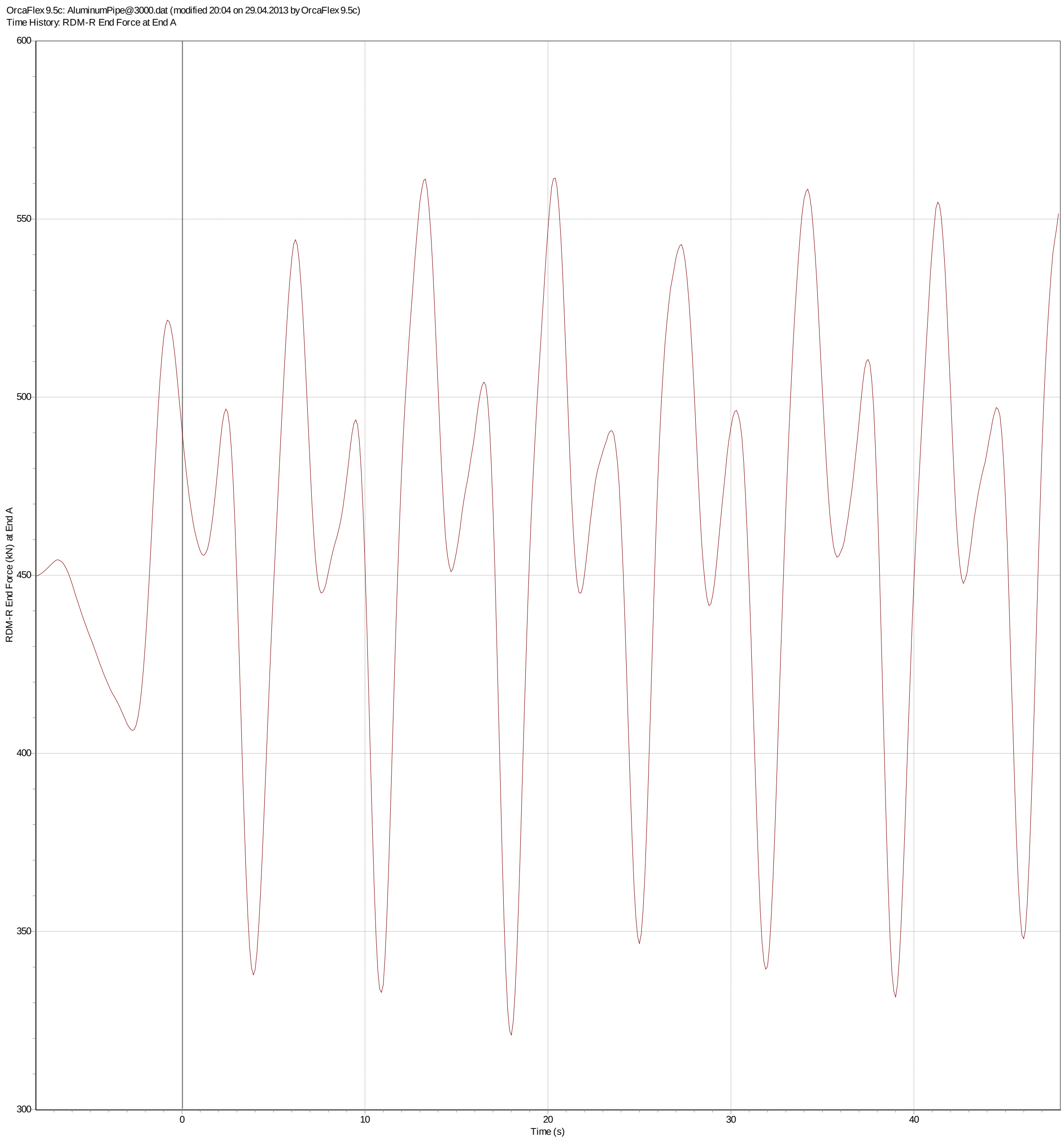
OrcaFlex 9.5c: AluminumPipe@3000.dat (modified 20:04 on 29.04.2013 by OrcaFlex 9.5c)
Time History: RDM-R End Force at End A
RDM-R End Force (kN) at End A
Time (s)
600
550
500
450
400
350
300
0
10
20
30
40

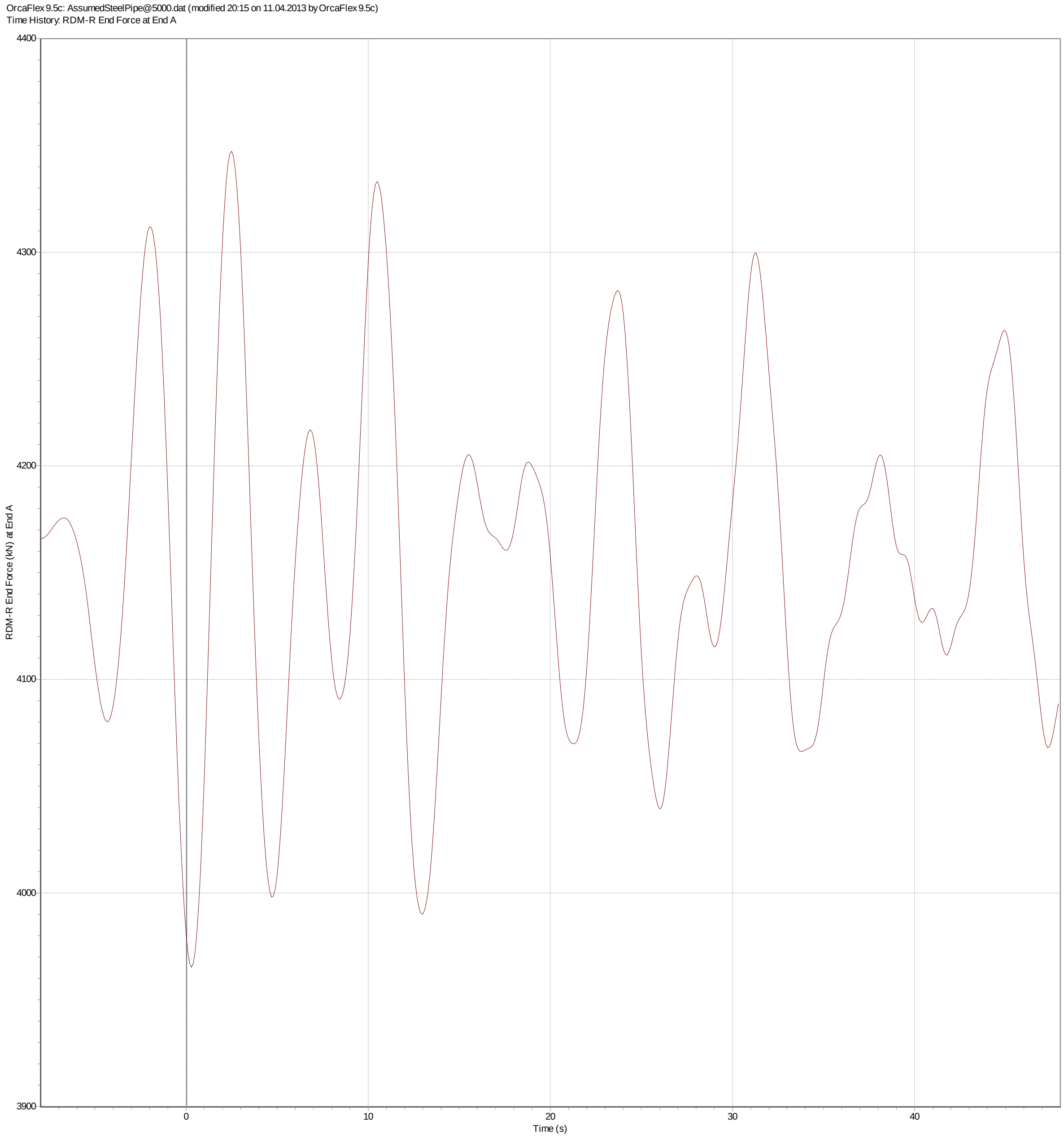
OrcaFlex 9.5c: AssumedSteelPipe@5000.dat (modified 20:15 on 11.04.2013 by OrcaFlex 9.5c)
Time History: RDM-R End Force at End A
RDM-R End Force (kN) at End A
4400
4300
4200
4100
4000
3900
0
10
20
30
40
Time (s)

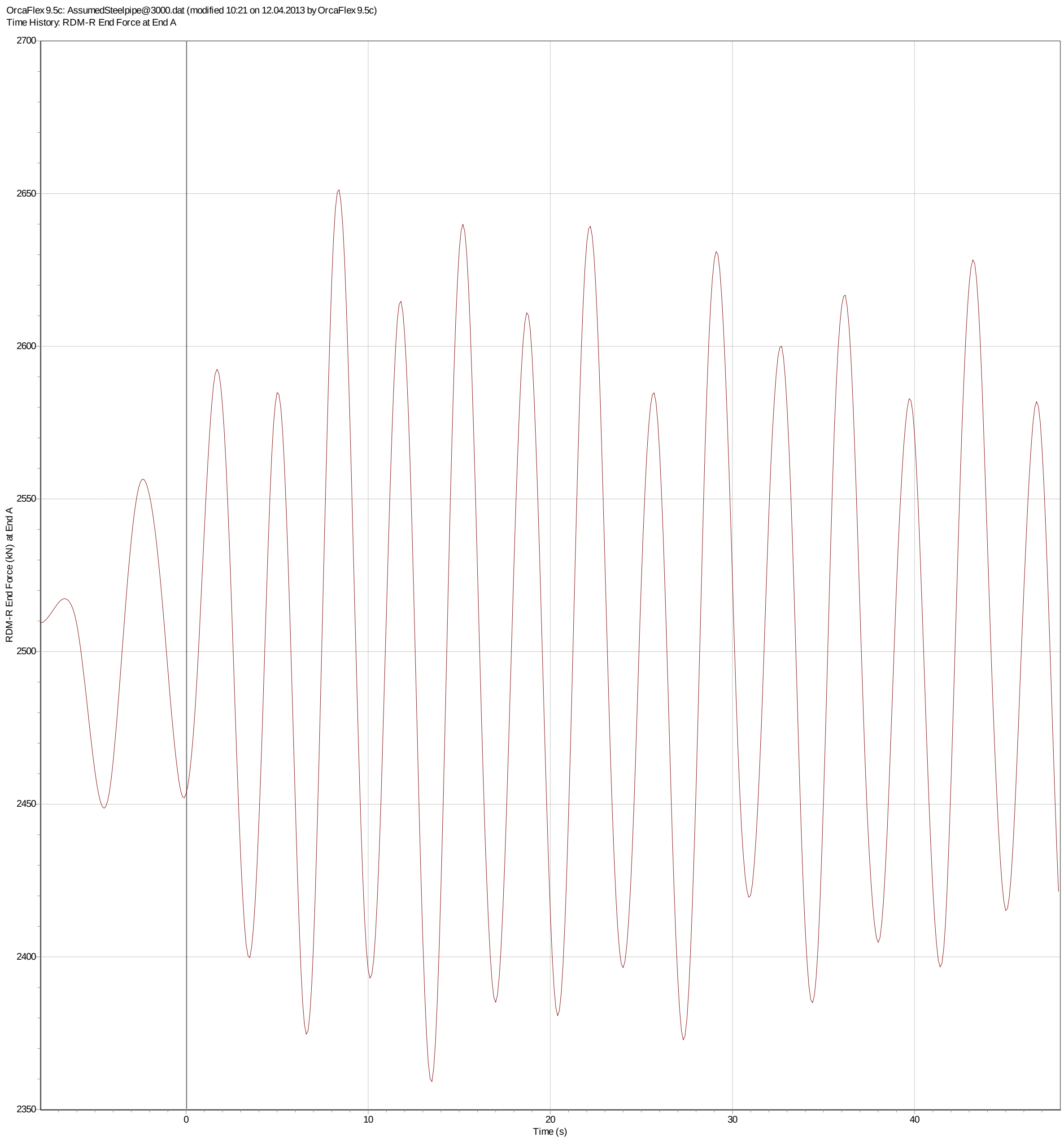
OrcaFlex 9.5c: AssumedSteelpipe@3000.dat (modified 10:21 on 12.04.2013 by OrcaFlex 9.5c)
Time History: RDM-R End Force at End A
RDM-R End Force (kN) at End A
2700
2650
2600
2550
2500
2450
2400
2350
0
10
20
30
40
Time (s)